

Nuclear Astrophysics in the Era of Multi-Messenger Astronomy

Xiao-Dong Tang

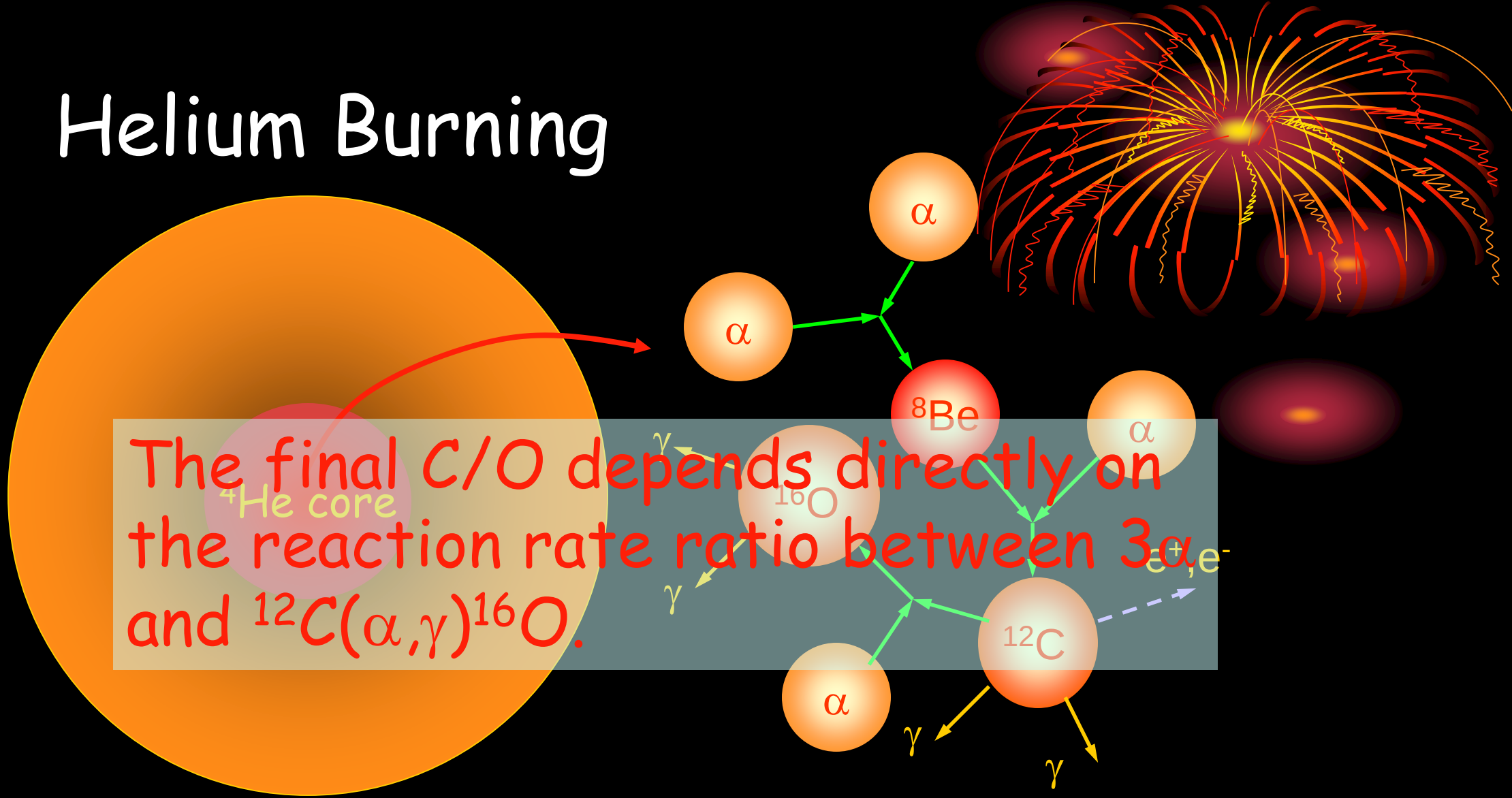
Institute of Modern Physics, CAS

Joint Department for Nuclear Physics, Lanzhou University and IMP, CAS

xtang@impcsa.ac.cn

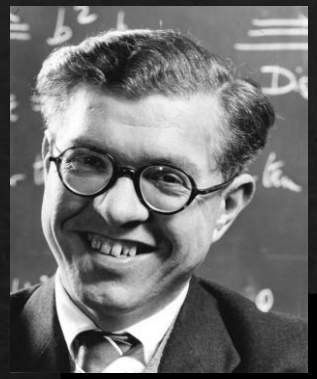
OECE School, Beijing, Nov.2-4, 2026

Helium Burning

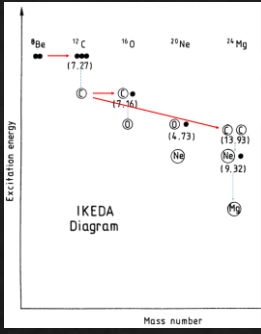


The final C/O depends directly on the reaction rate ratio between 3α and $^{12}C(\alpha,\gamma)^{16}O$.

T ~ 0.2 billion Kelvin



Helium burning :3α and $^{12}C(\alpha,\gamma)^{16}O$



Reaction rates determined by α cluster state configurations providing strong resonances!

$\theta_\alpha^2 \approx 1$

0.0 MeV 0^+

-.092 MeV

$\theta_\alpha^2 \approx 1$

7.654 MeV 0^+

7.367 MeV

9.580 MeV 1^- $\theta_\alpha^2 \approx 0.7$

7.117 MeV 1^- $\theta_\alpha^2 \approx 0.3$

6.917 MeV 2^+ $\theta_\alpha^2 \approx 0.8$

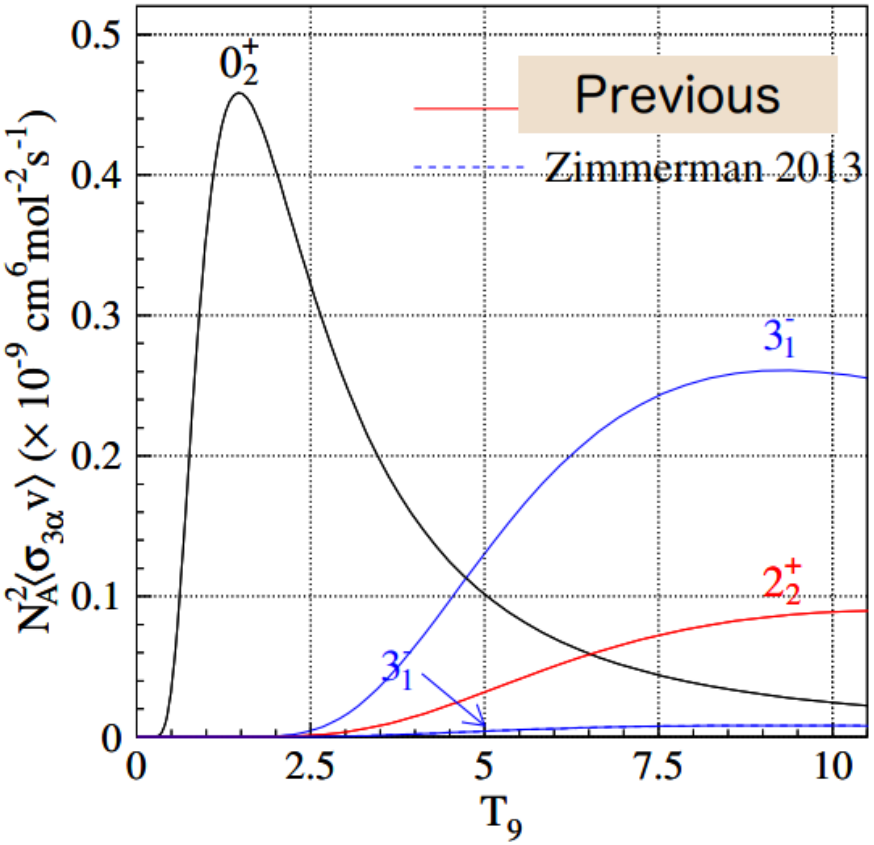
7.162 MeV

^4He ^8Be ^{12}C ^{16}O

Triple Alpha Reaction Rate

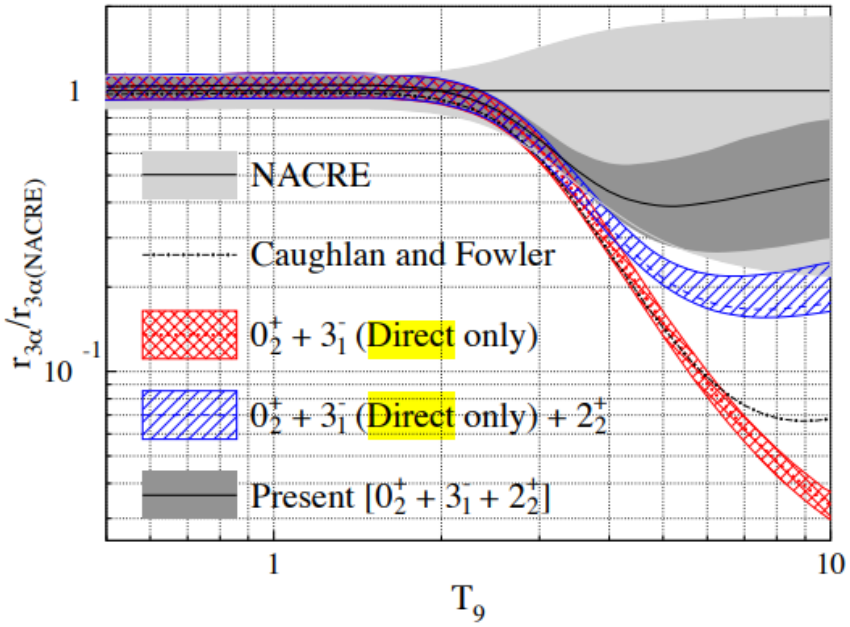
Higher temperature

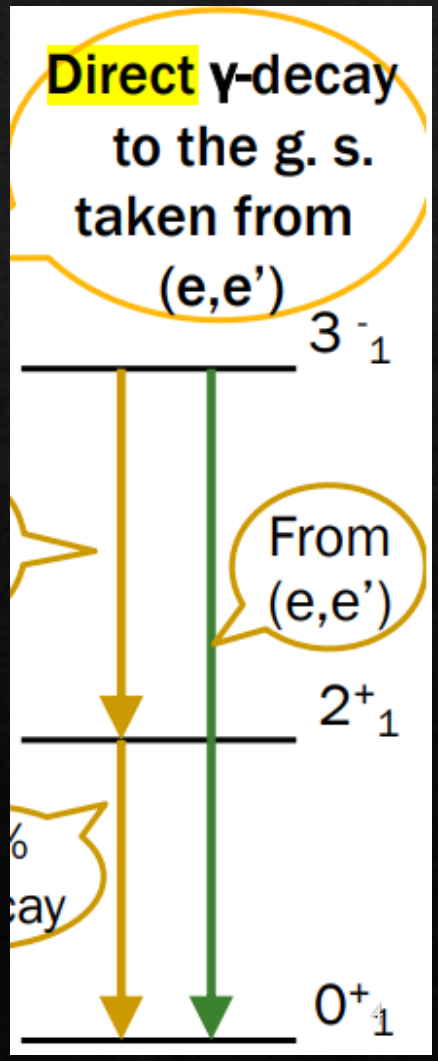
Triple reaction rate was calculated using the measured Γ_γ/Γ



NACRE
3^-_1
Γ_γ = 2 meV

Present
3^-_1
Γ_γ = 44 meV





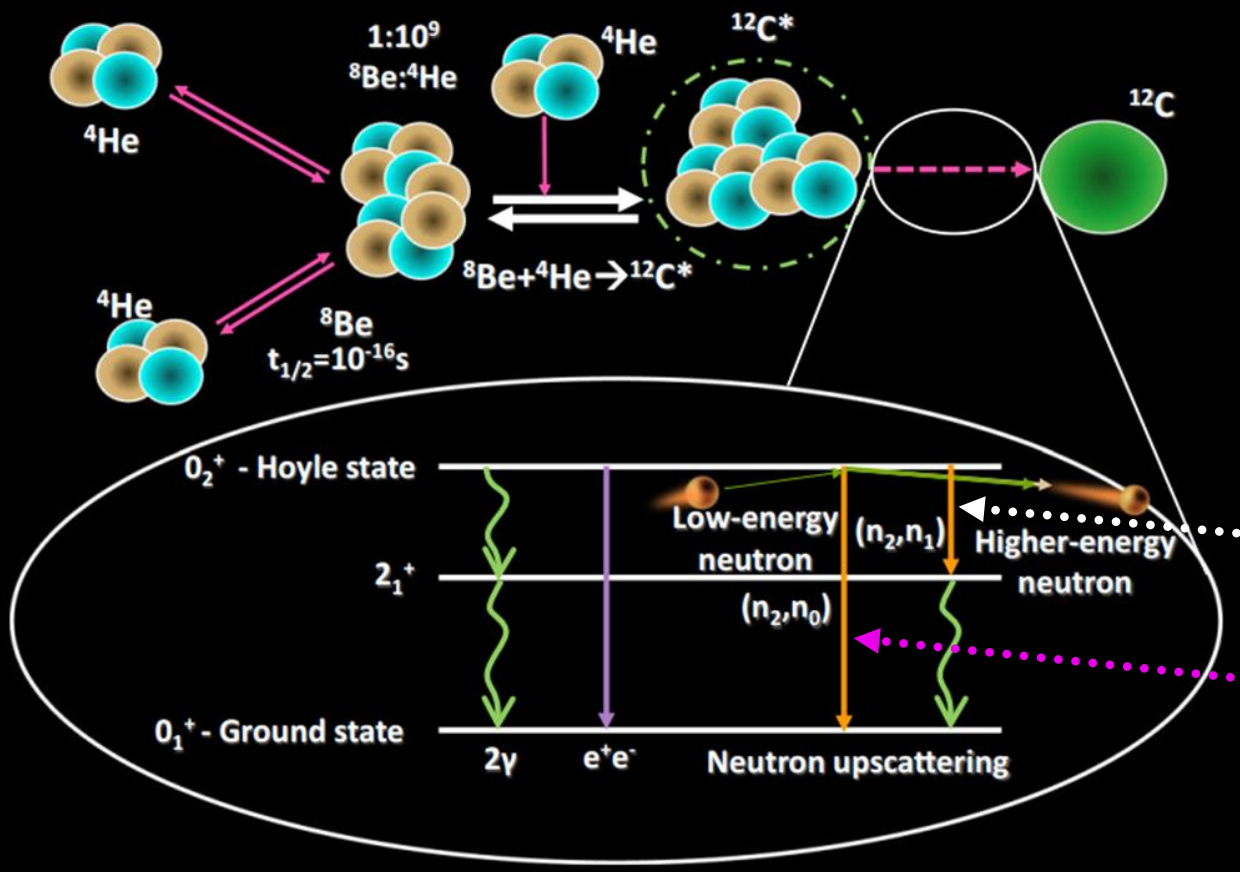
The 3α rate is partially restored, and consistent with NACRE...

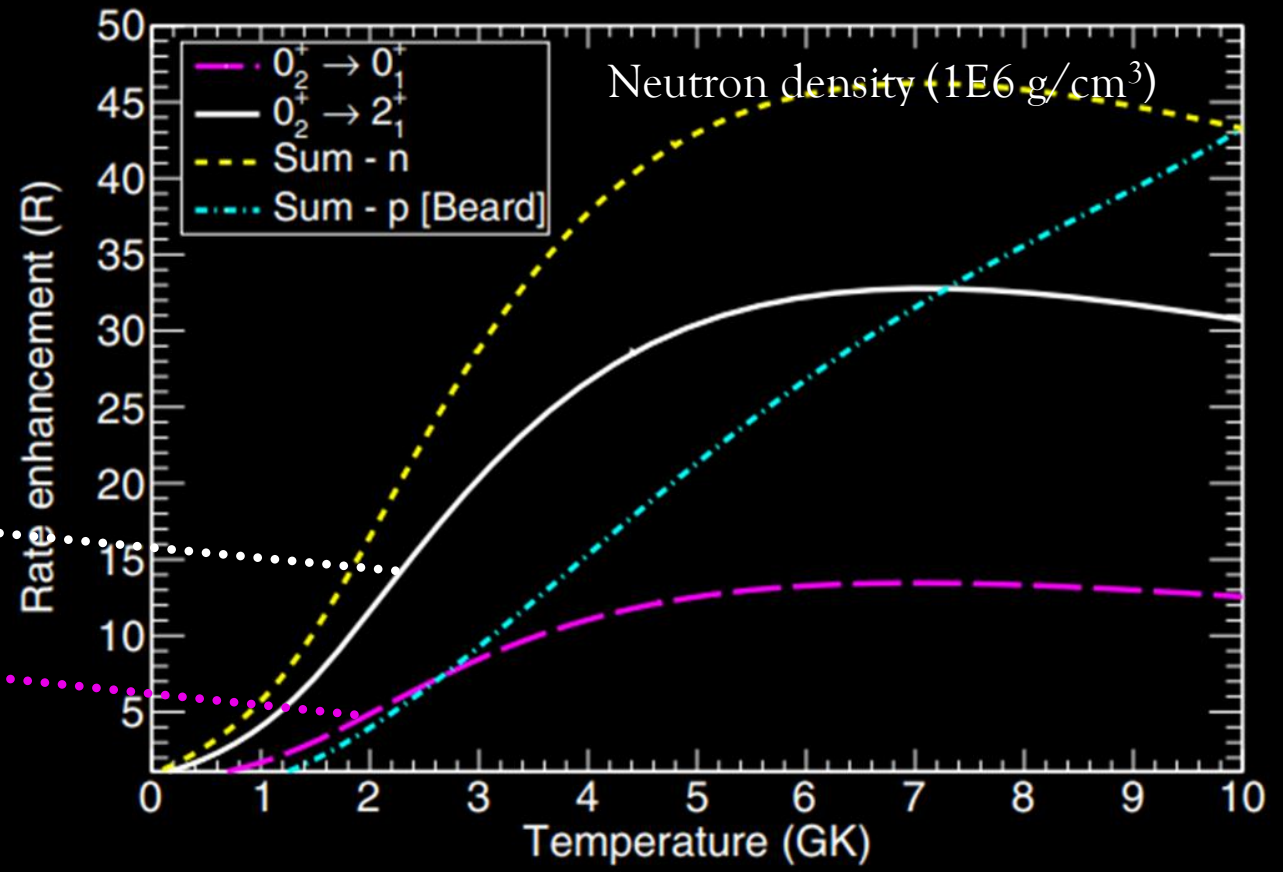
Recently published in M. Tsumura, T. K. et al., Phys. Lett. B 817, 136283 (2021).

https://www2.yukawa.kyoto-u.ac.jp/~nuc2021/slides/kawabata_t.pdf

Upscattering enhances the Hoyle state's decay rate to the bound states of ^{12}C

Upscattering: Low energy proton/neutron + ^{12}C(7.654 MeV)→Higher energy neutron + ^{12}C(g.s.)/^{12}C(4.44 MeV)

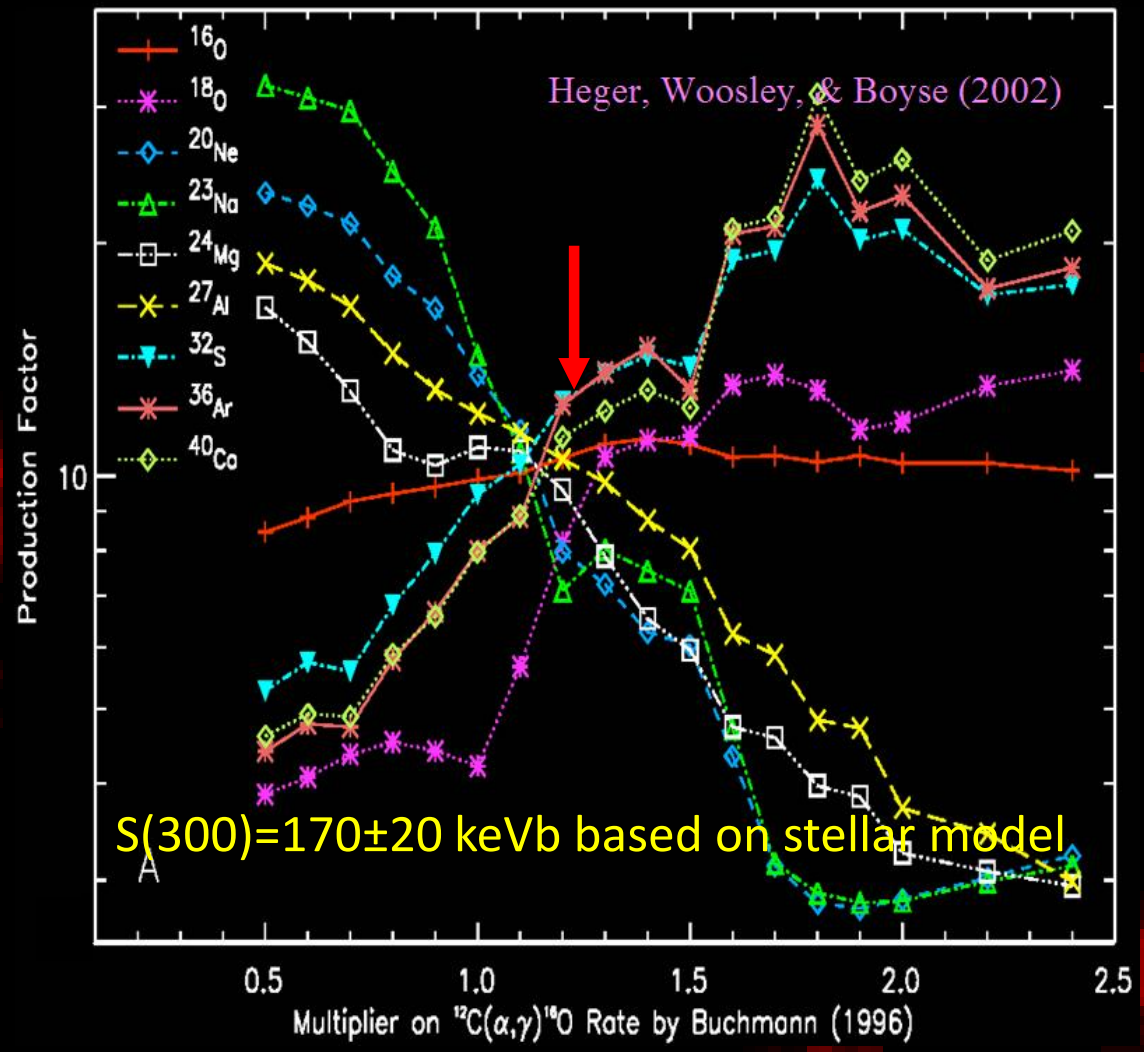




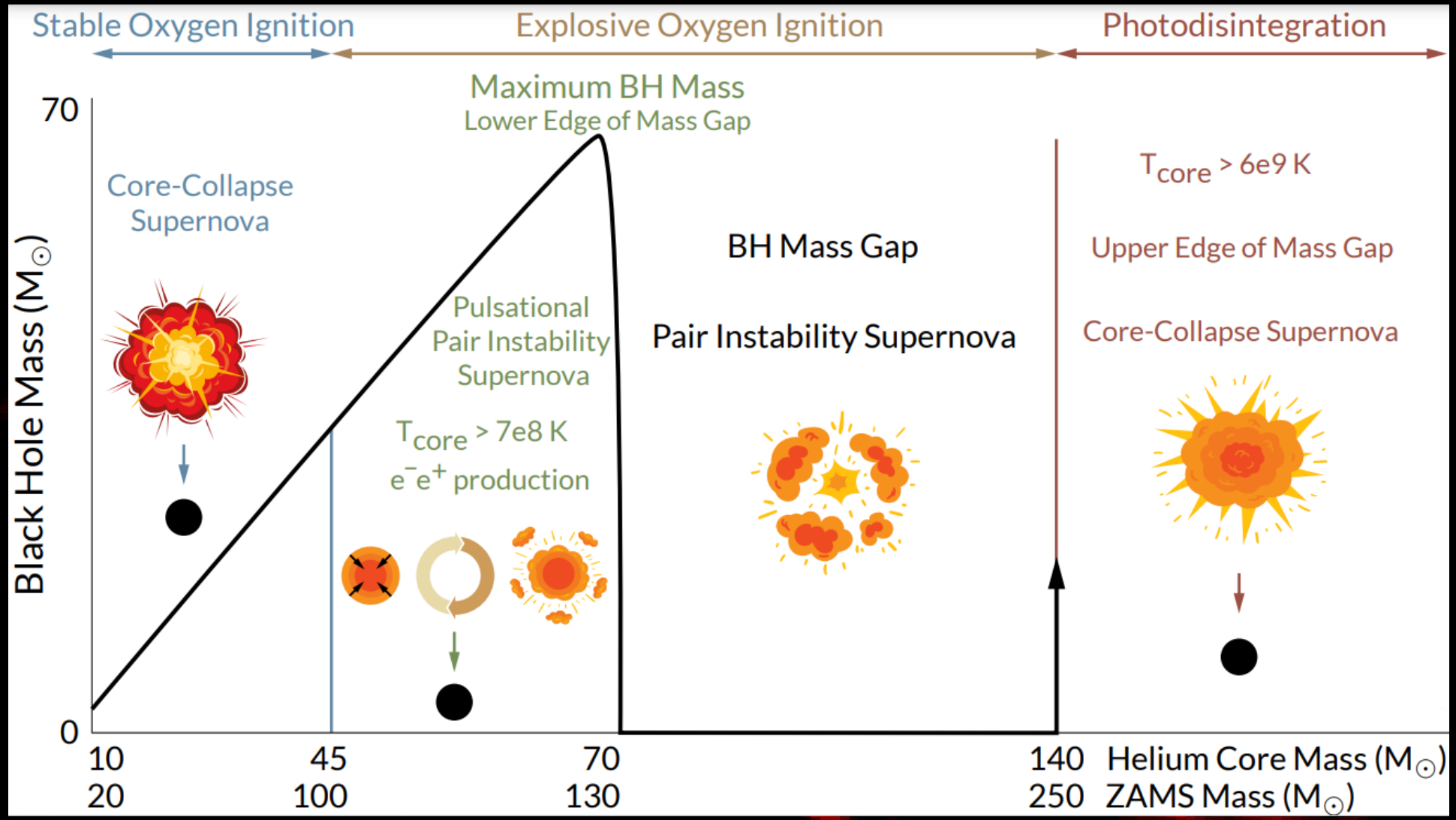
Bishop et al., Nat Commun **13**, 2151 (2022); Beard et al., Phys. Rev. Lett. 119, 112701 (2017); Jin et al., Nature 588, 57–60 (2020); p+^{12}C experiment@JAEA(CENS)

Influences of the uncertainty in the $^{12}C(\alpha,\gamma)^{16}O$ reaction rate in Nucleosynthesis

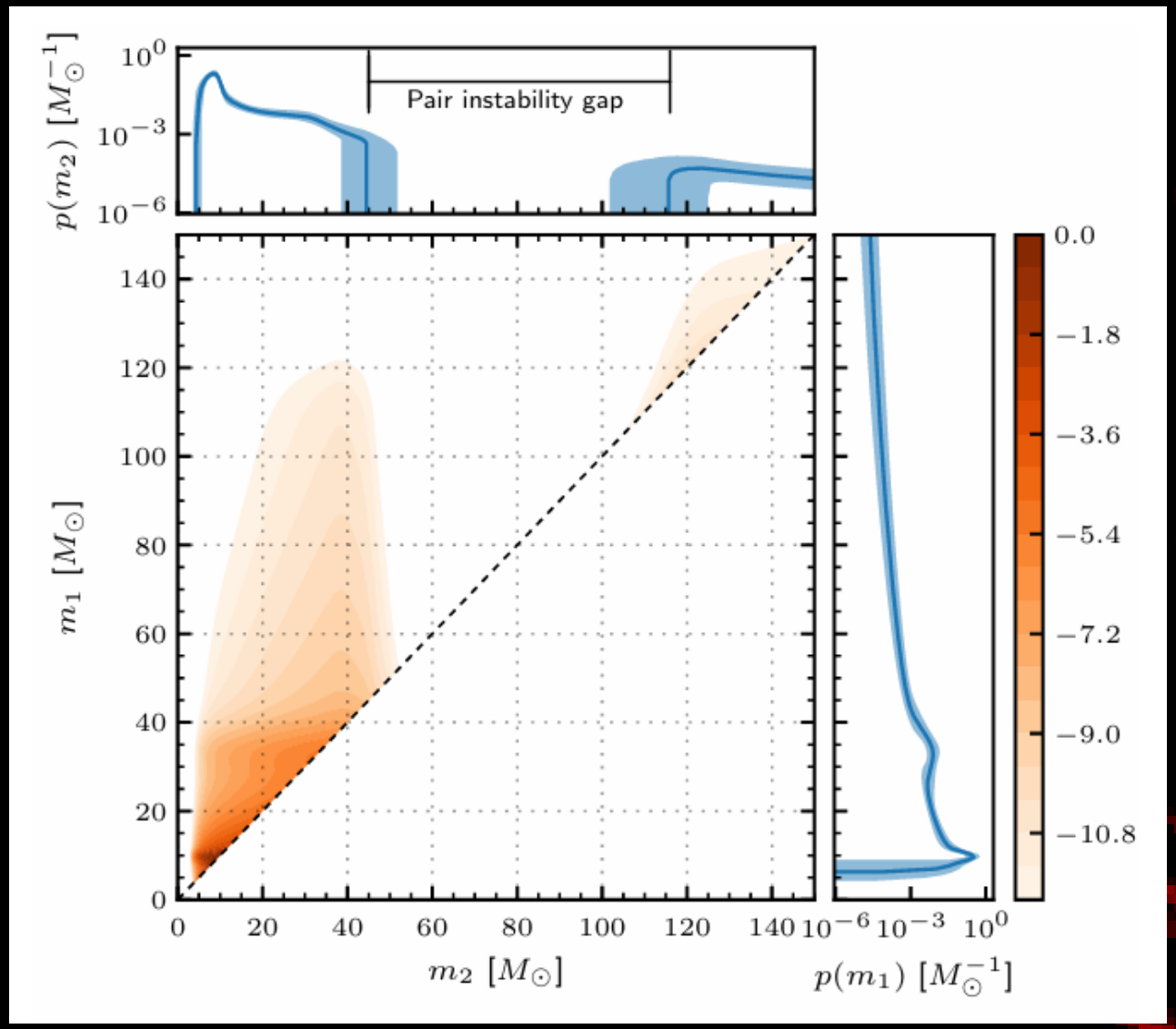
A uncertainty of ~10% is needed!



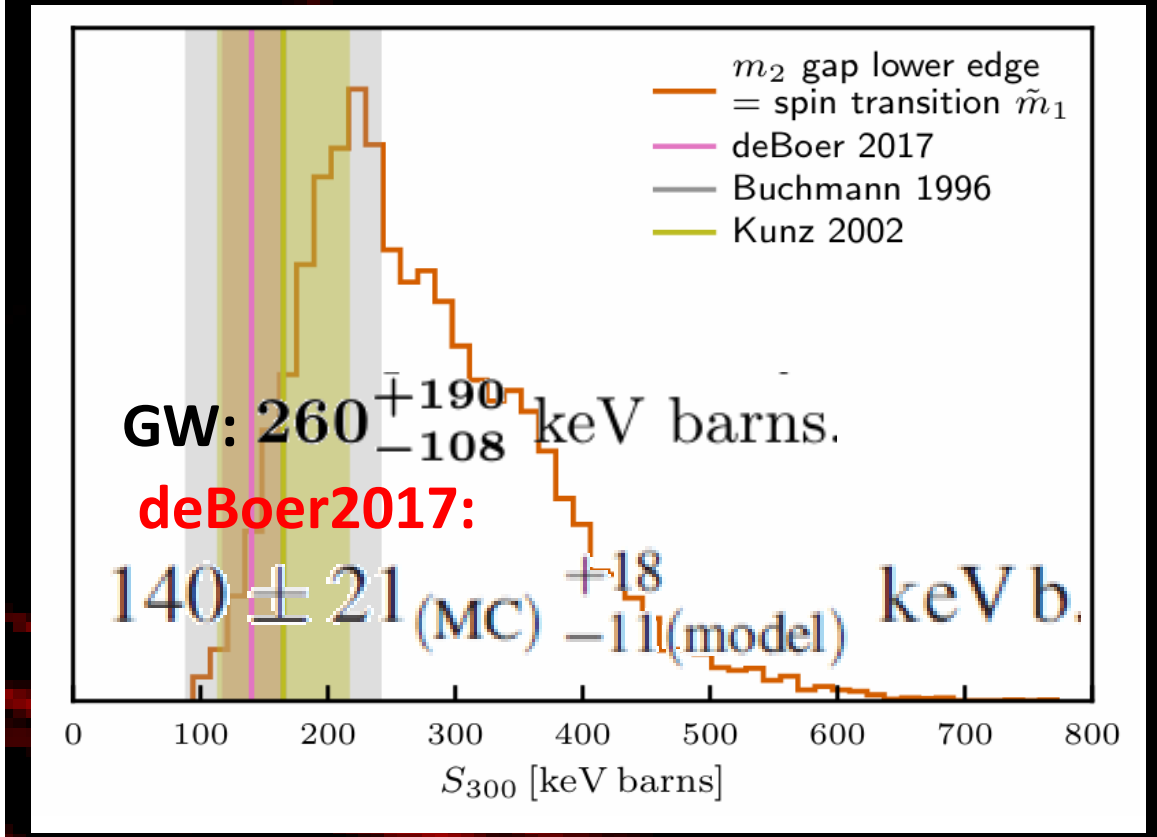
Black hole mass gap



Evidence of the pair-instability gap from black-hole masses

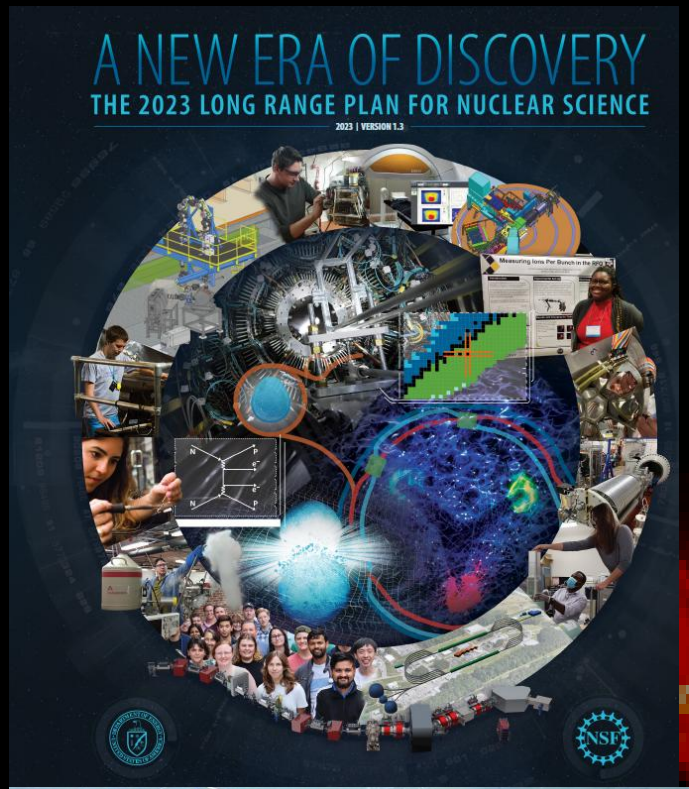




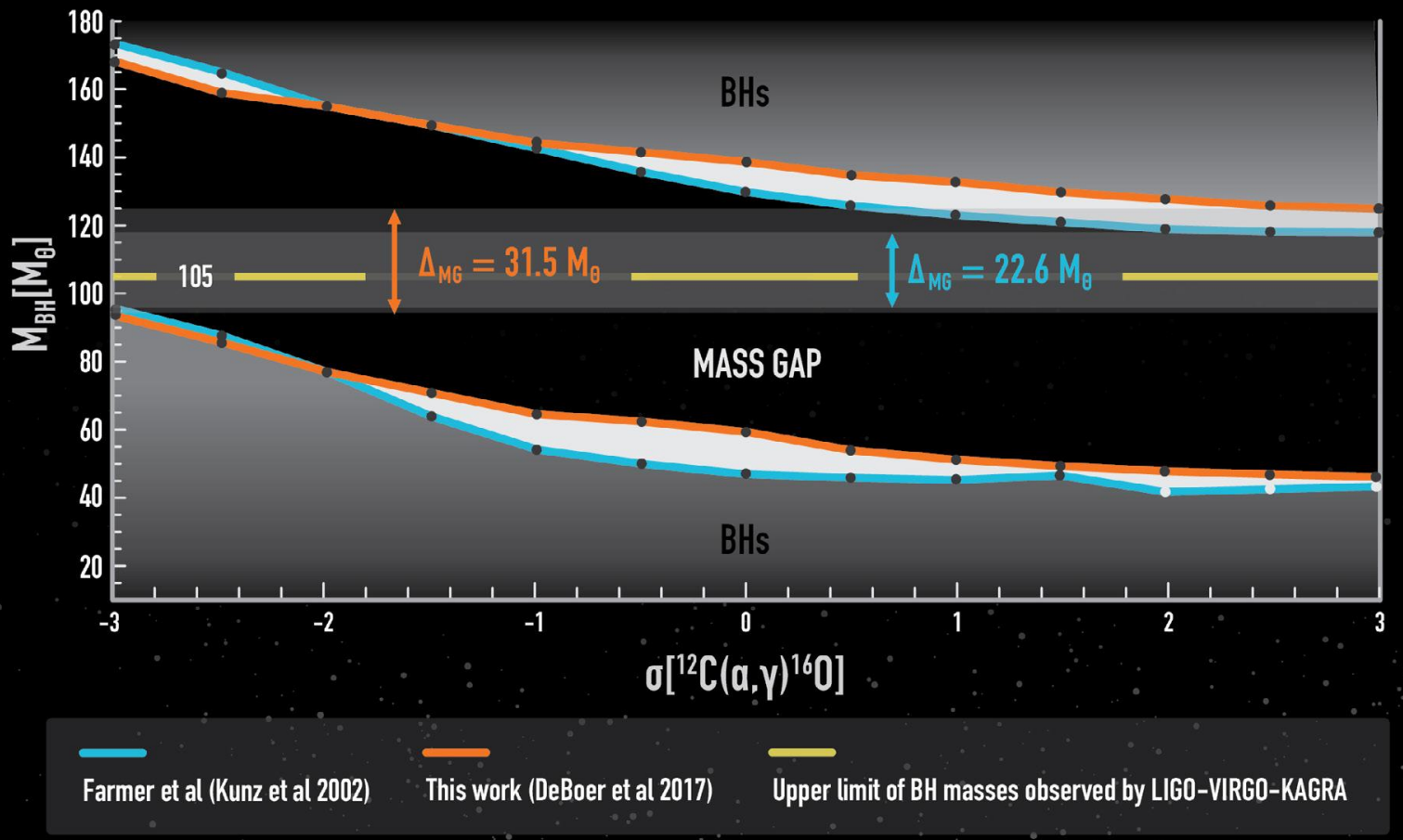


Hui Tong et al., https://arxiv.org/pdf/2509.04151
Nature volume 652, pages874–877 (2026)

Impact on Multi-Messenger Astronomy







Farmer et al., ApJ 902:L36(2020)
NSAC LONG RANGE PLAN (2023)

Holy grail for nuclear astrophysicists

Uncertainty in the $^{12}C(\alpha,\gamma)^{16}O$ reaction rate affects not only the nucleosynthesis but also the explosion itself.

The determination of the ratio C/O produced in helium burning is a problem of paramount importance in Nuclear Astrophysics.

W. Fowler, Nobel lecture, 1983

We hope that…will keenly motivate experimentalists to undertake the difficult task of accurately measuring this rate.

Weaver & Woosley, Phys. Rep. 227 (1993) 65

The fusion of ^{4}He and ^{12}C nuclei to ^{16}O is the most important nuclear reaction in the development of massive stars.

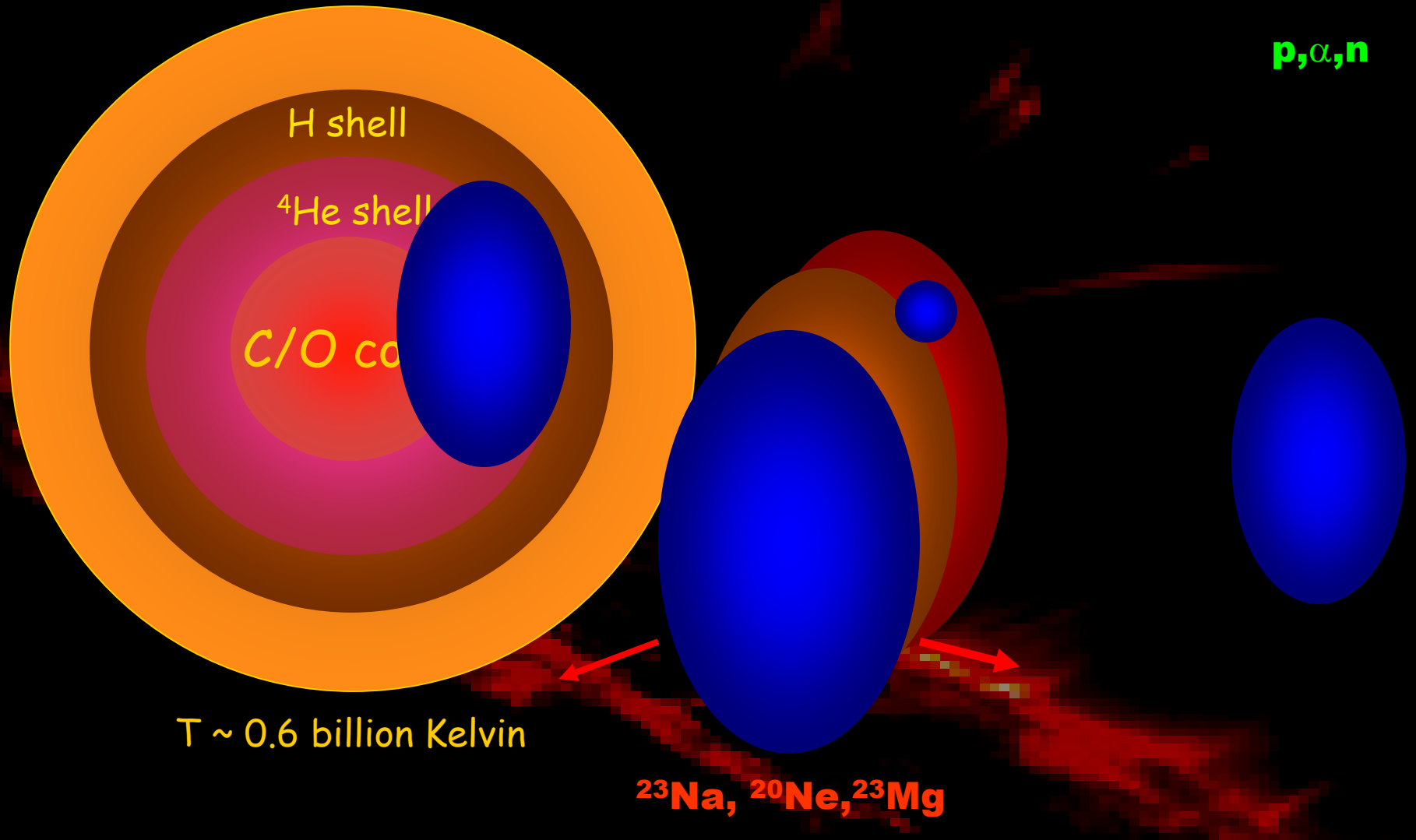
NuPECC Long Range Plan

Life of a 20 solar mass star

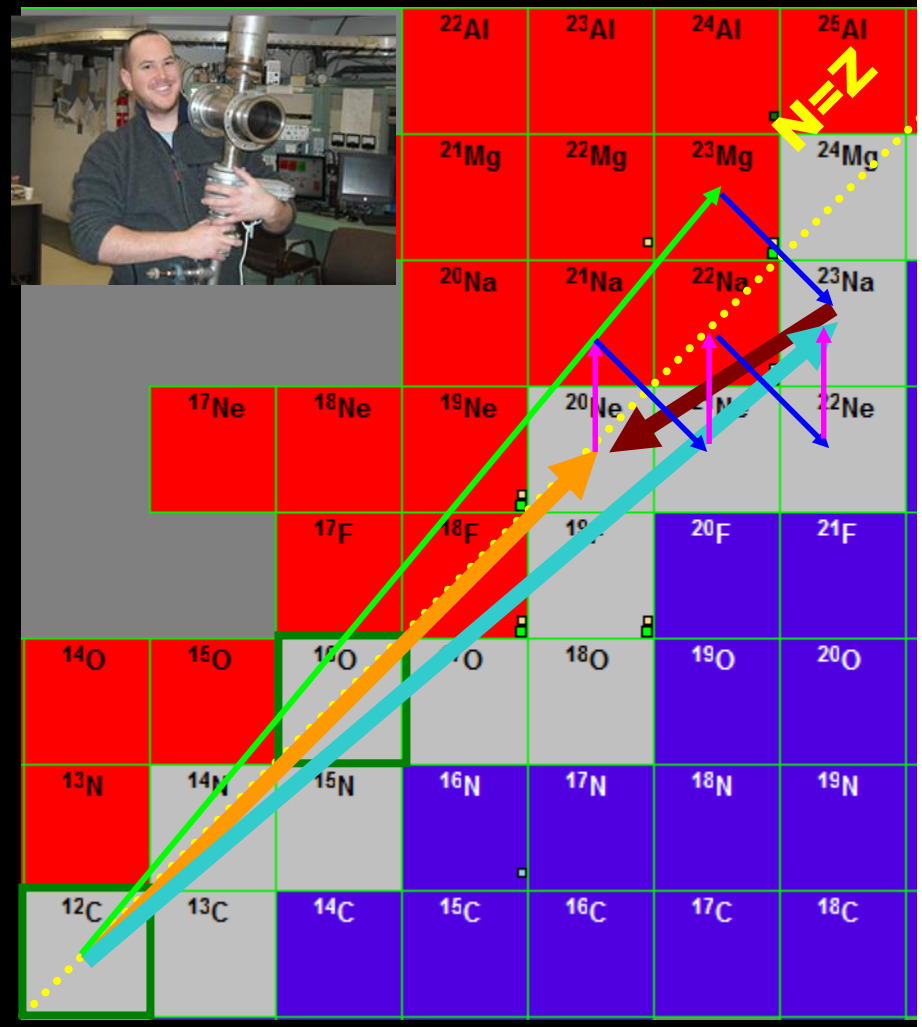
Fuel	Primary Products	Secondary products	Approximate temperature (10^9 K)	Approximate duration
Hydrogen	^{4}He	^{14}N	0.02	10^7 yr
Helium	C,O	^{18}O,^{22}Ne s-process	0.2	10^6 yr
Carbon	Ne,Mg	Na	0.8	10^3 yr
Neon	O,Mg	Al, P	1.5	3 yr
Oxygen	Si, S	Cl, Ar, K, Ca	2.0	0.8 yr
Silicon	Fe	Ti, V, Cr Mn, Co, Ni	3.5	1 week

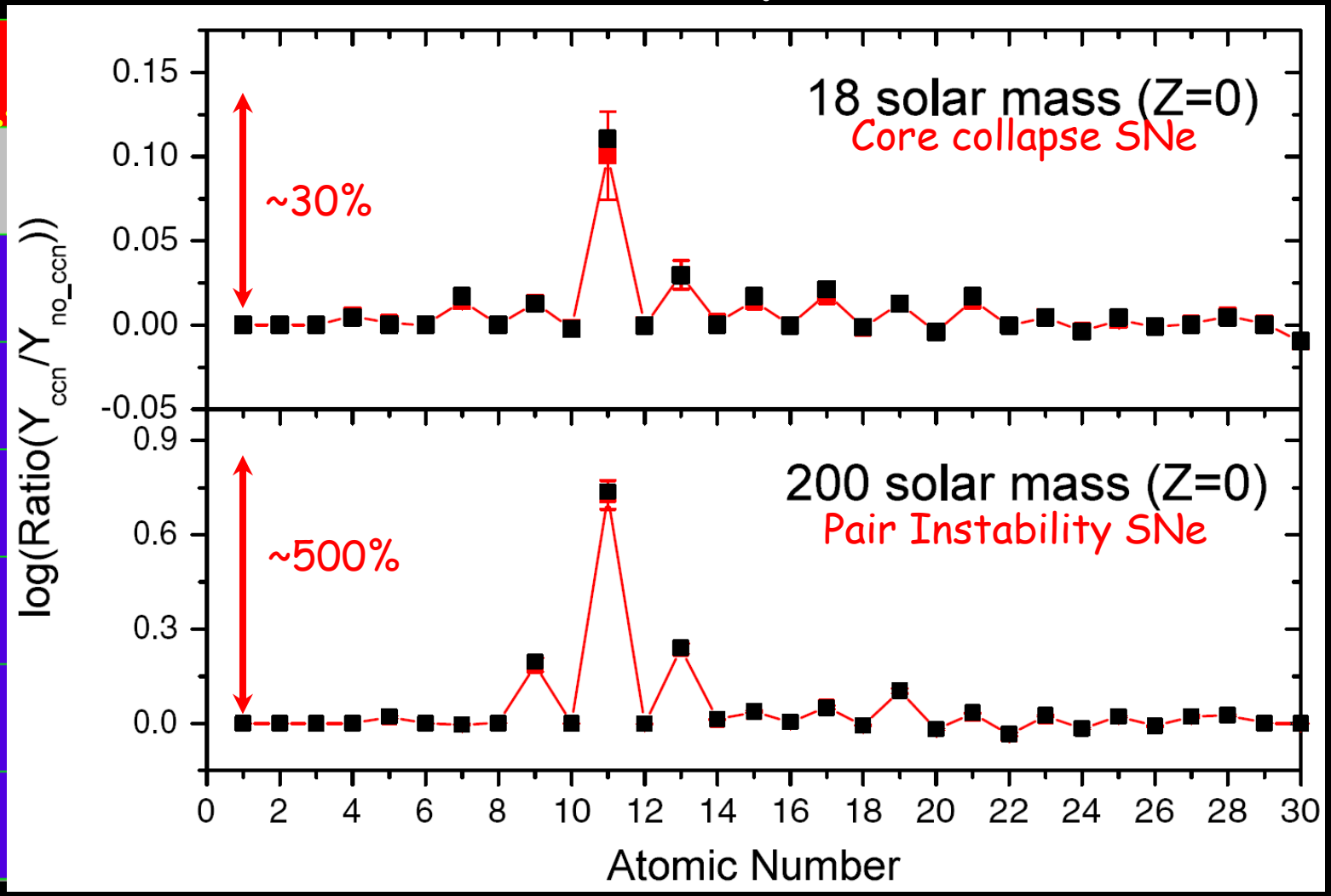


Carbon burning



$^{12}C(^{12}C,n)^{23}Mg$: neutron source in Pop-III stars





- Decay of ^{23}Mg changes the electron fraction and the even-odd pattern in the production yield
- Direct measurement was performed within Gamow window

Bucher et al., PRL(2015)



nature › articles › article

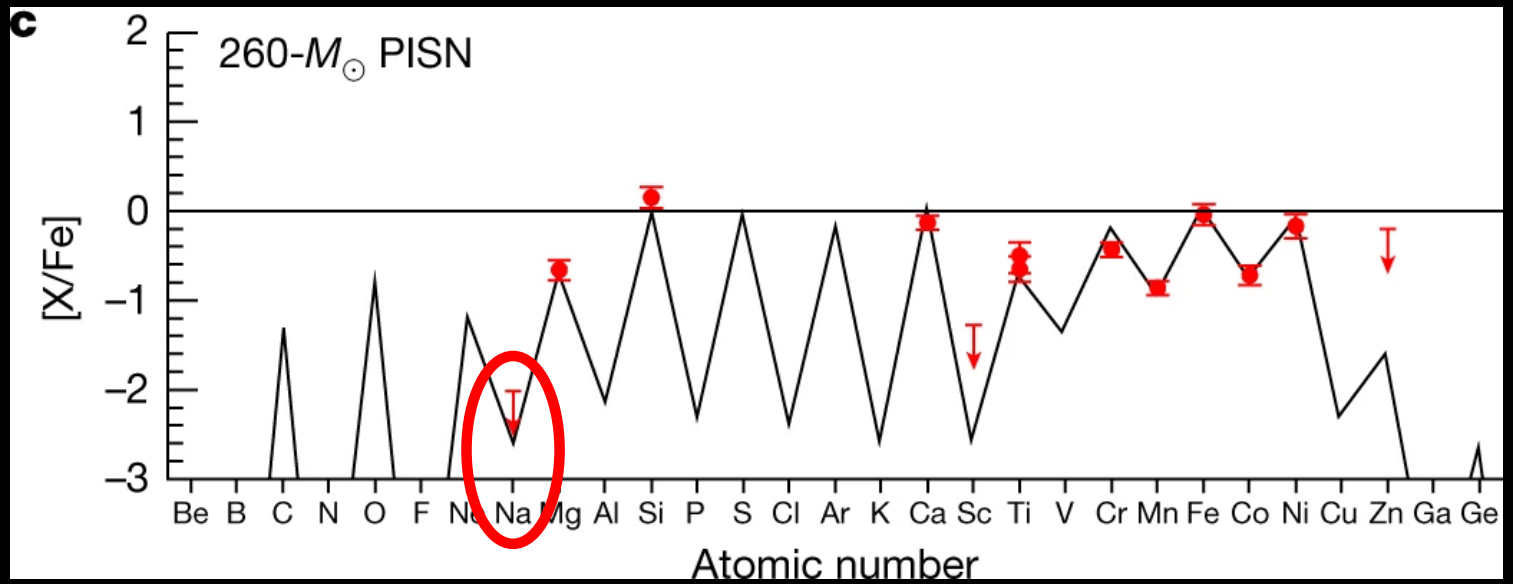
Article | Open access | Published: 07 June 2023

A metal-poor star with abundances from a pair-instability supernova

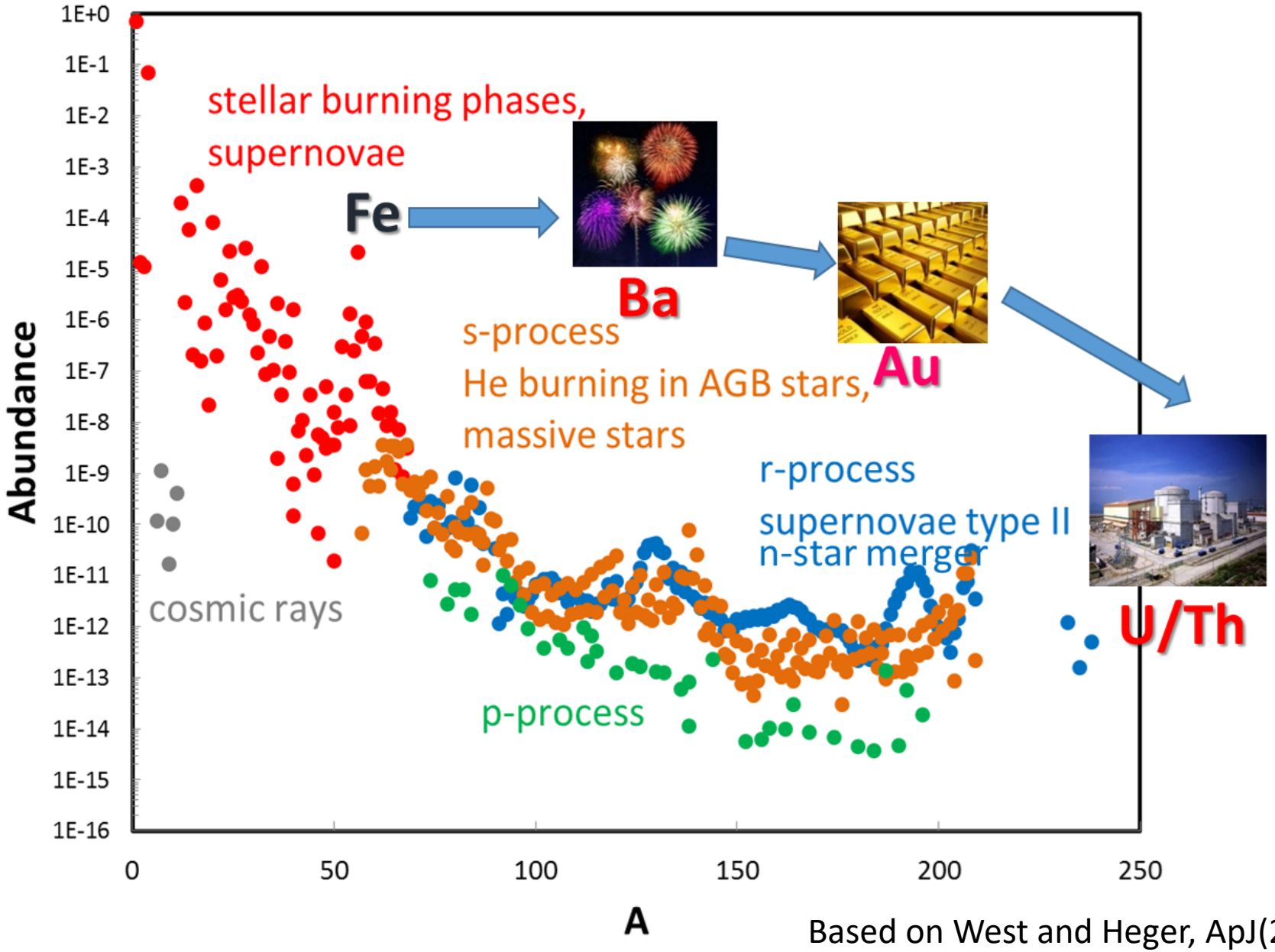
Qian-Fan Xing, Gang Zhao ✉, Zheng-Wei Liu, Alexander Heger, Zhan-Wen Han, Wako Aoki, Yu-Qin Chen, Miho N. Ishigaki, Hai-Ning Li & Jing-Kun Zhao

Nature **618**, 712–715 (2023) | Cite this article

Our rate has been used in KEPLER to predict the production of Na in PISN

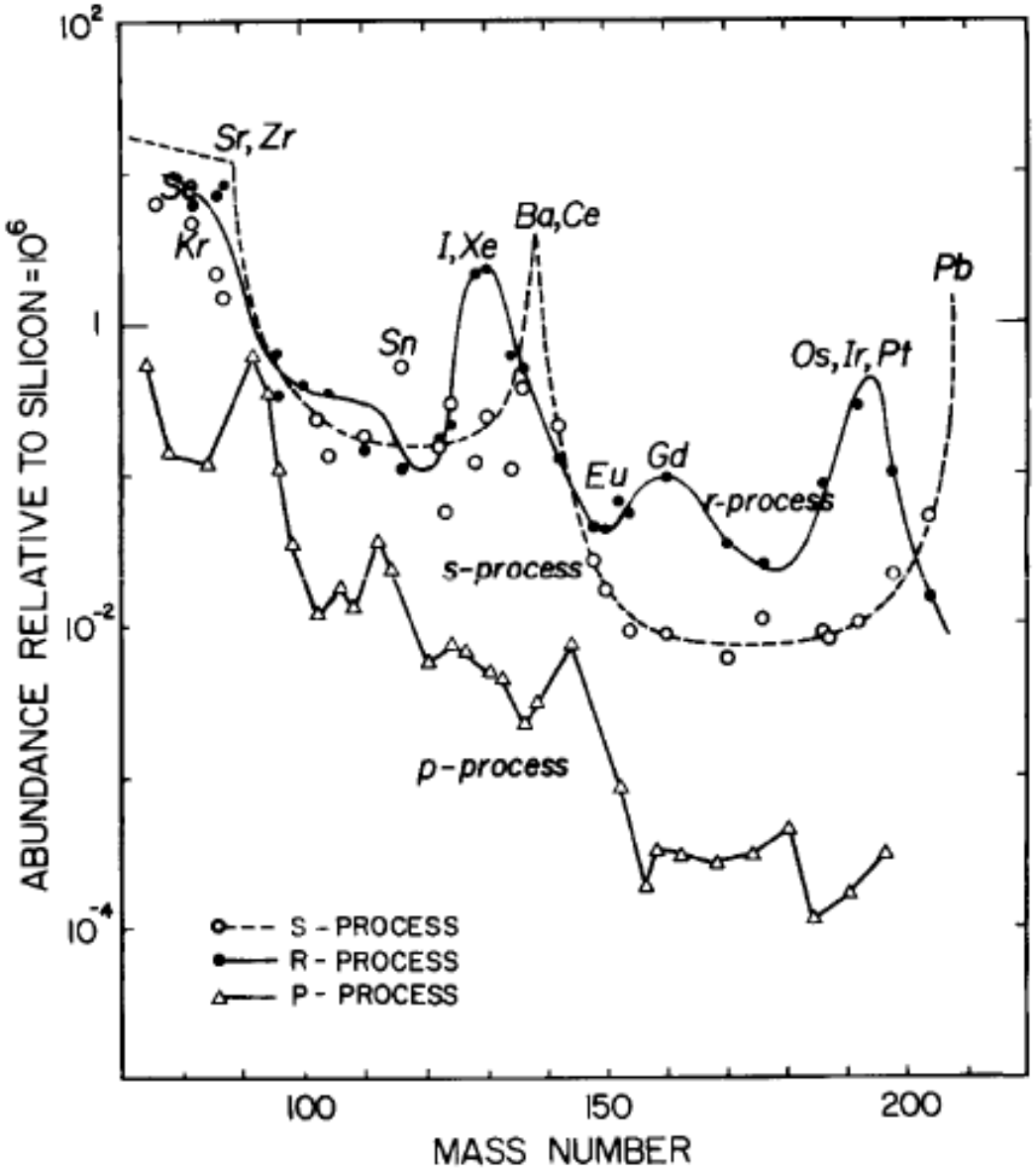


Origin of Heavy elements

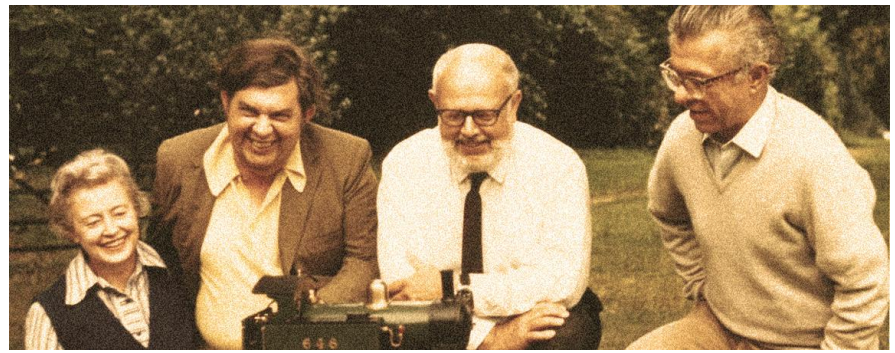


Based on West and Heger, ApJ(2013)

The origin of heavy elements in the solar system



(Pagel, Fig 6.8)

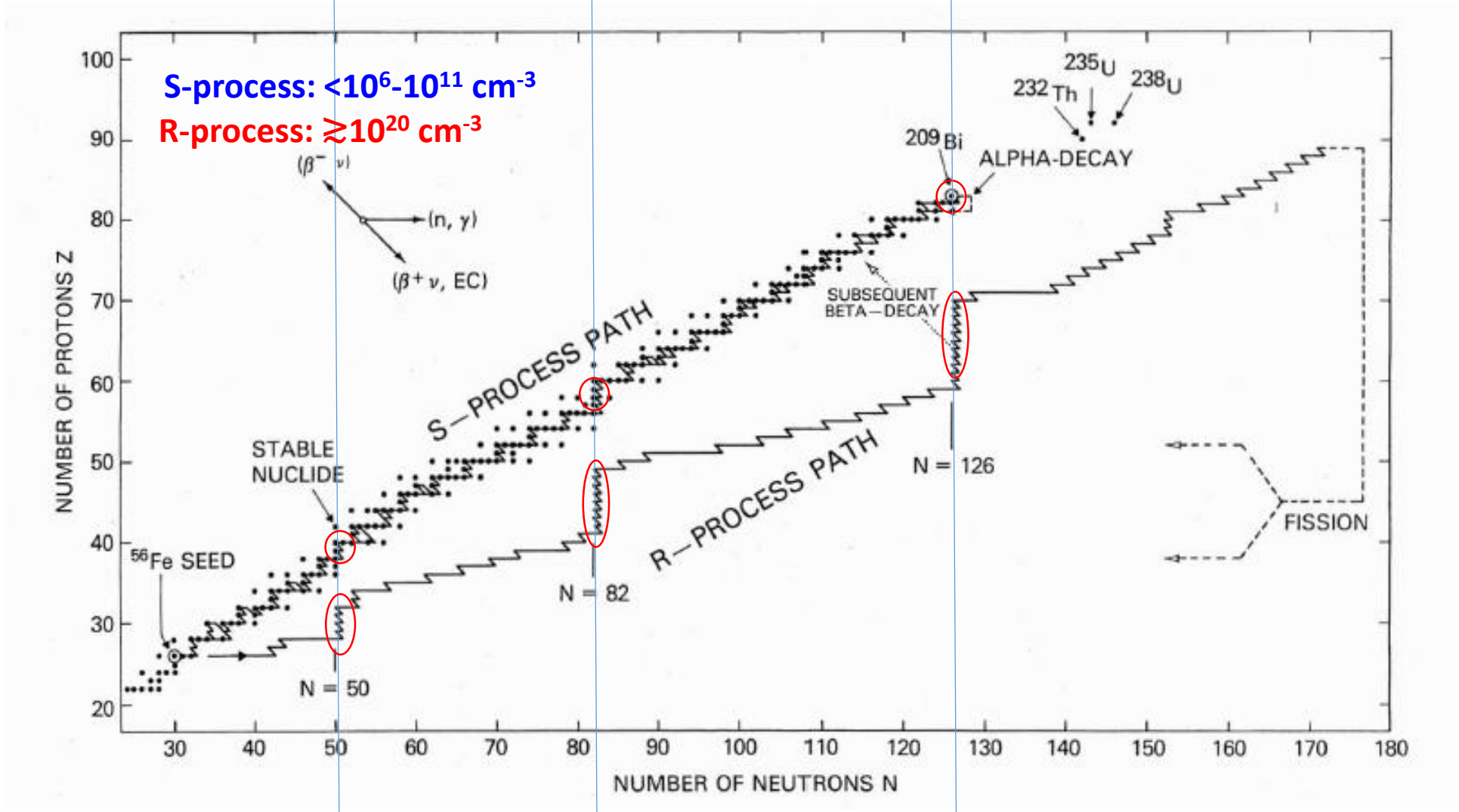


B2FH Synthesis of the Elements in Stars (1957)

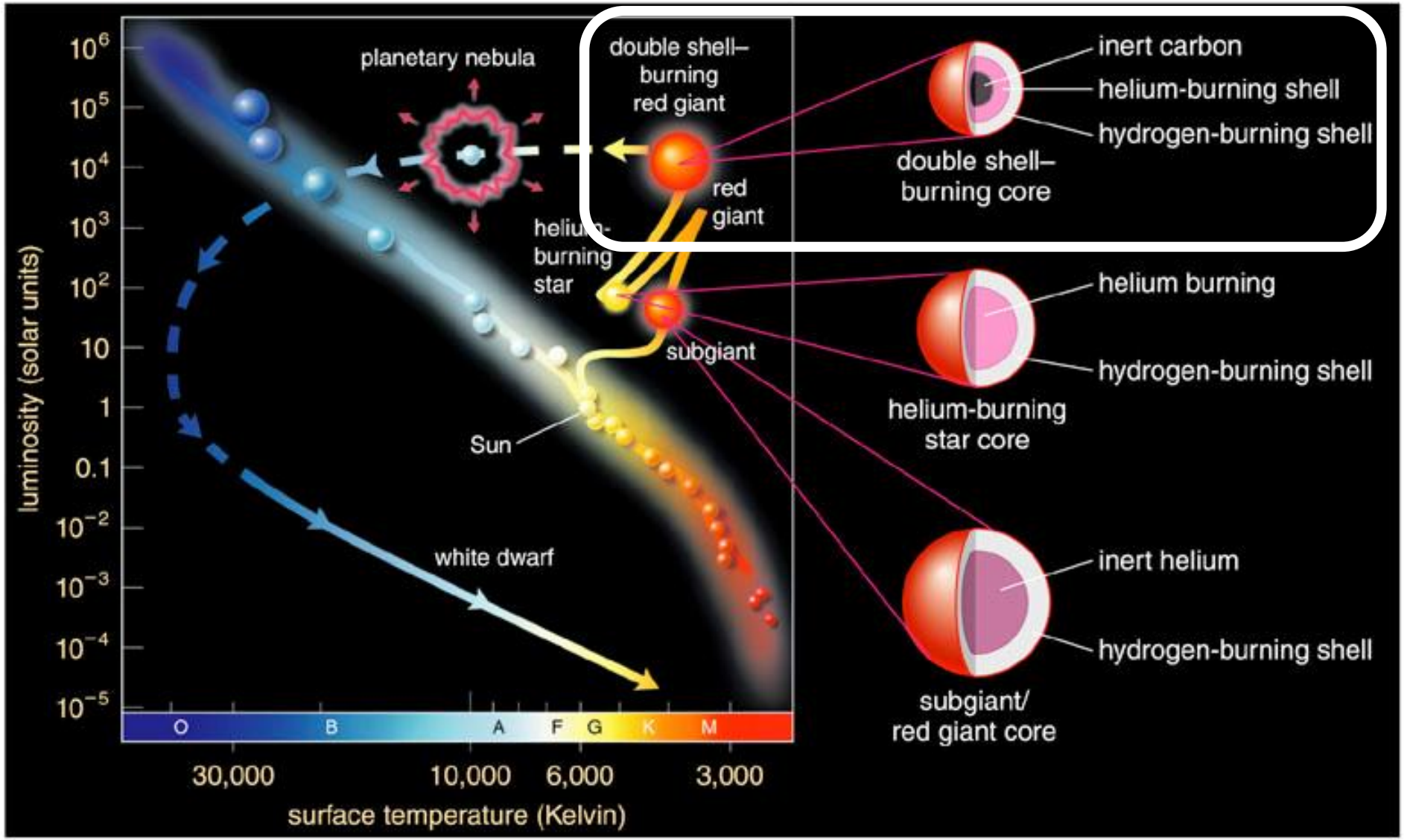


Cameron
Nuclear Reactions in Stars and Nucleogenesis (1957)

each process contribution is a mix of many events !


S-process: <10^6-10^11 cm^-3
R-process: ≳10^20 cm^-3
NUMBER OF PROTONS Z
NUMBER OF NEUTRONS N
(β⁻ ν)
(n, γ)
(β⁺ ν, EC)
S—PROCESS PATH
R—PROCESS PATH
STABLE NUCLIDE
56Fe SEED
N = 50
N = 82
N = 126
209Bi
ALPHA-DECAY
232Th
235U
238U
SUBSEQUENT BETA—DECAY
FISSION

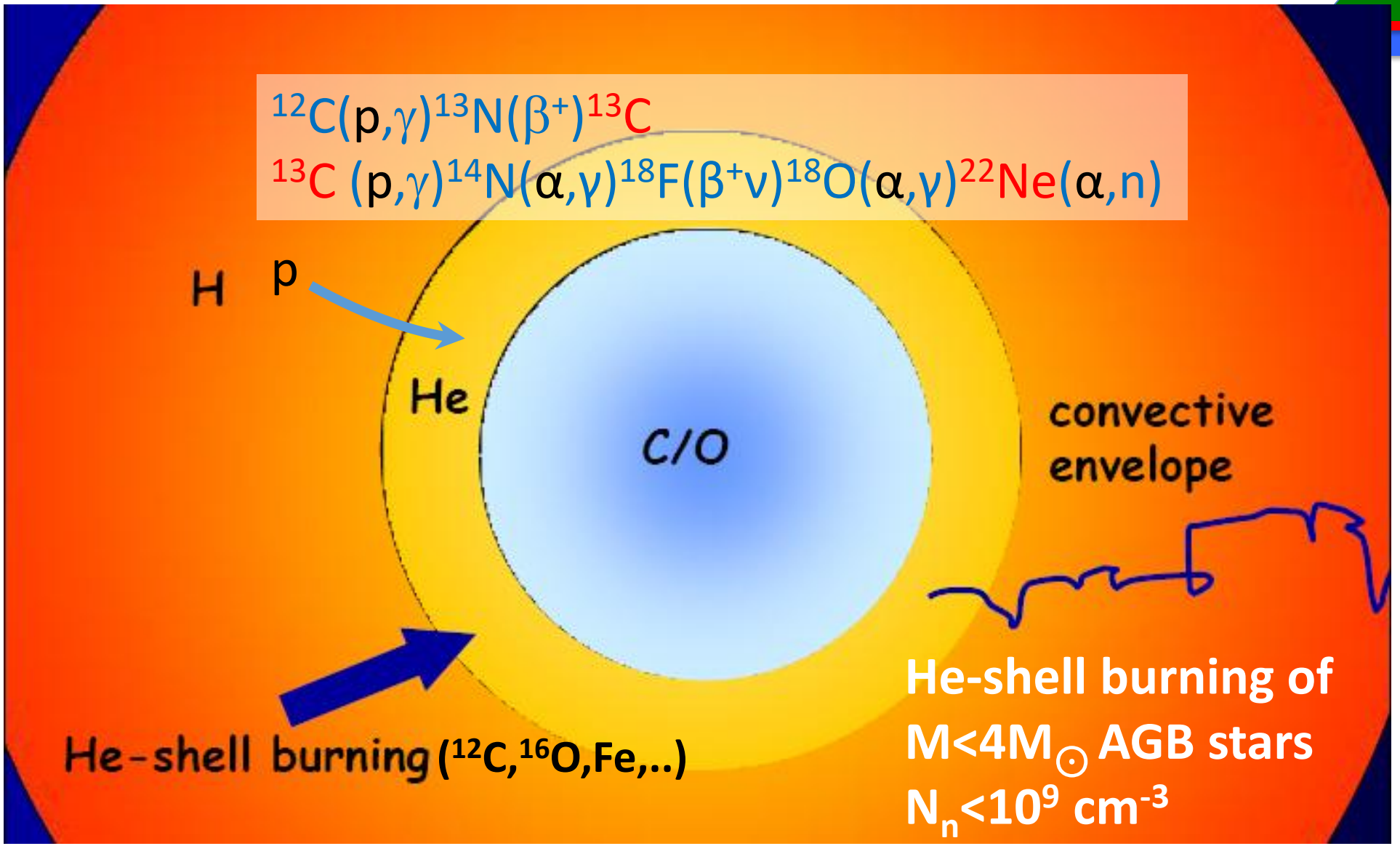
Asymptotic Giant Branch star



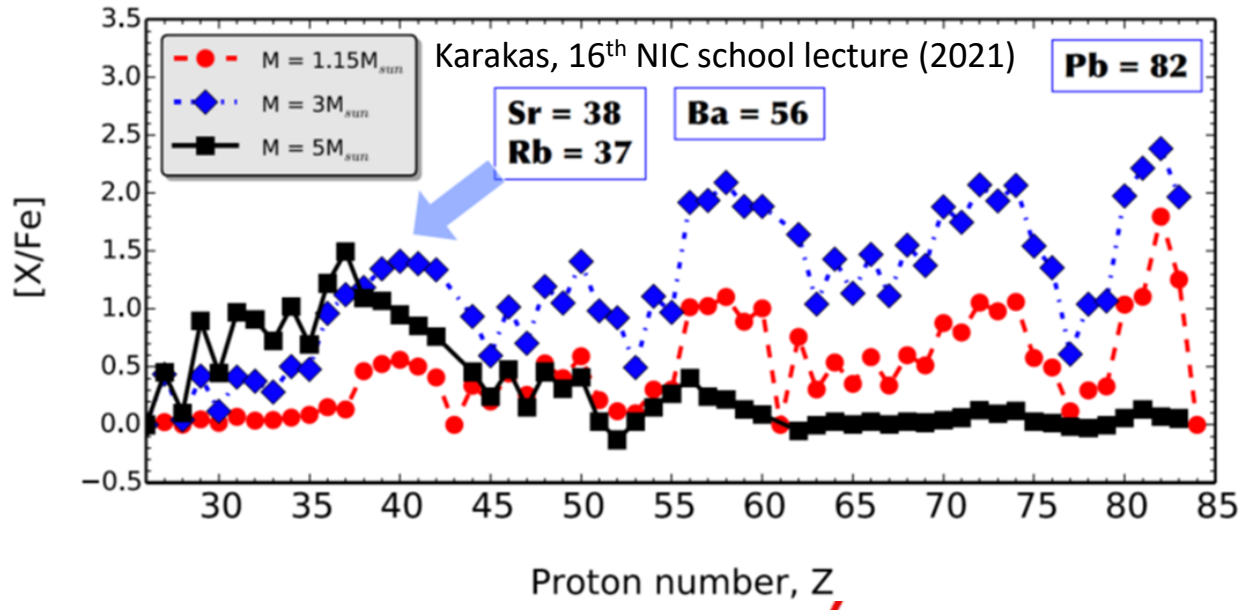
Stars with <10 solar mass go through the asymptotic giant branch (AGB) before becoming white dwarfs.

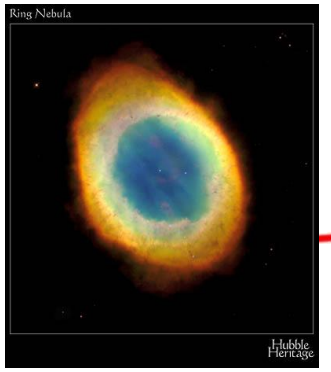
Taken from Lugaro's lecture

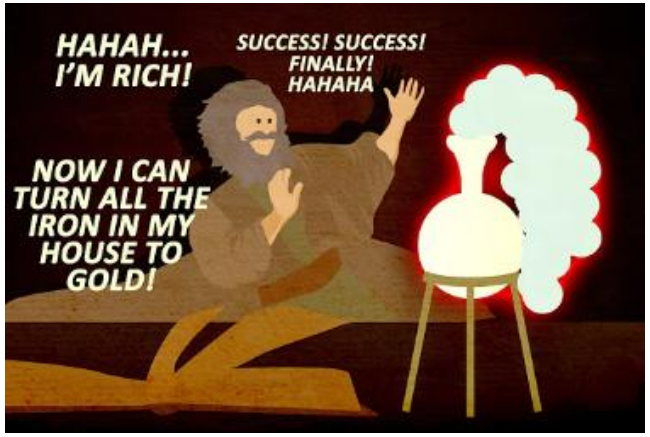
Neutrons in Asymptotic Giant Branch

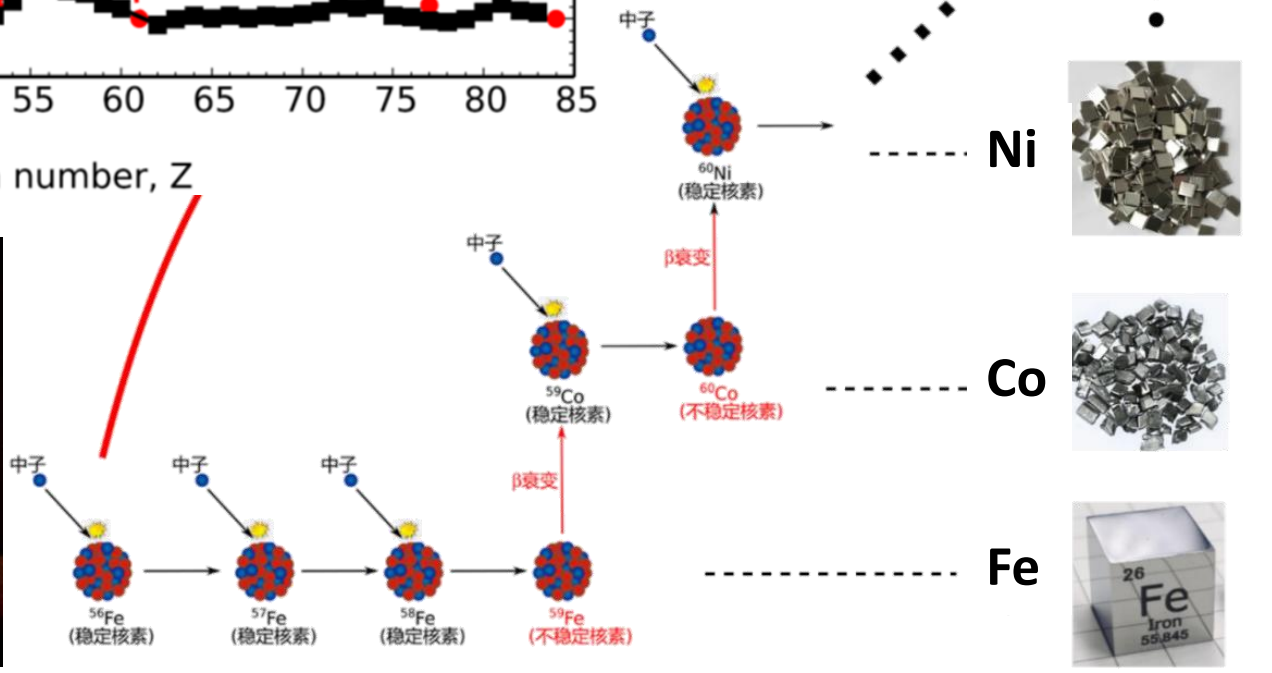


Neutron: Magic Bullet







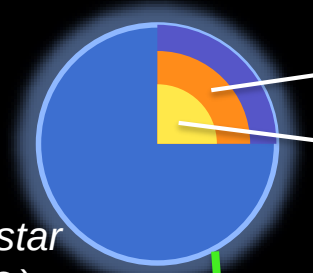


Now I can turn all the iron in my house to gold?

10 billion neutrons → 1E-14 gram gold → 1E-12 USD

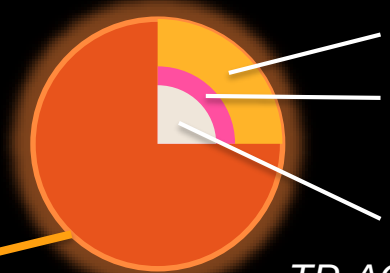
The sites of the s-process

weak s-process: core He/ shell C burning in massive stars

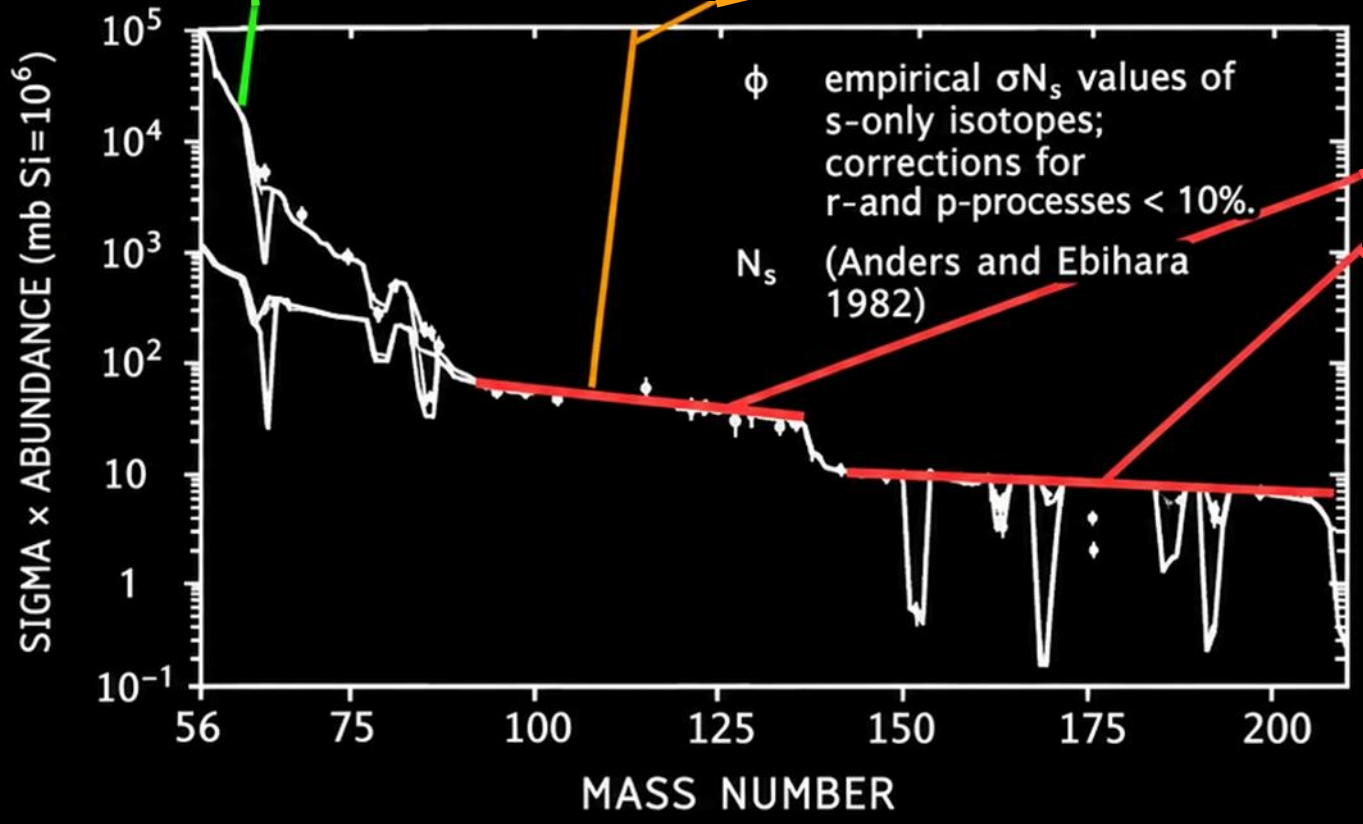


massive star (≳ 8 M⊙)

main s-process: He shell flashes in low mass TP-AGB stars



TP-AGB star (~1–4 M⊙)



approx. steady flow

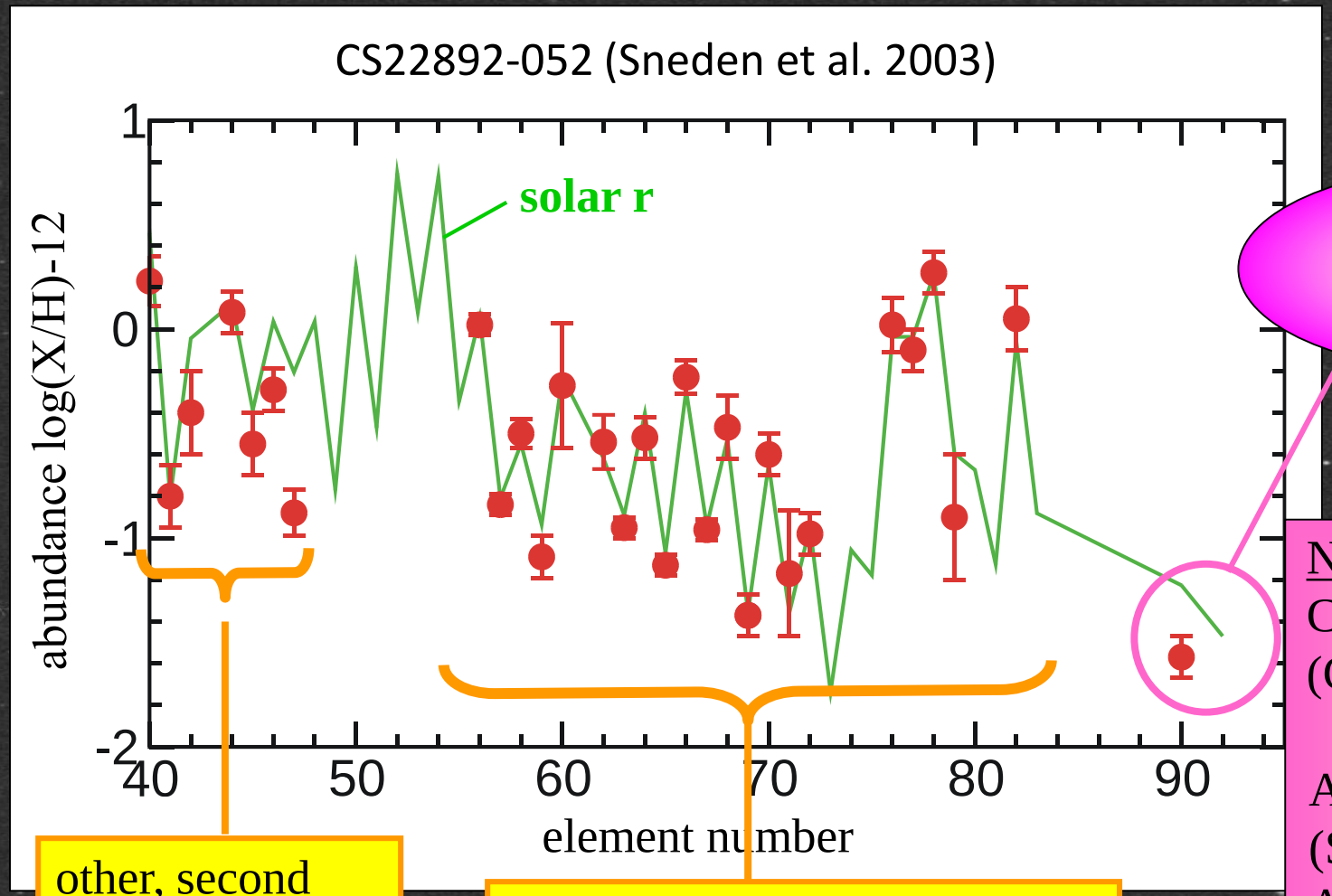
$Y_n \propto Y\sigma_{(n,\gamma)} \approx \text{const}$

↓

can easily interpolate s-contribution for s+r-nuclei **if neutron capture cross sections are known**

Adapted from Schatz's lecture

A single (or a few) r-process event(s)



Cosmo Chronometer

NEW:
CS31082-001 with U
(Cayrel et al. 2001)

Age: 16±3 Gyr
(Schatz et al. 2002
ApJ 579, 626)

other, second r-process to fill this up ?
(weak r-process)

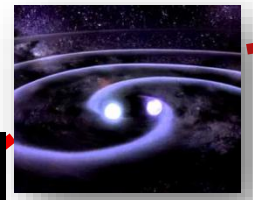
main r-process
matches exactly solar r-pattern
conclusions ?

Adapted from Schatz's lecture

The origin of heavy elements from iron to uranium (rapid neutron capture process)

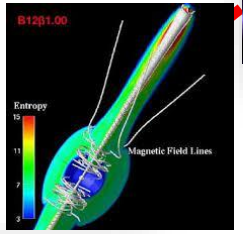
Neutron Density~10^{20} cm^{-3}

- Astrophysics sites?
- Nuclear properties?

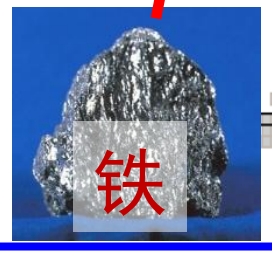


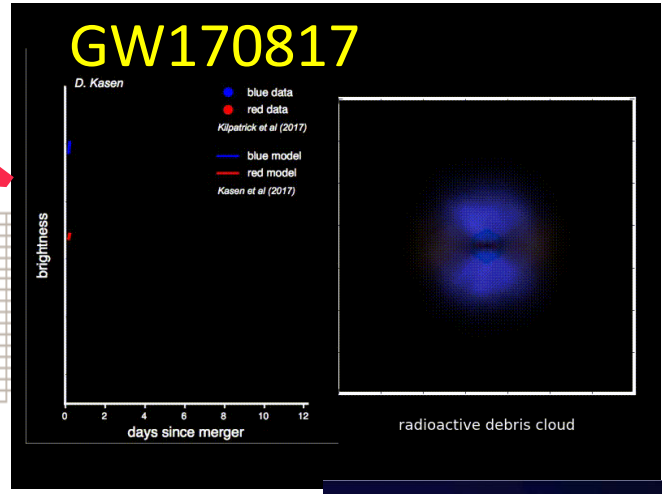


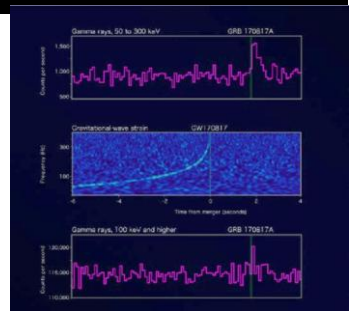










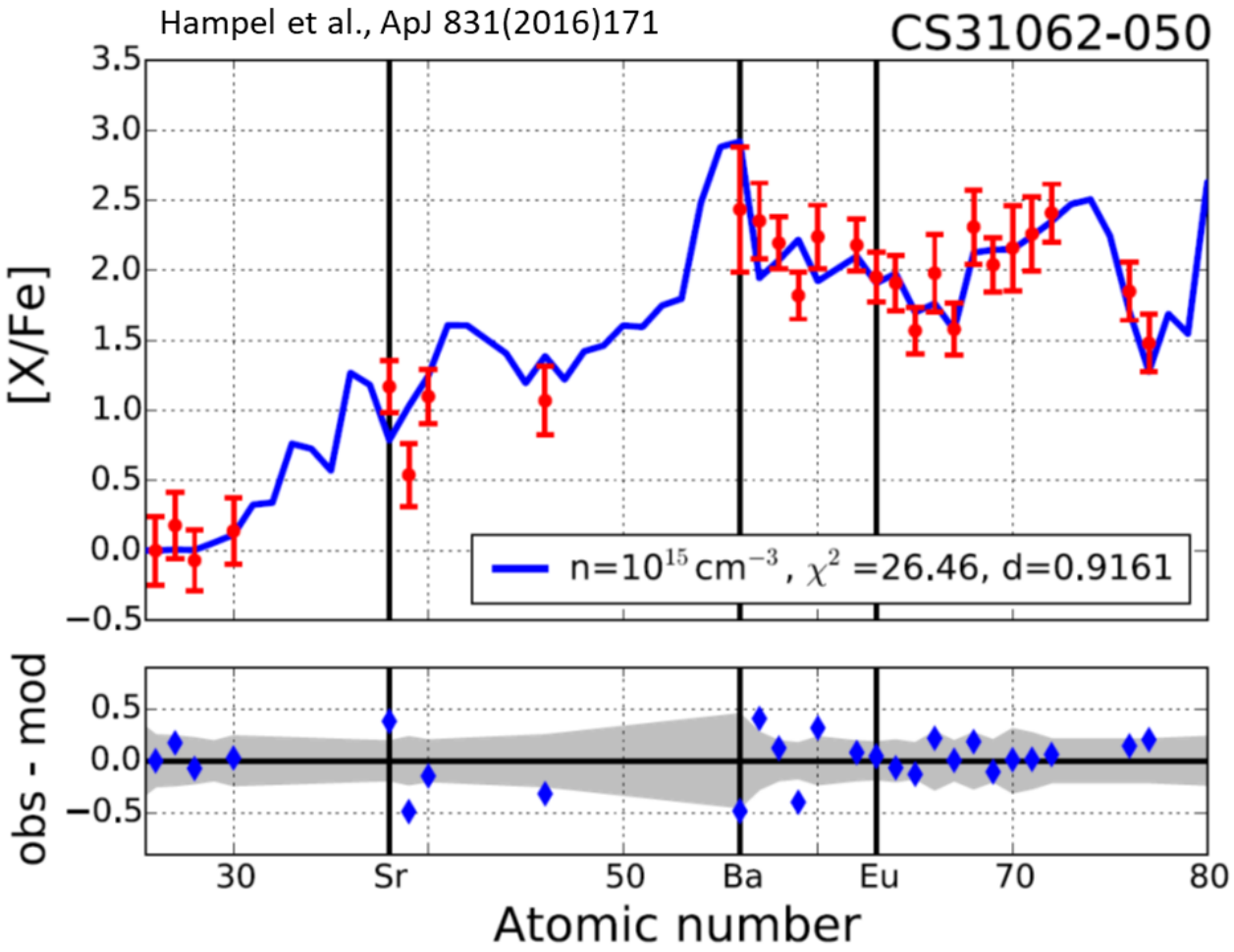


- **Mass**
- **Lifetime**
- Decay branching
- Neutron capture reaction
- Fission **Termination point of r-process**

Experiment+Theory+Observation

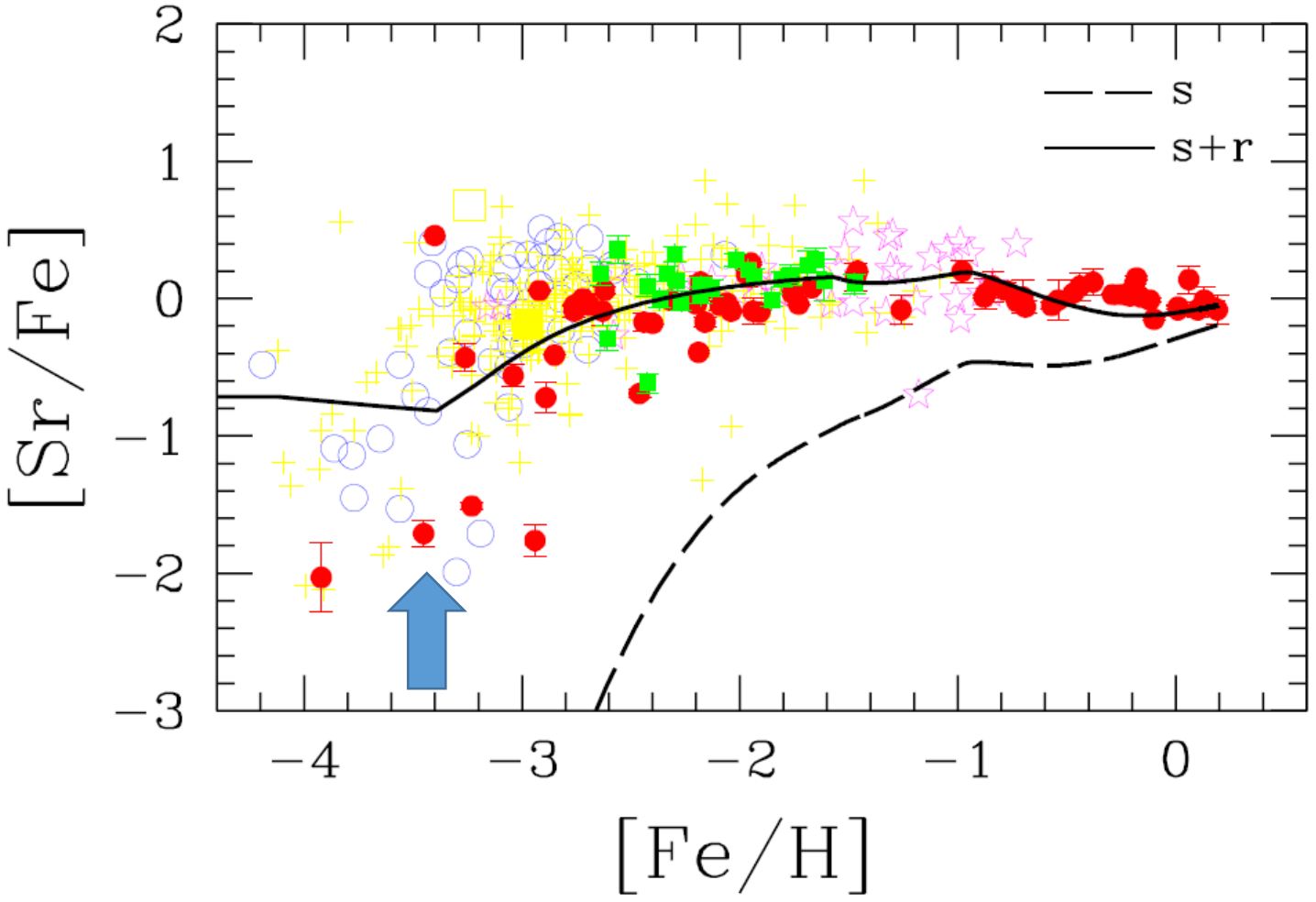
Improving the predictive power of stellar models by eliminating nuclear uncertainties

Carbon-Enhanced Metal-Poor(CEMP) stars



- R-process: $\gtrsim 10^{20}$ cm^{-3} S-process: <10^{6}-10^{11} cm^{-3}
- Intermediate-process (i-process): 10^{13}-10^{16} cm^{-3}
- $^{13}C(\alpha,n)^{16}O$ is the neutron source (AGB? Metal-poor star?...)

Impact on Galactic Chemical Evolution



From Kobayashi, Karakas & Lugaro (2020)

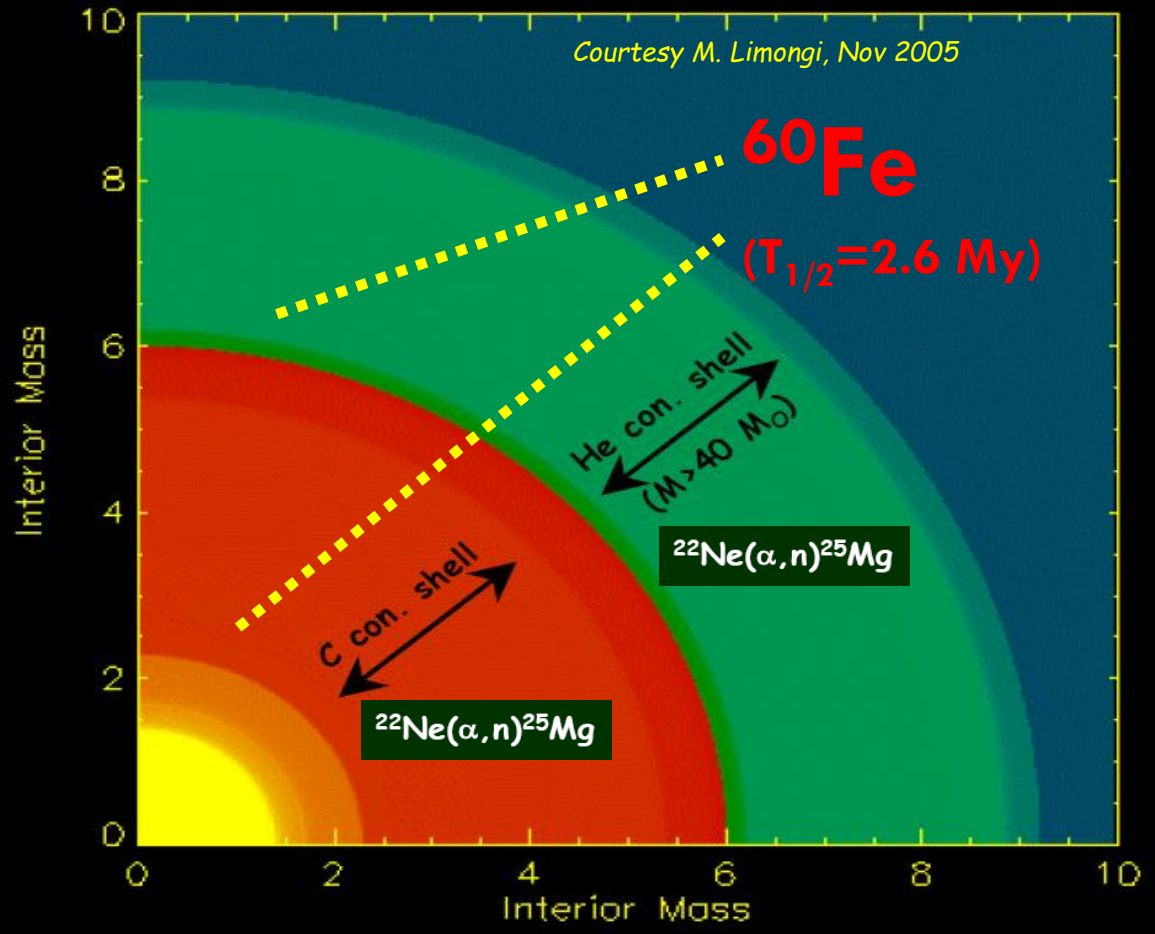
This model matches the solar composition of Sr with yields from s- and r-processes alone.

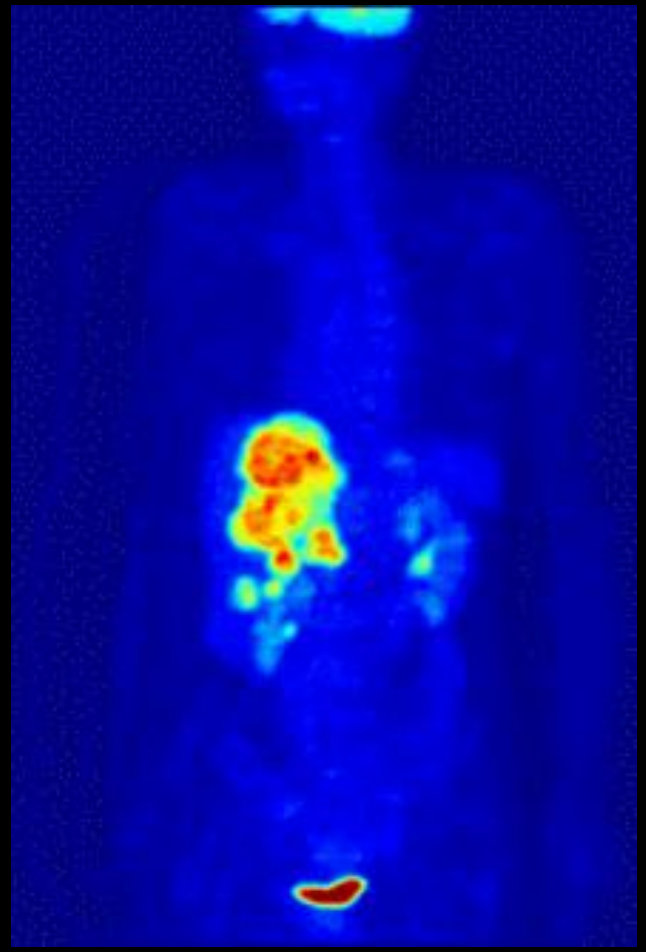
Do we even need an i-process? Maybe, at low metallicities?

Côté et al. 2018 suggests important for the first s-process peak (Sr, Y, Zr)

Taken from Karakas's lecture. 16th NIC school
https://indico.ihep.ac.cn/event/15049/overview

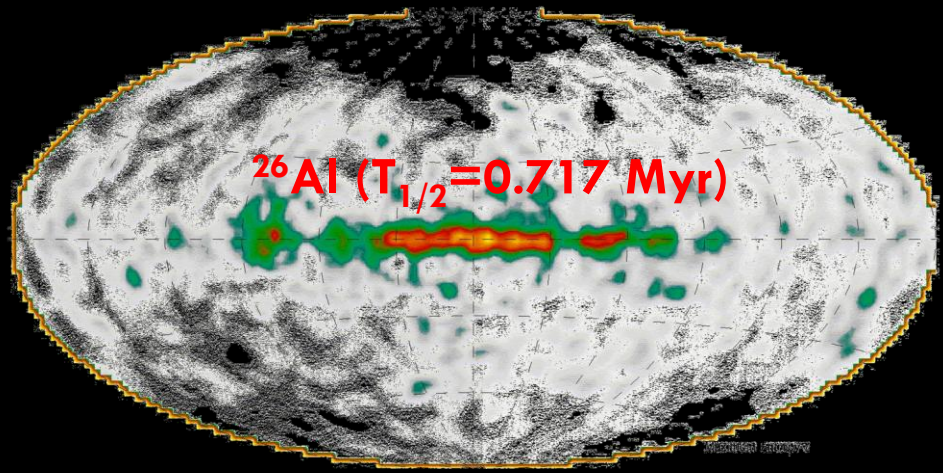
Gamma Ray Astronomy: ^{60}Fe from Supernova

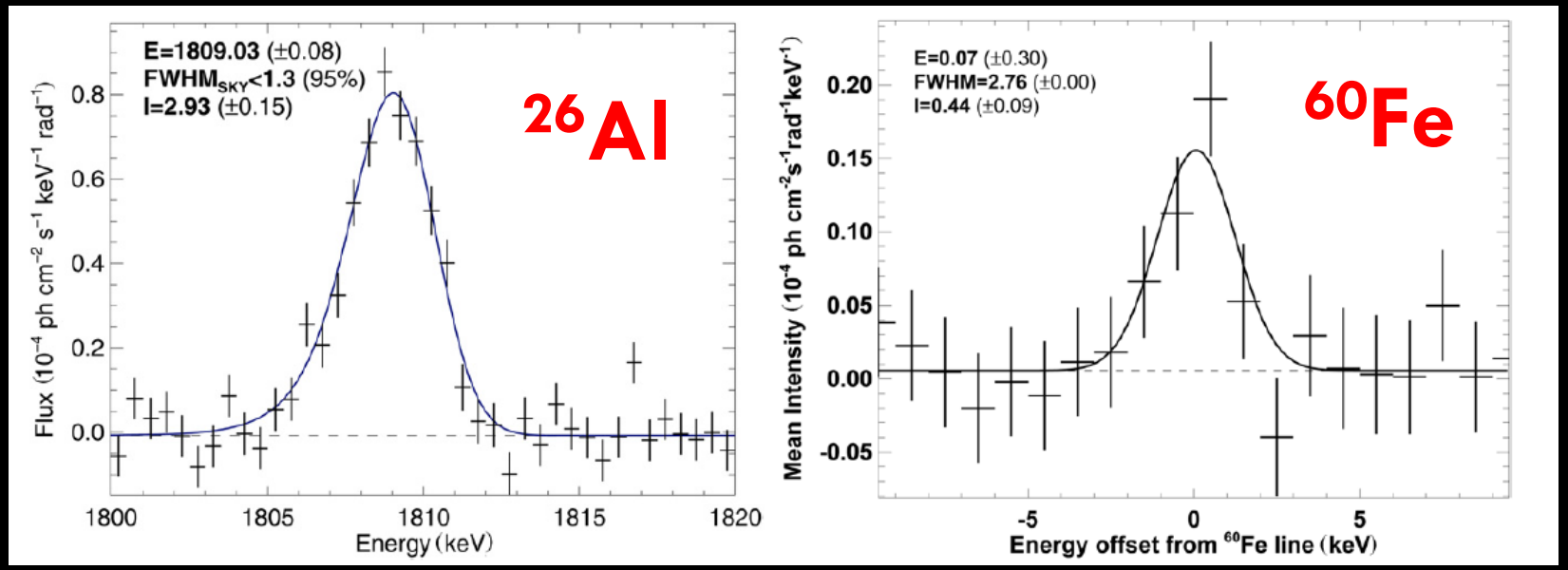




Galactic Radioactivity







Diehl R *et al* 2006 *Astron. Astrophys.* **449** 1025–31 Wang W *et al* 2007 *Astron. Astrophys.* **469** 1005–12

MeV Gamma-Ray Observatory (MeVGRO)
---design and recent development

Courtesy of X.L. Wang (IHEP)

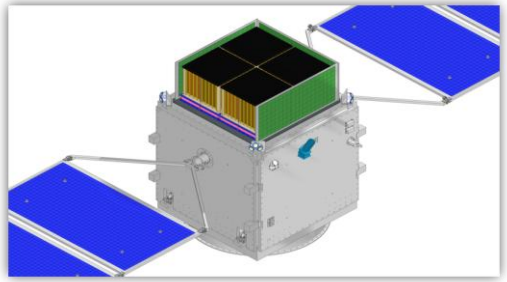
Aim to observe ~0.3~3MeV (extendable to 100 MeV) gamma-rays in wide-field

-Energy spectrum: nuclear lines and continuum

-Imaging

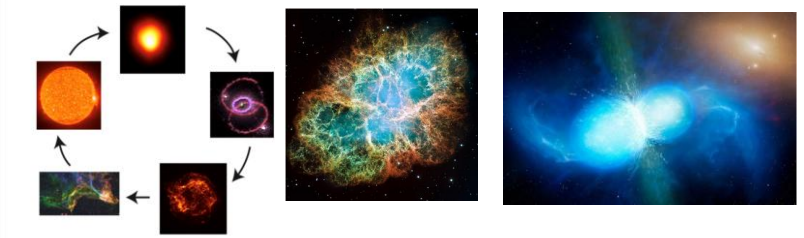
-Timing

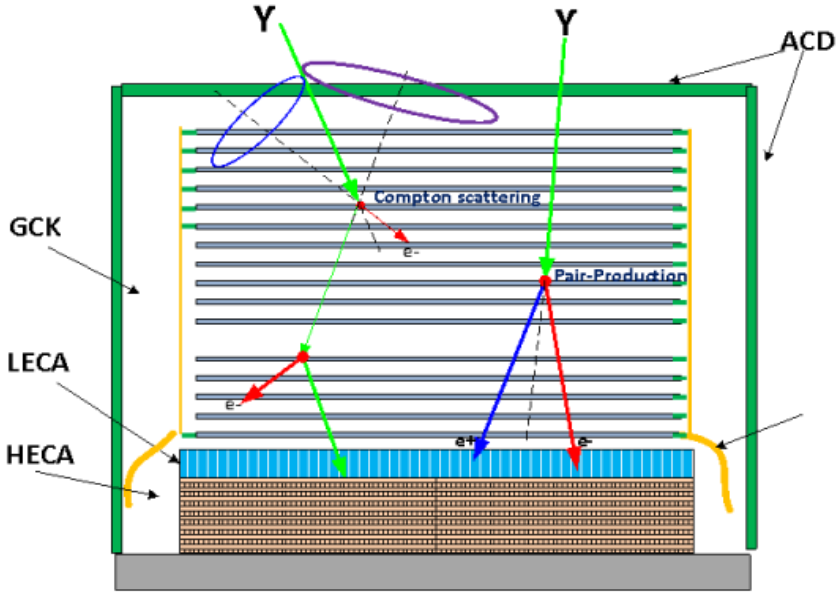
-Polarization

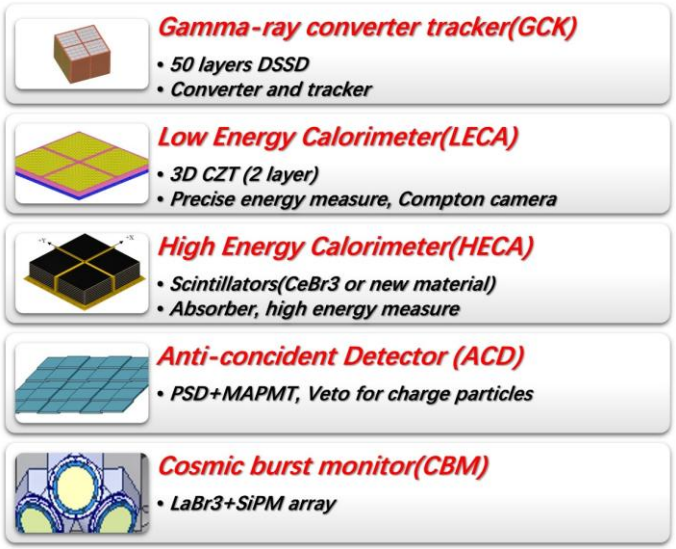


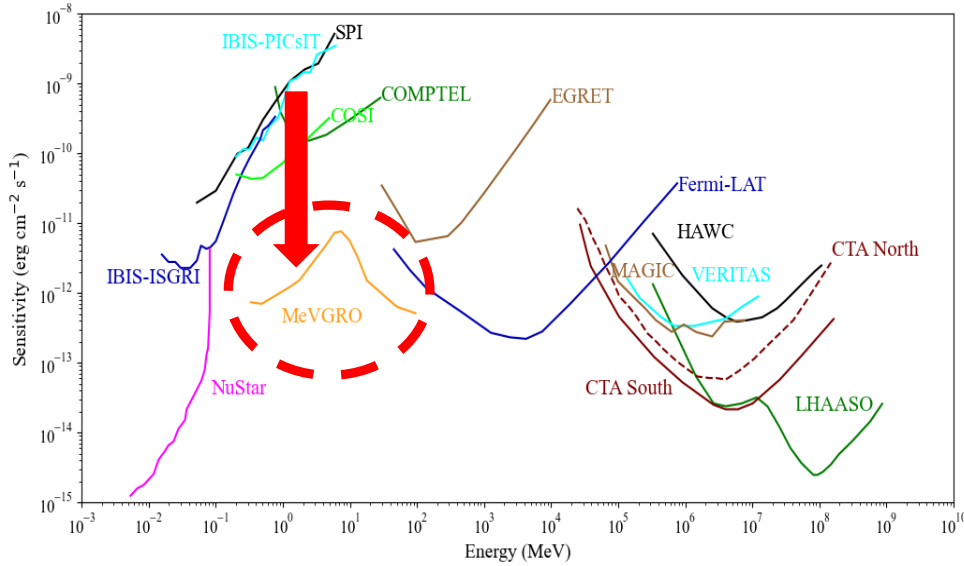
Key Scientific objectives:

1. Exploration of Supernova Explosion Mechanism
2. Tracing Heavy Element Formation and Evolution
3. Indirect Search of Dark Matter









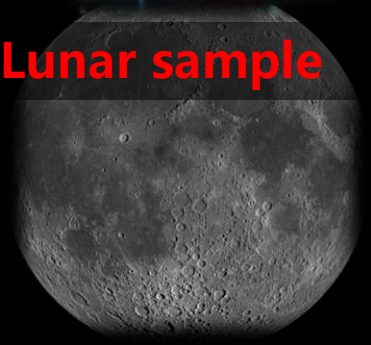
^{60}Fe found on Earth!



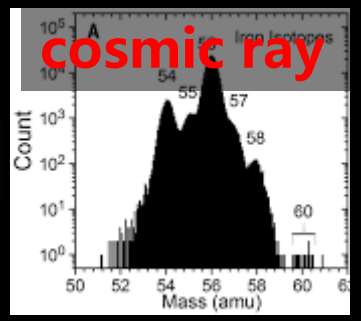
Ice sample Antarctica



Lunar sample

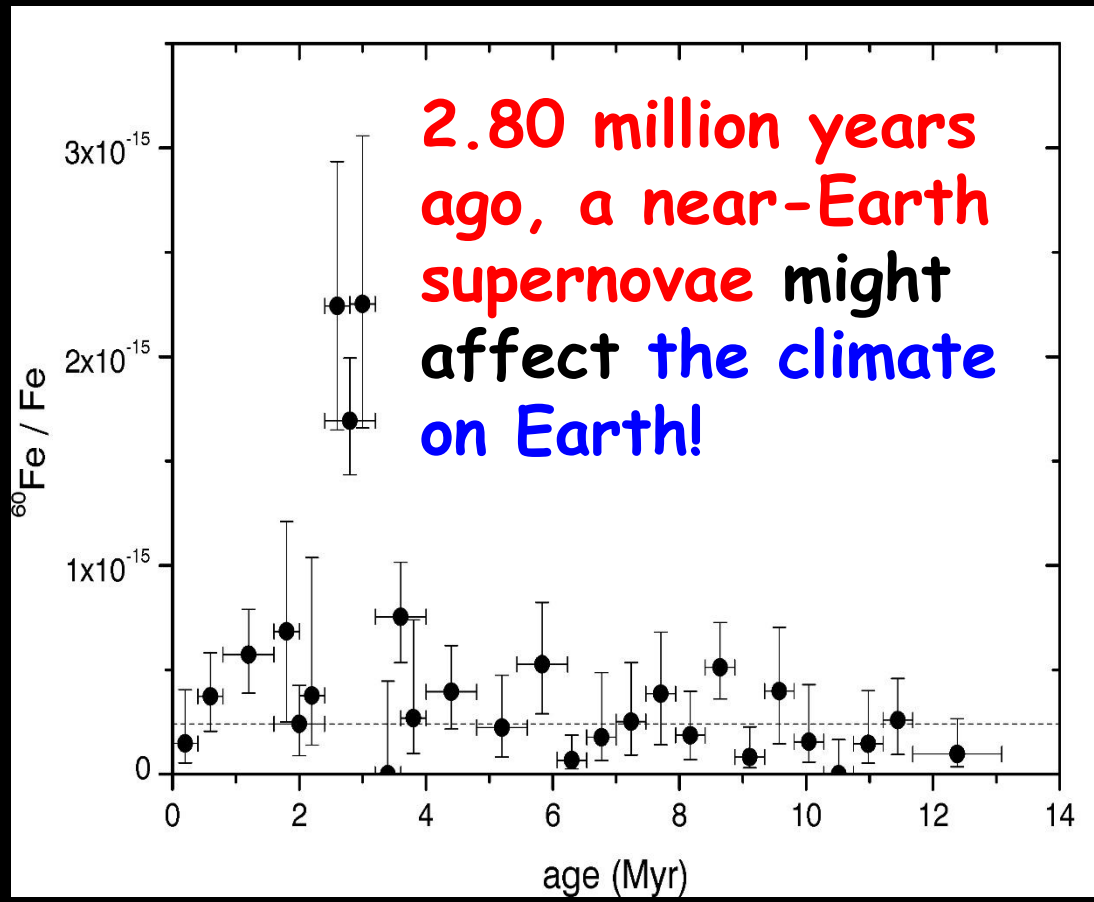


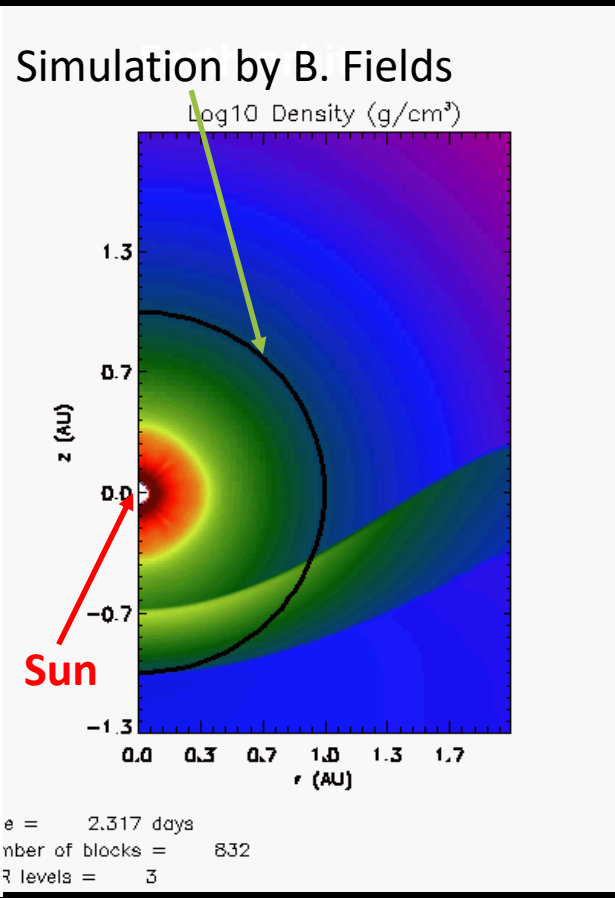
cosmic ray



Deep Sea Crust







A. Wallners doi:10.1038/nature17196

Knie, K. et al. Phys. Rev. Lett. 93, 171103 (2004); Fimiani, L. et al., Phys. Rev. Lett. 116, 151104 (2016); Breitschwerdt et al., Nature(2016); Wallner et al., Nature(2016)



First humans lived 2.8 million years ago, jawbone shows

5 March 2015 Last updated at 15:19 GMT

BBC

Scientists have found a jawbone that they say proves the first humans were alive much earlier than we thought.

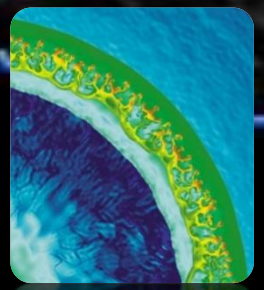
$^{60}Fe/^{26}Al$ abundance puzzle

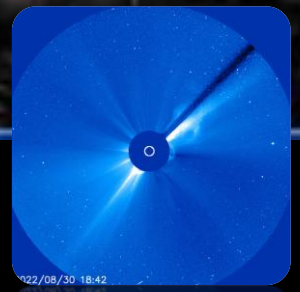
Prediction : $^{60}Fe/^{26}Al$ = 0.45
Observation: $^{60}Fe/^{26}Al$ = 0.15±0.04

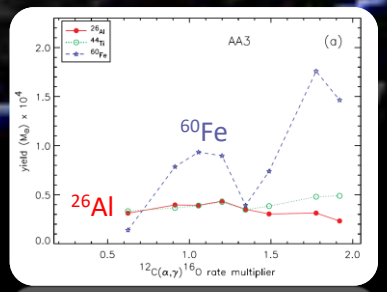
Model Ingredients:

- Initial Mass Function and birth rate
- **Stellar evolution (nuclear reactions,** convection, mixing…**)**
- Stellar Wind Model(s) (Mass loss during evolution)
- **Nucleosynthesis Yields (depends on nuclear physics)**
- **Explodability (explode as SNe or collapse to black holes)**





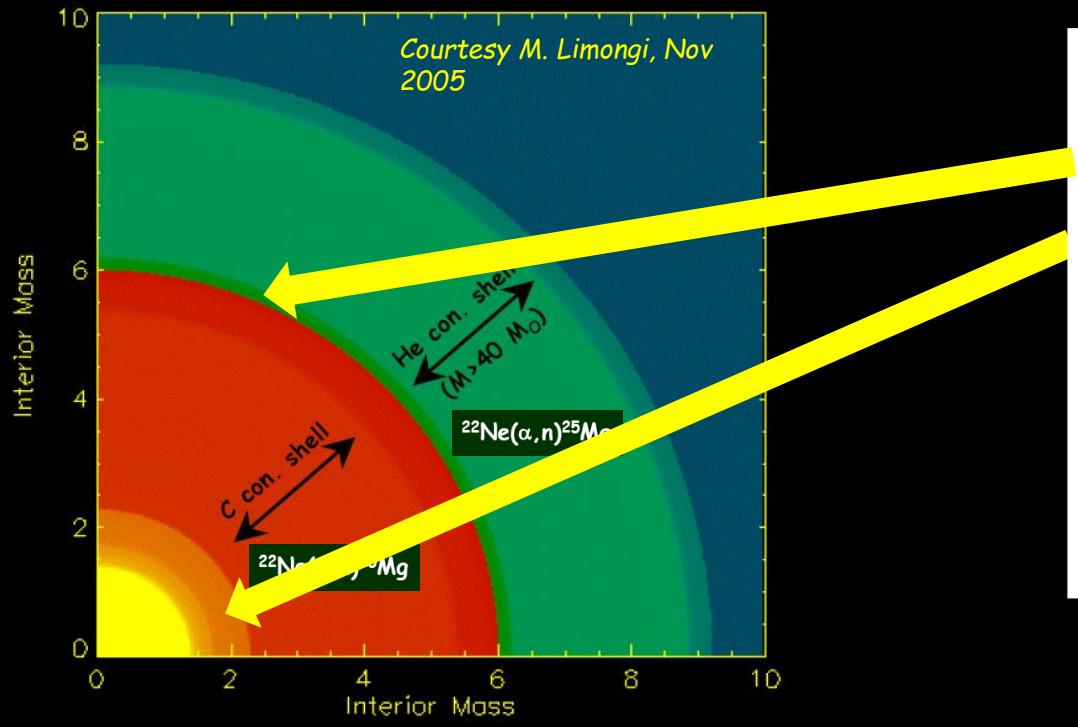


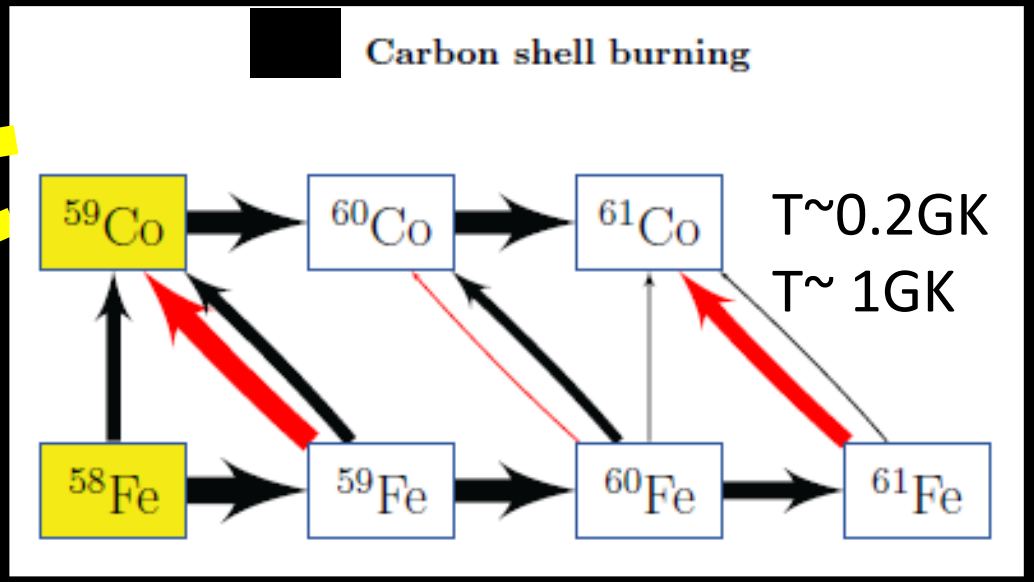




Diehl, Lugaro, Heger, Sieverding, Tang et al., PASA (2021), 38, e062

^{60}Fe nucleosynthesis



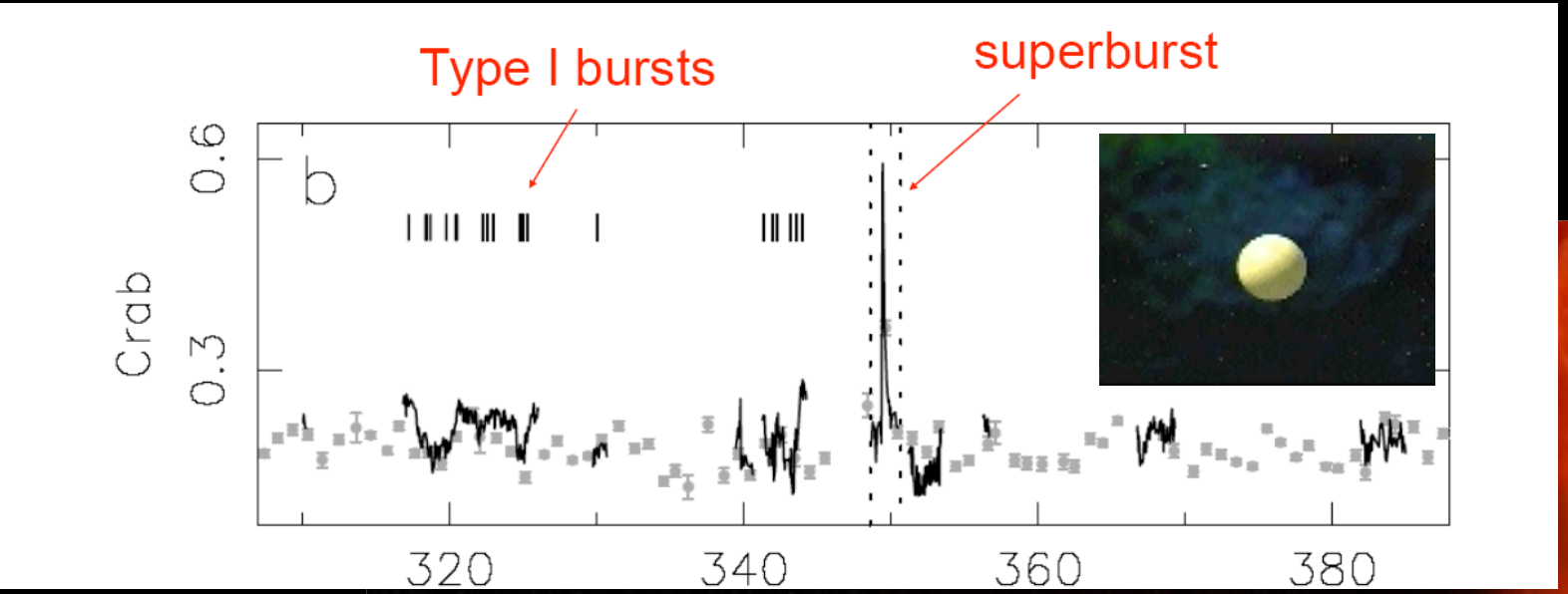


Calculation using NUNET; Flux in log scale

Important nuclear reactions or decays

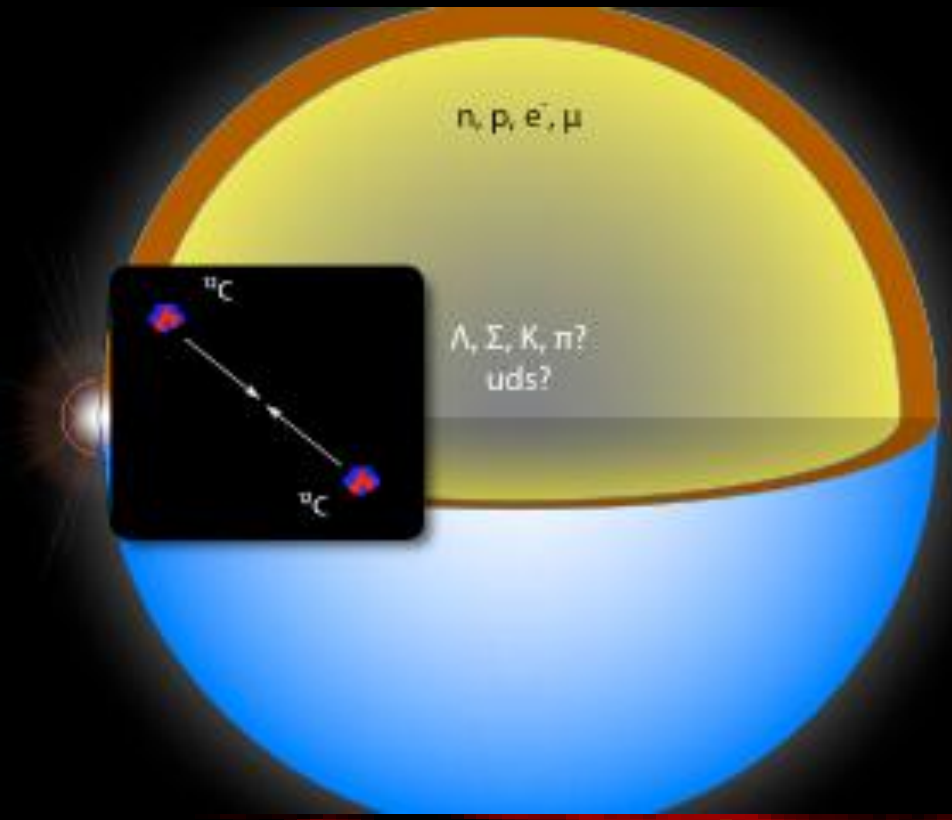
- Neutron sources: ^{22}Ne(α,n)^{25}Mg
- Stellar decay rate of ^{59}Fe (Ground state decay 44.5 days + Excited state decay)
- ^{12}C(α,γ)^{16}O, ^{12}C+^{12}C, ^{59}Fe(n,γ), ^{60}Fe(n,γ)

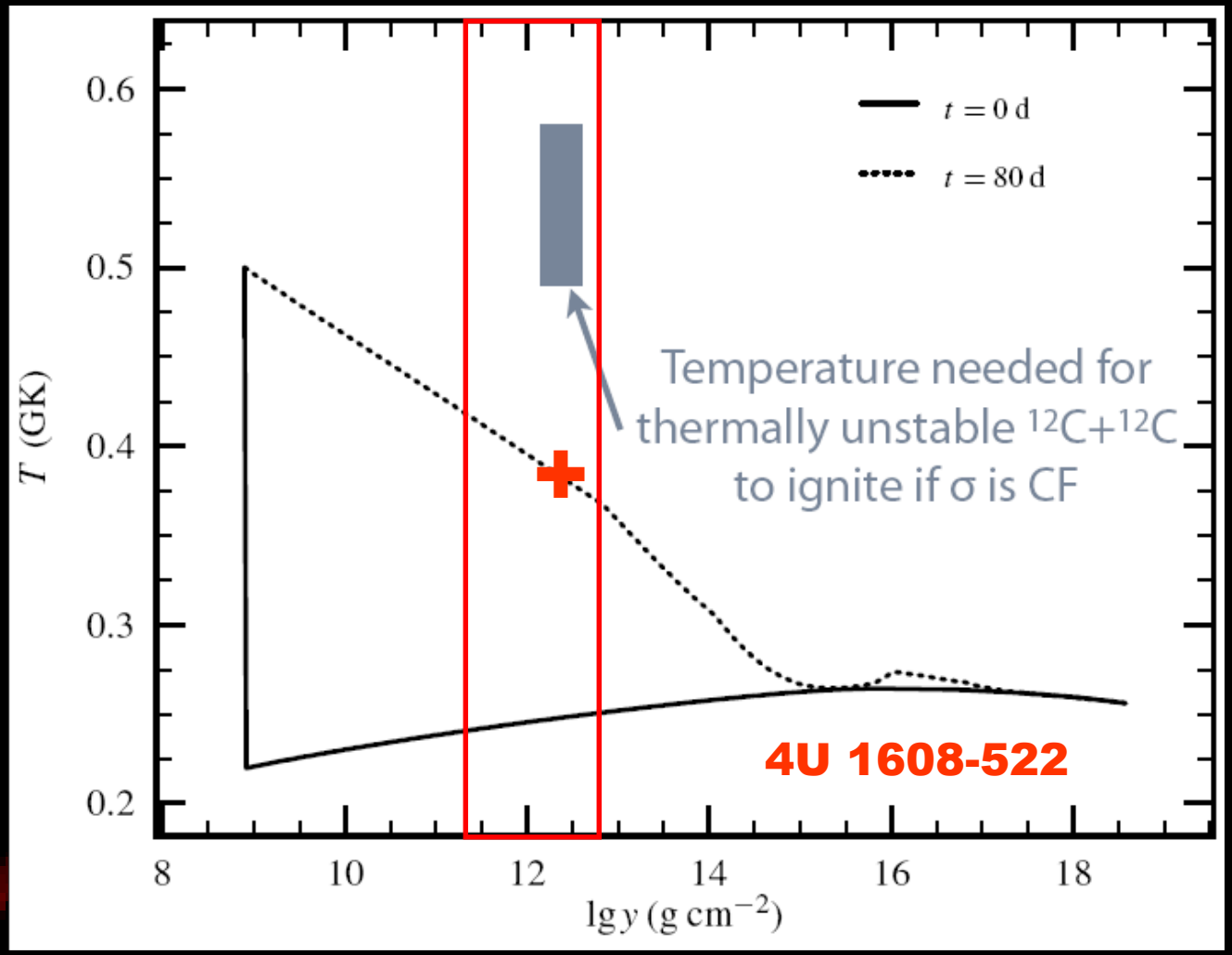
Diehl, Lugaro, Heger, Sieverding, Tang et al., PASA (2021), 38, e062



credits: NASA/CXC/M. WEISS

How does the carbon fusion reaction to trigger the explosion?





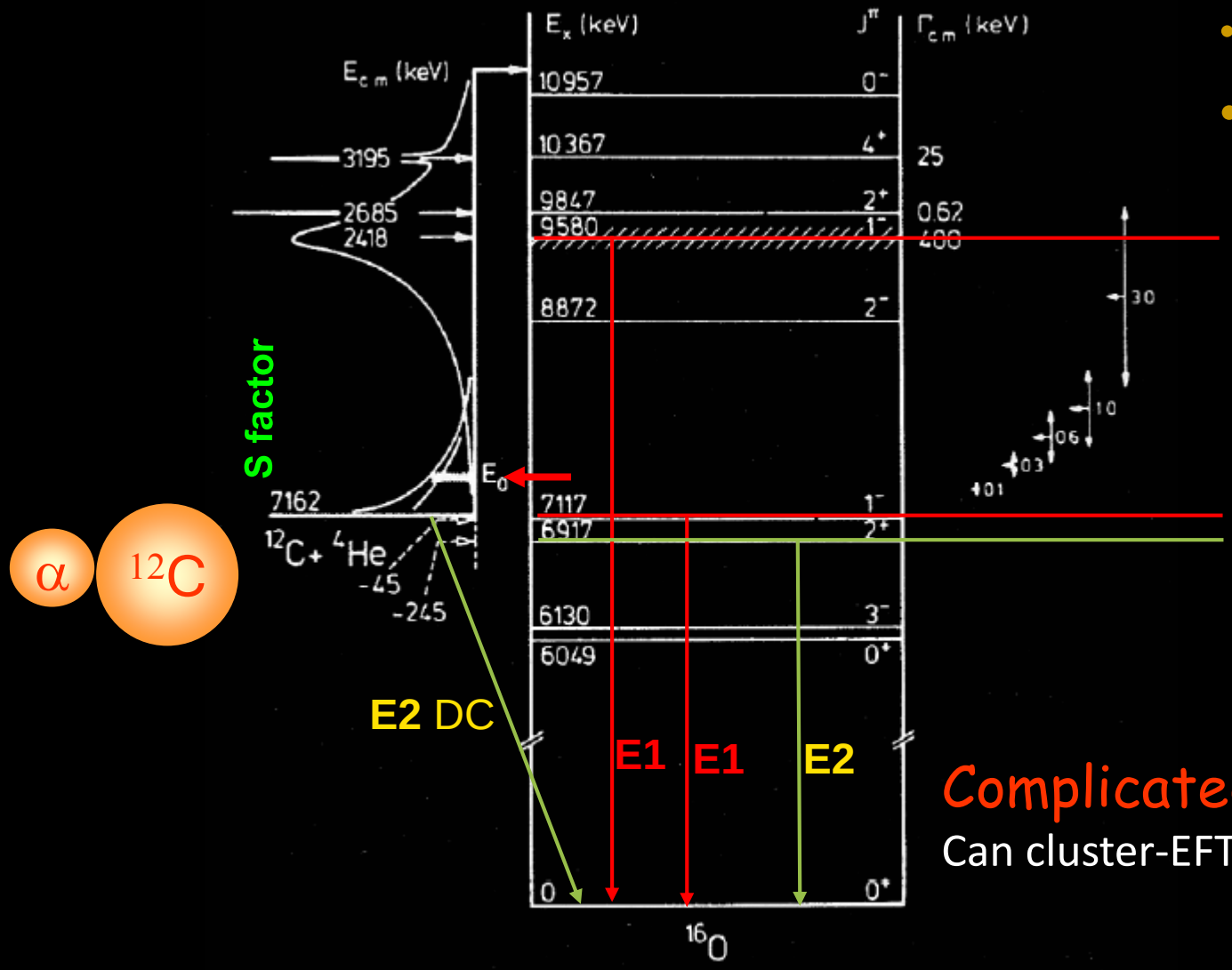
(MSU)

Keek et al. (2007), Astron. & Astrophys. 479: 177
Cooper, Steiner and Brown, ApJ (2009)

How to get precise reaction rates?

- $^{12}C(\alpha,\gamma)^{16}O$
- $^{12}C+^{12}C$

Level Scheme of ^{16}O



- **3 resonances**
- **1 direct capture**

resonance
(high lying)

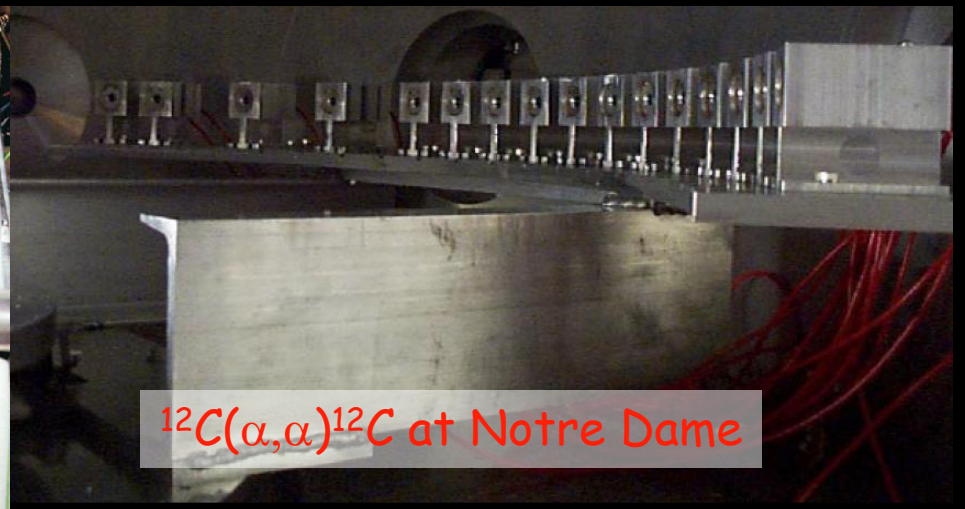
resonance
(sub threshold)

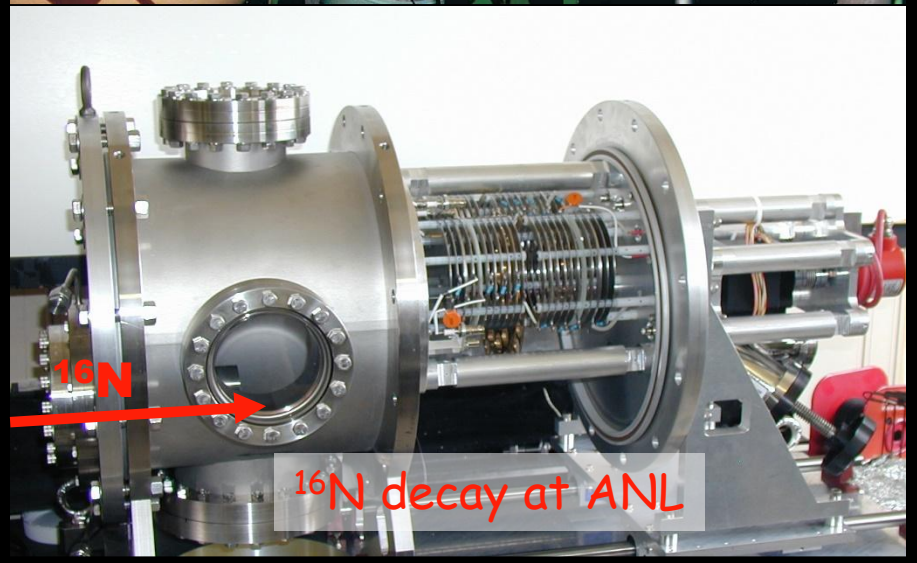
resonance
(sub threshold)

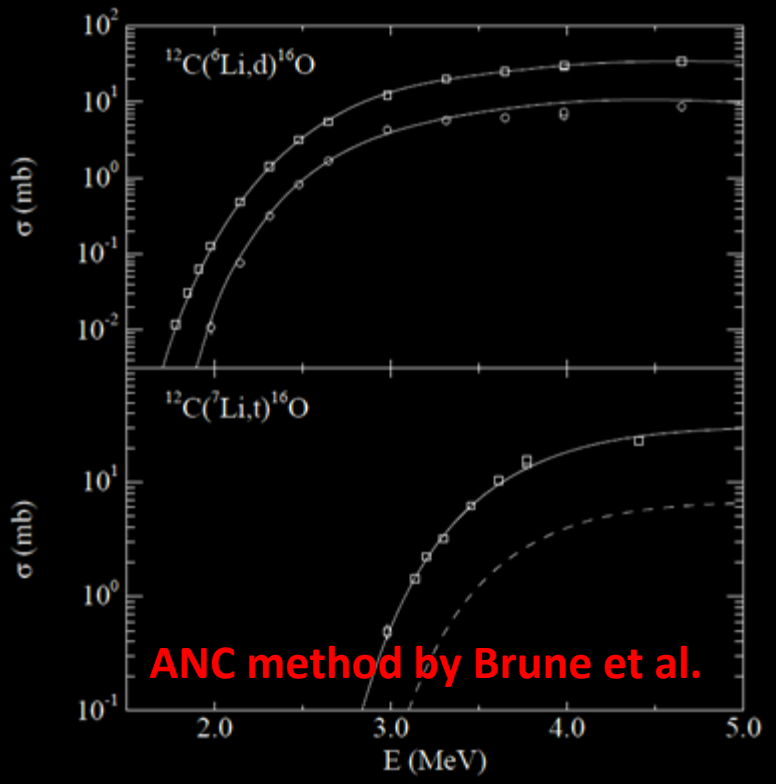
Complicated reaction mechanism

Can cluster-EFT predict the sign of interference?

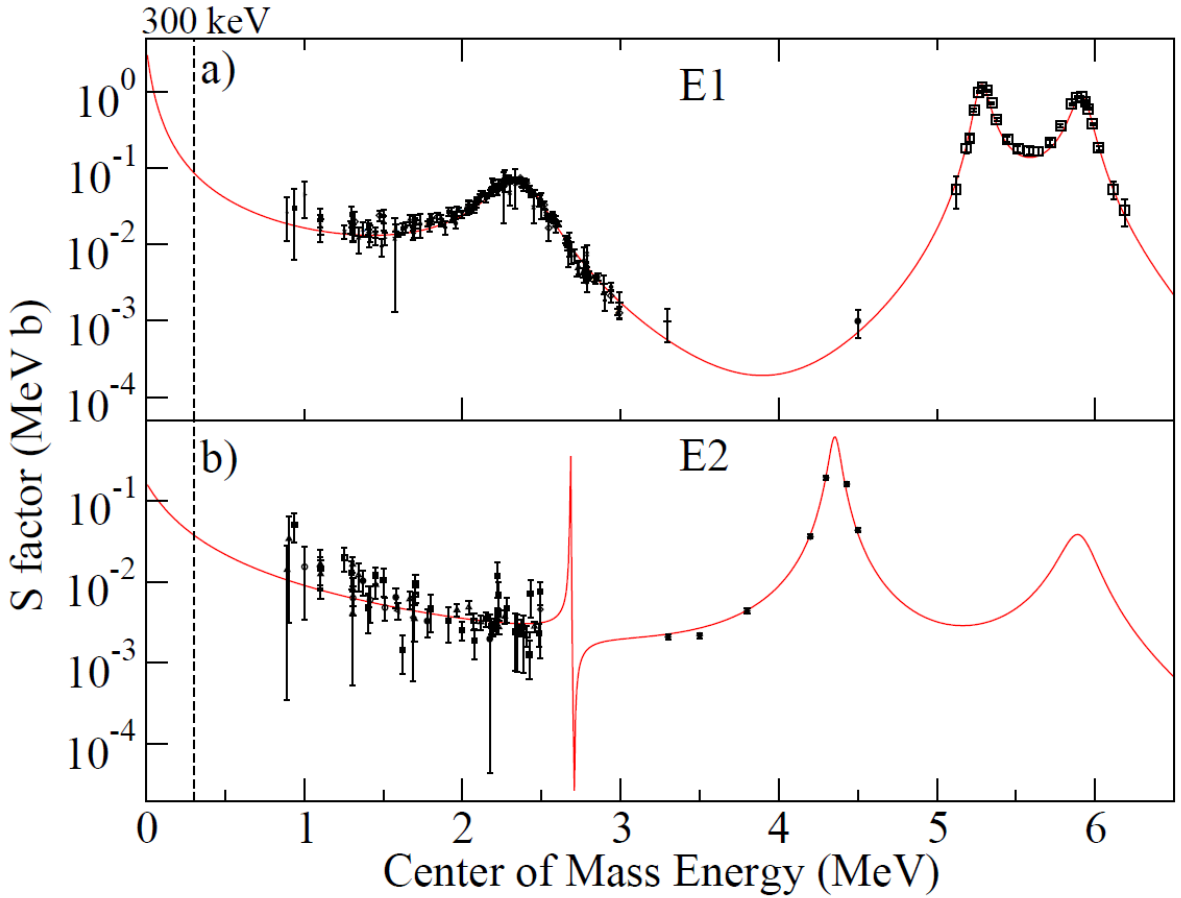

0.5 mA α
$^{12}C(\alpha,\gamma)^{16}O$ at Stuggart

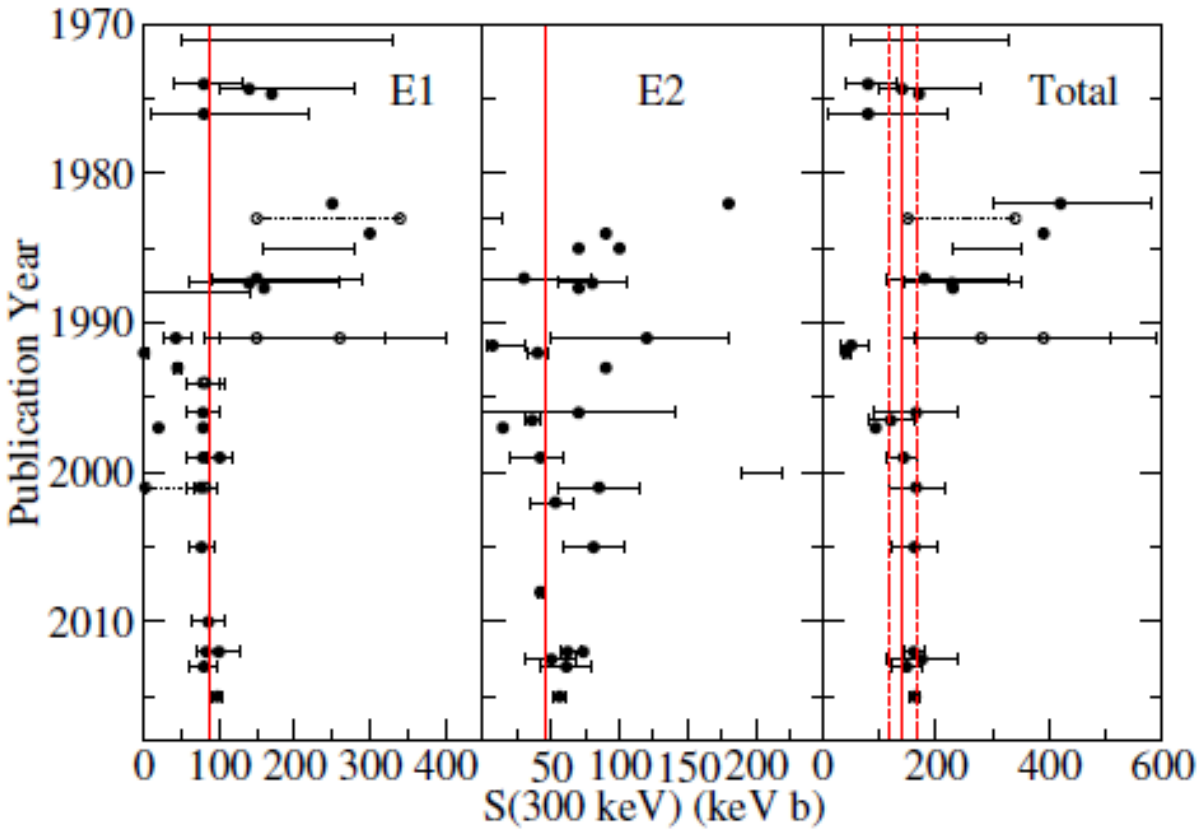

$^{12}C(\alpha,\alpha)^{12}C$ at Notre Dame


^{16}N
^{16}N decay at ANL


$^{12}C(^{6}Li,d)^{16}O$
$^{12}C(^{7}Li,t)^{16}O$
σ (mb)
E (MeV)
ANC method by Brune et al.

Recommended S factor of $^{12}C(\alpha,\gamma)^{16}O$





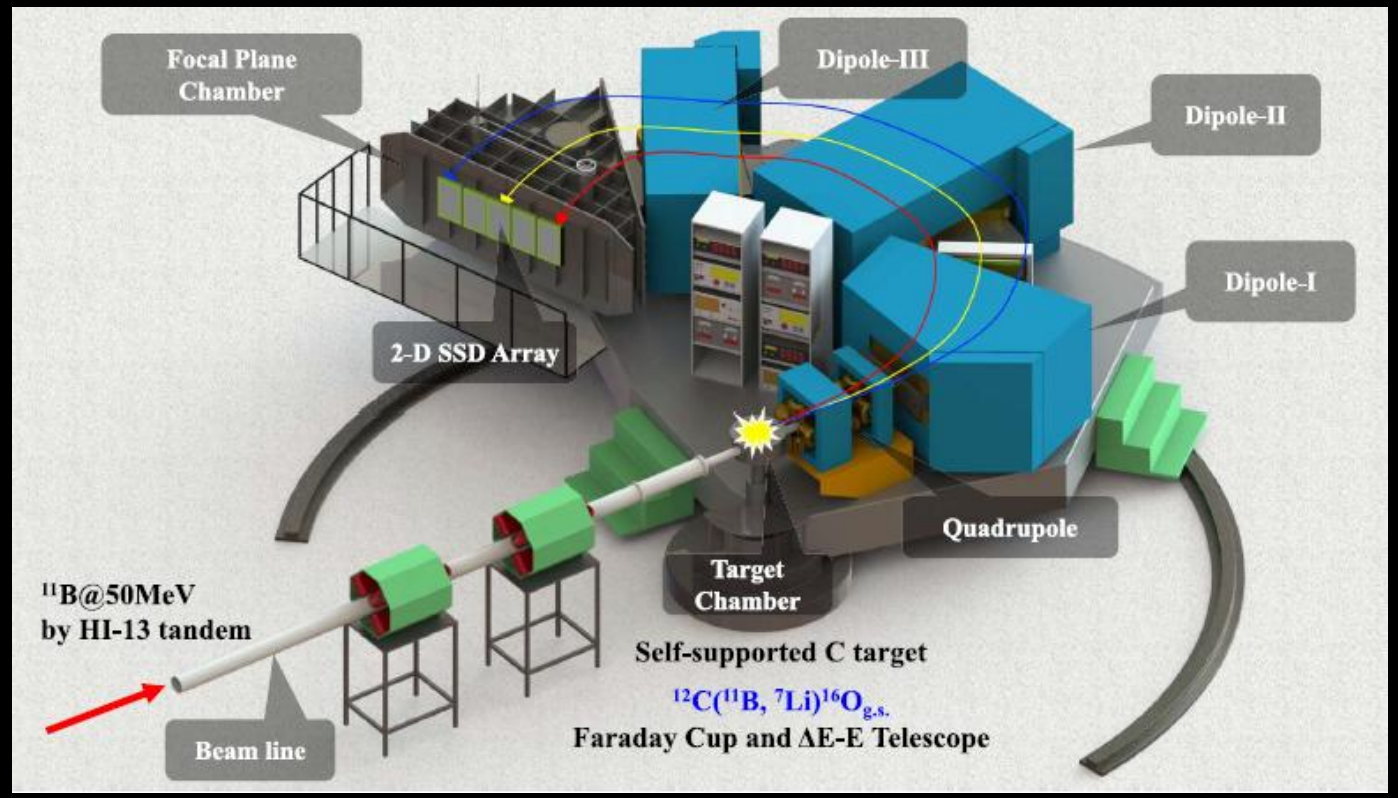
S(E1)=86.3 keVb; S(E2)=45.3 keVb; S(cascade)=7 keVb

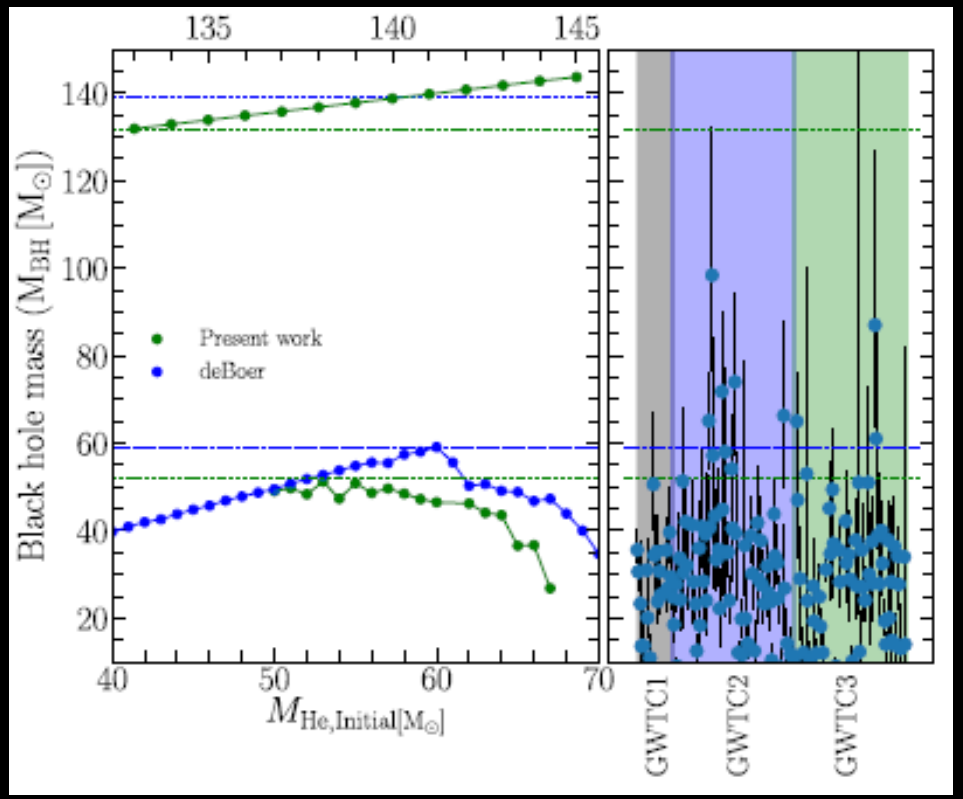
Total S factor = $140 \pm 21_{(\mathrm{MC})}\ ^{+18}_{-11\,(\mathrm{model})}$ keV b.

ANC plays the key role to fix the strengths of the subthreshold states and direct capture

deBoer et al., RMP(2017)

New measurement of ANC of ^{16}O(g.s.) leads to larger S(E2)

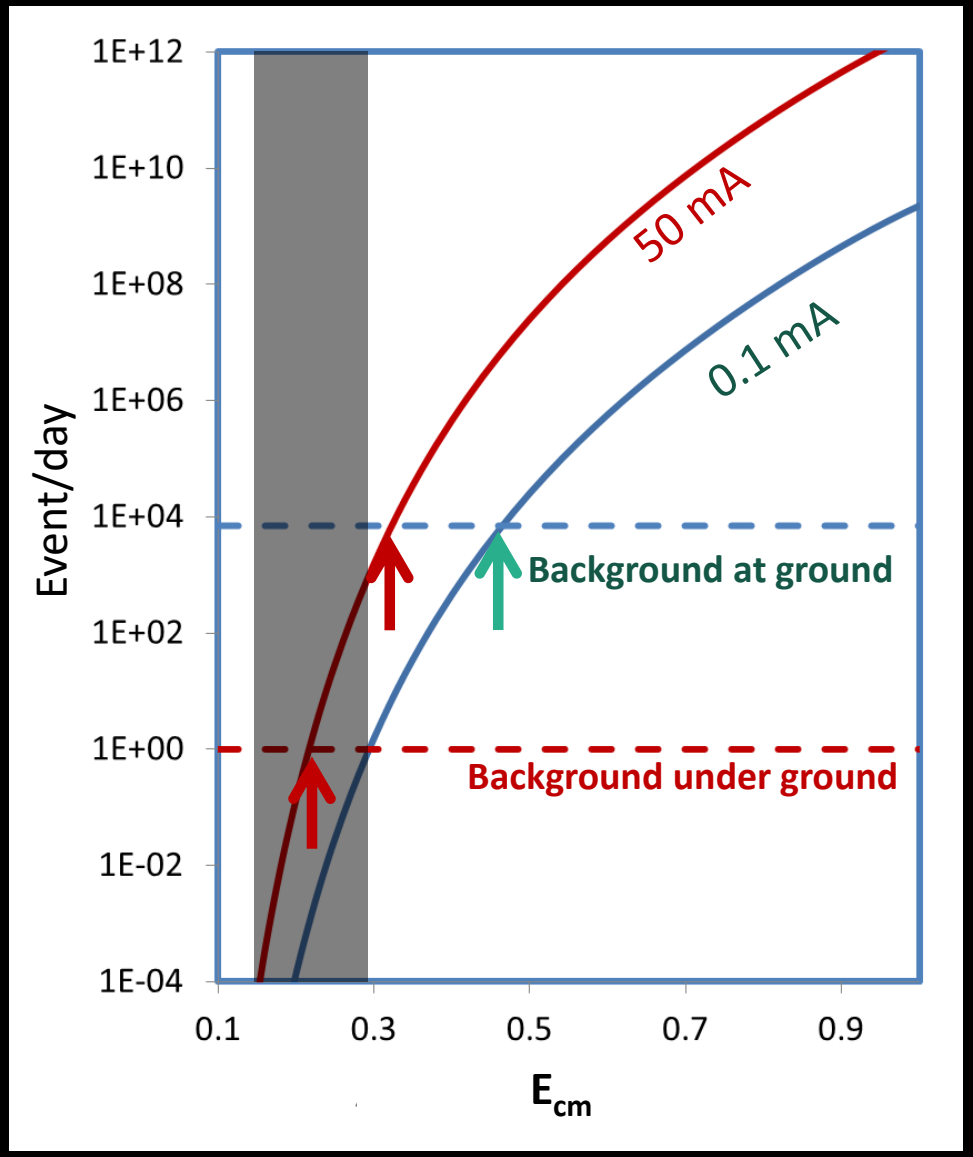


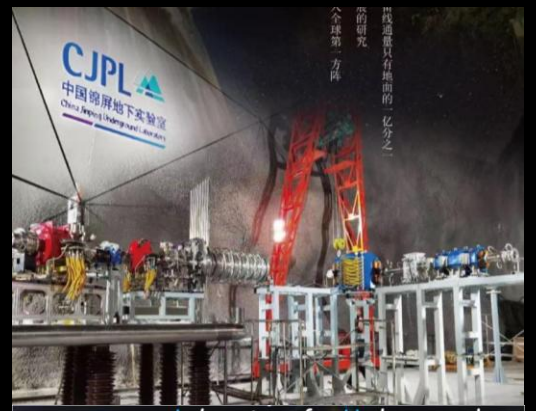


- S(E2) increases from 45 keVb to 70±7 keVb → Total S factor = 162 keVb (err TBD)
- The updated $^{12}C(\alpha, \gamma)^{16}O$ reaction rate decreases the lower and upper edges of the black hole mass gap about 12% and 5%, respectively.

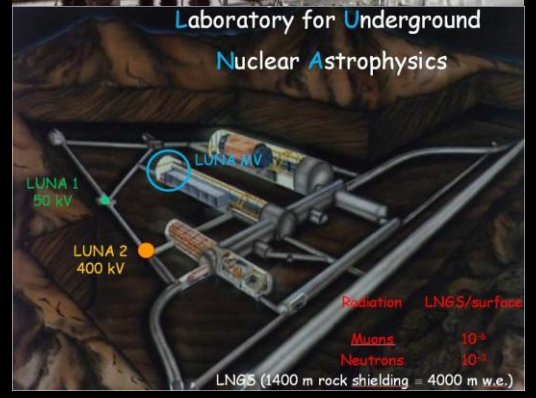
Shen … DeBoer… Tang… et al, PRL(2022), ApJ(2023)

Challenging the tiny cross-sections

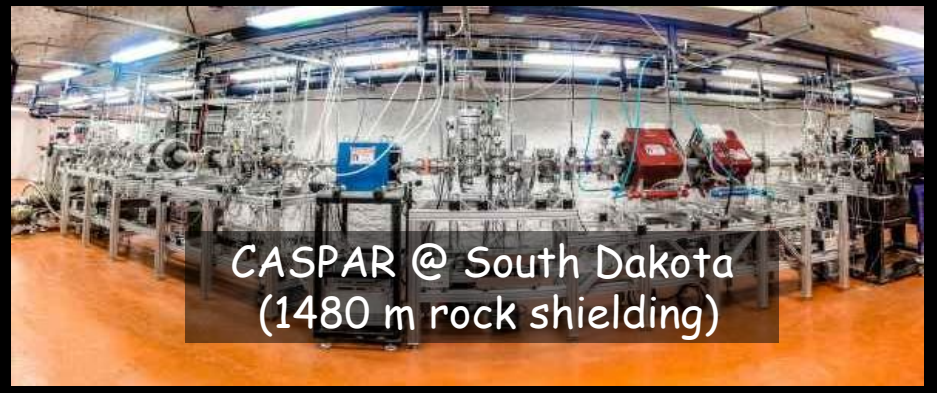




JUNA@China Jinping Underground Laboratory
(2400 m rock shielding)

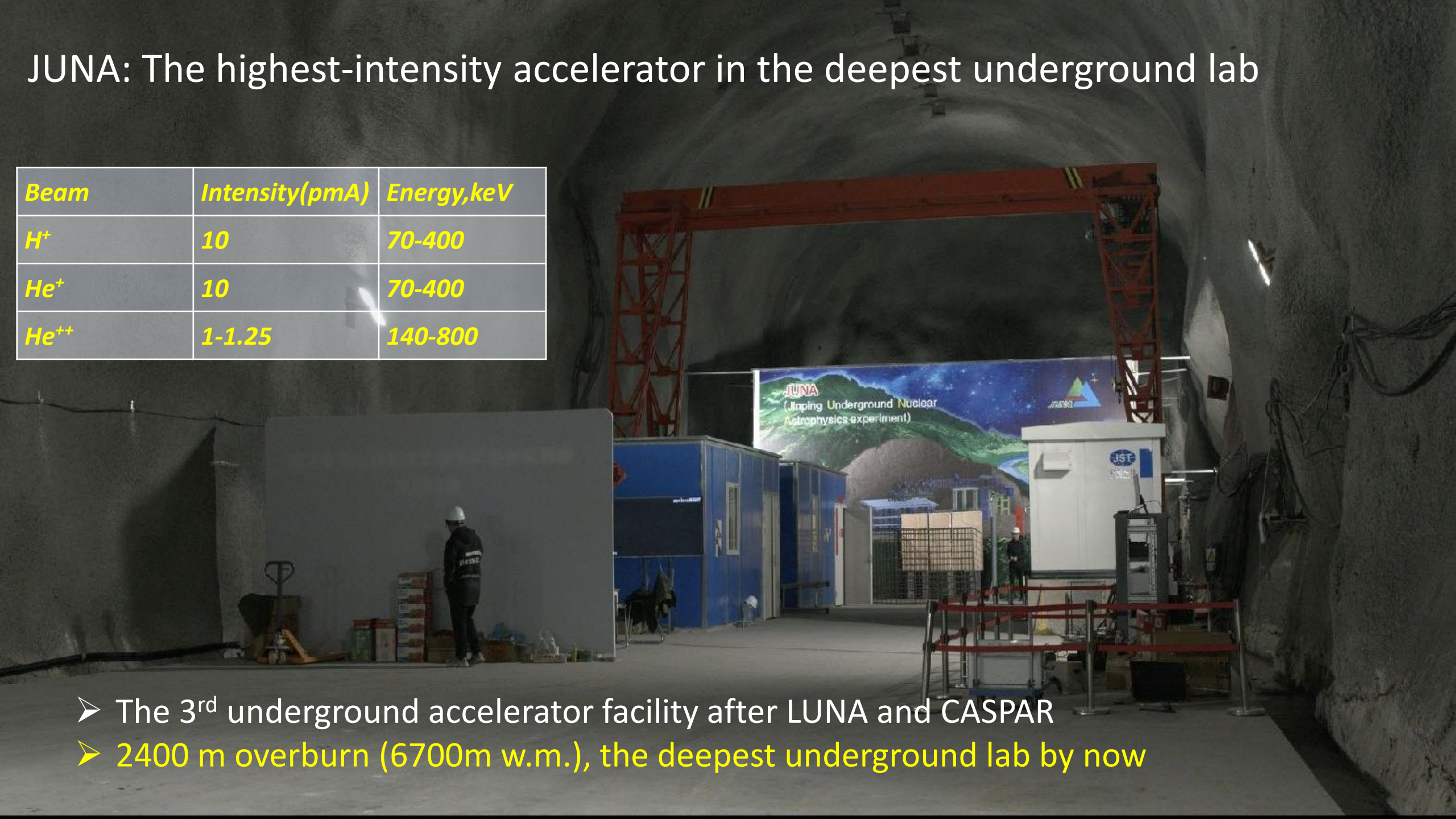


LUNA @ Gran Sasso Italy
1400m rock shielding



JUNA: The highest-intensity accelerator in the deepest underground lab

Beam	Intensity(pmA)	Energy,keV
H^+	10	70-400
He^+	10	70-400
He^{++}	1-1.25	140-800



- The 3rd underground accelerator facility after LUNA and CASPAR
- 2400 m overburn (6700m w.m.), the deepest underground lab by now

Jinping Underground Nuclear Astrophysics(JUNA) projects (2015-2021)



CIAE, W.P. Liu
12C(α,γ)16O



BNU, J.J. He
19F(p,α)16O
19F(p,γ)20Ne



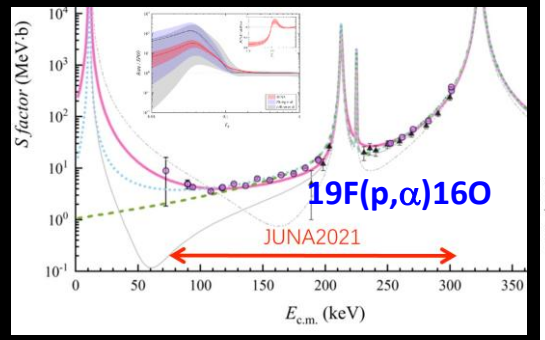
CIAE, Z.H. Li
25Mg(p,γ)26Al



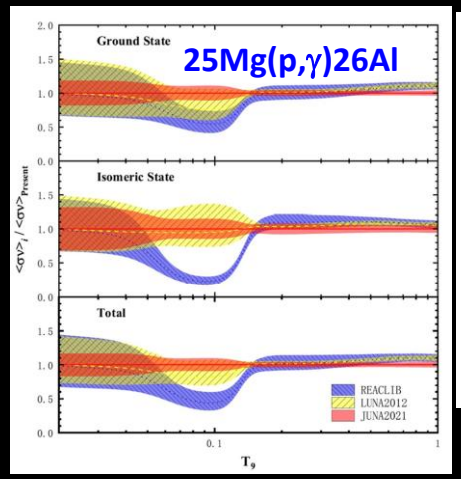
IMP, X.D. Tang
13C(α,n)16O



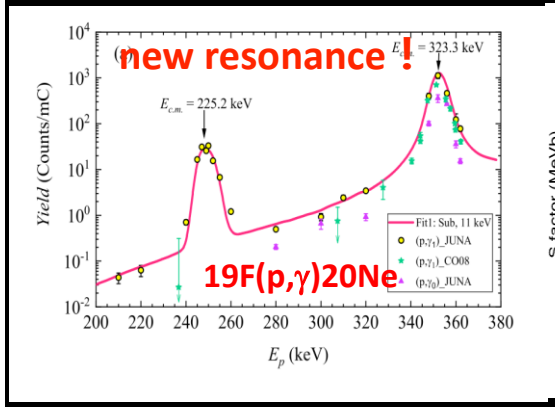
CIAE, G. Lian
Accelerator and Infrastructure



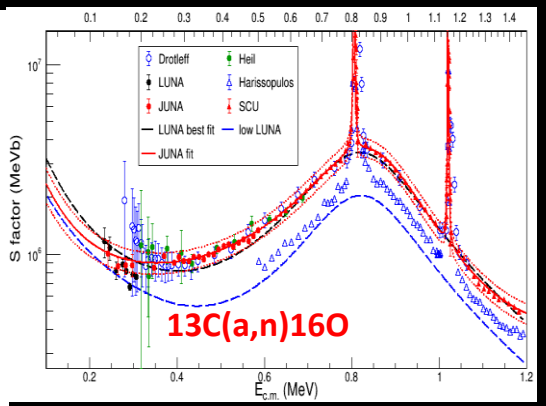
Zhang et al., PRL(2021)



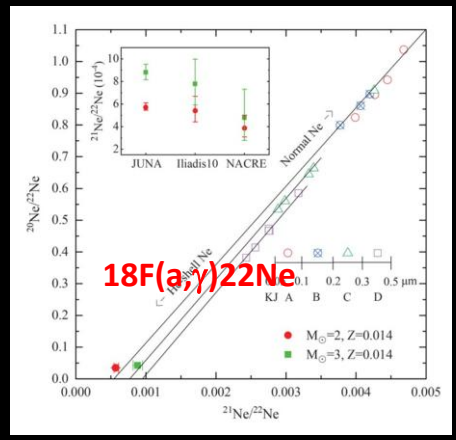
Su et al., Science Bulletin(2022)



Zhang et al,
Nature (2022)



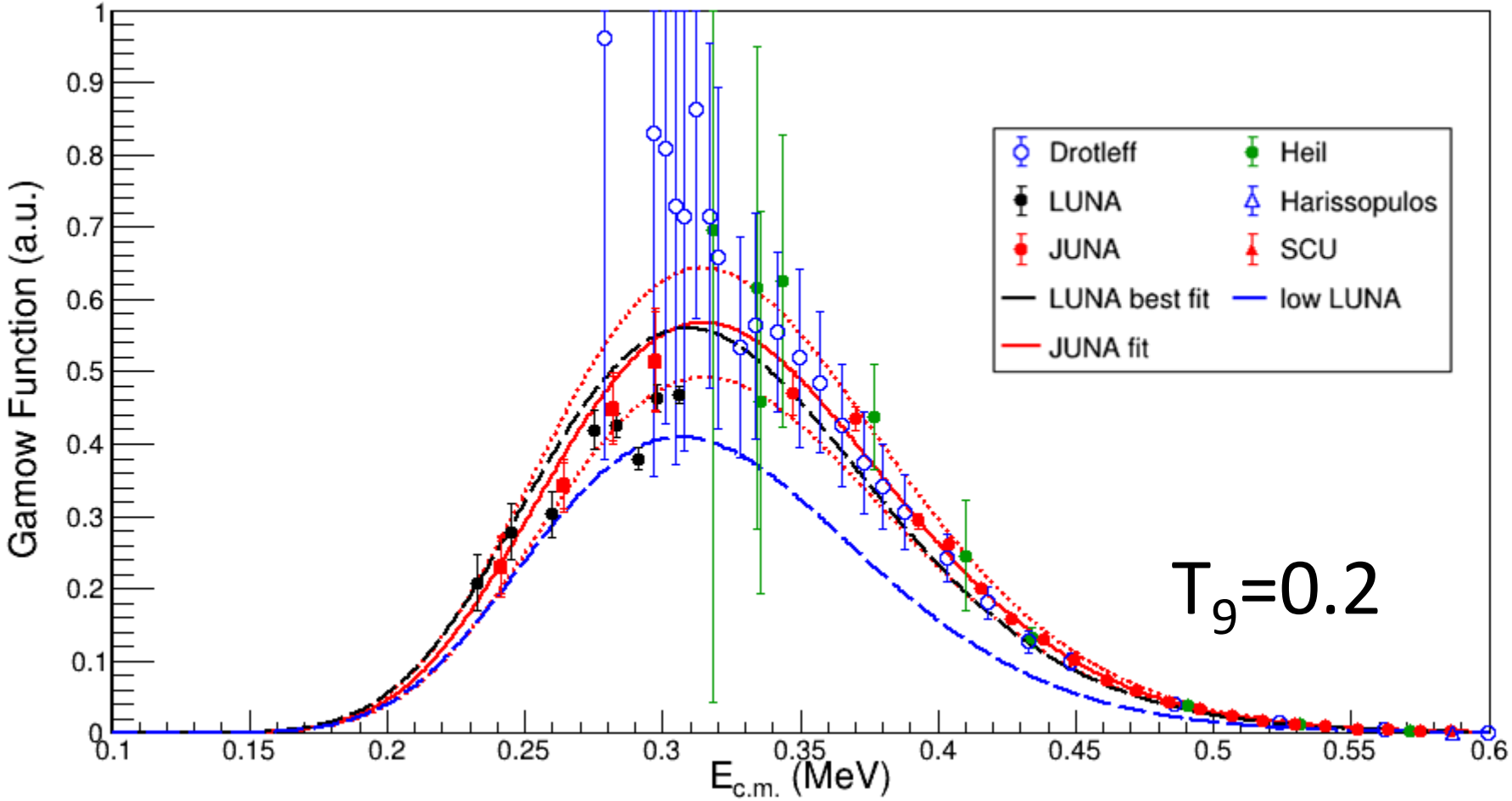
B.S. Gao et al,
PRL (2022)



Wang et al,
PRL (2023)

Gamow peak of $^{13}C(a,n)^{16}O$ for i-process

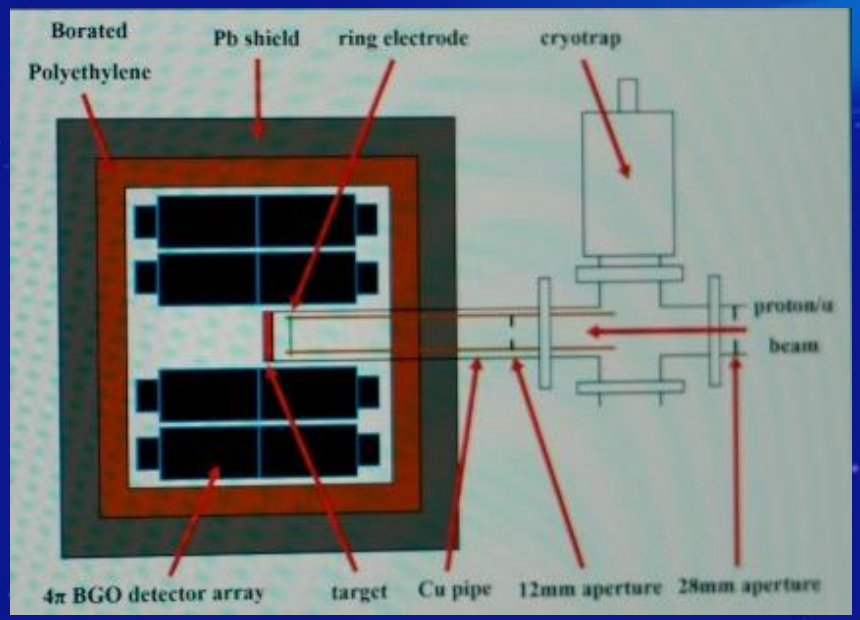
$$\langle \sigma v \rangle = \left(\frac{8}{\pi\mu}\right)^{1/2} \frac{1}{kT^{3/2}} \int_0^\infty \sigma(E) E \exp\left(-\frac{E}{kT}\right) \mathrm{dE}$$

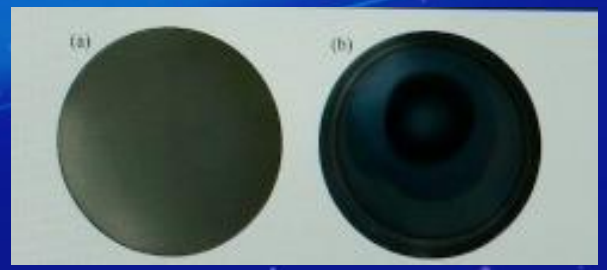


- Cover almost the entire Gamow window for i-processs (0.2-0.3 GK)
- Uncertainty drops from 60% to 15%, disagree with the upturning trend

B.S. Gao et al, PRL (2022)

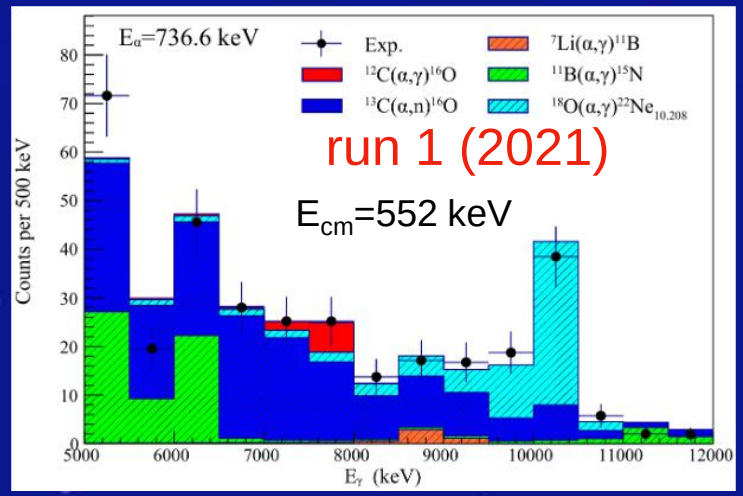
$^{12}C(\alpha,\gamma)^{16}O$: from Run 1 to Run 2

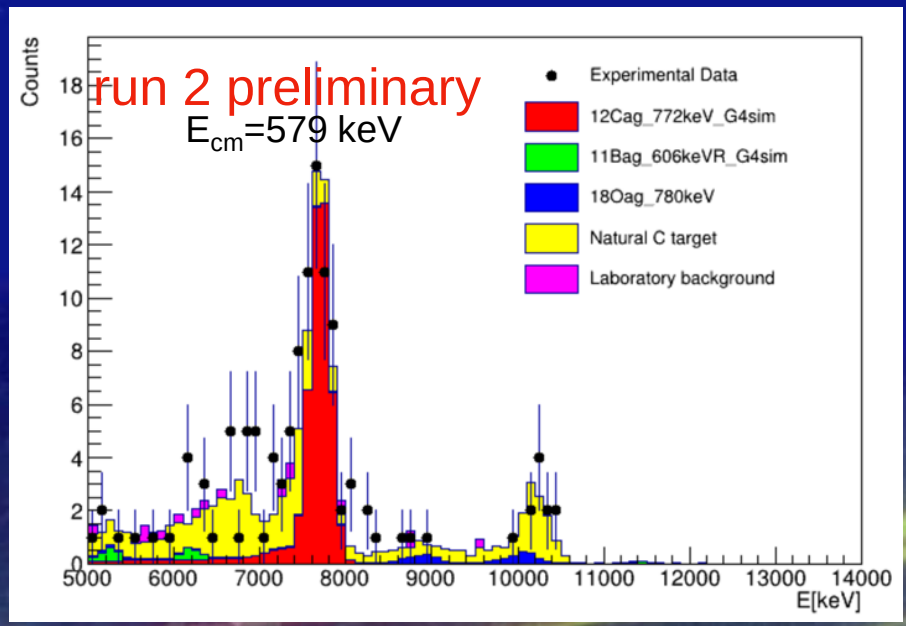


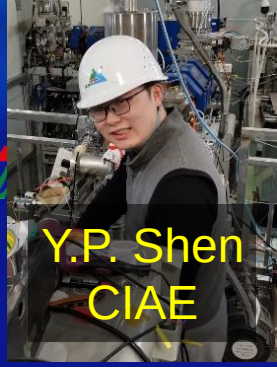


run 2 improve
Target C to Diamond
BGO 40% larger
^{18}O and ^{13}C much reduced
S/N from 1:1 to 5:1

- 48X 60X60X120 mm BGO for g detection
- full efficiency 85 % @7700 keV
- Out layer for anti coincidence, inner for signal hit: 24 % @7700 keV
- Background 0.048/h @6-10 MeV
- 99.99% ^{12}C diamond with Mo backing, $^{13}C < 10^{-5}$

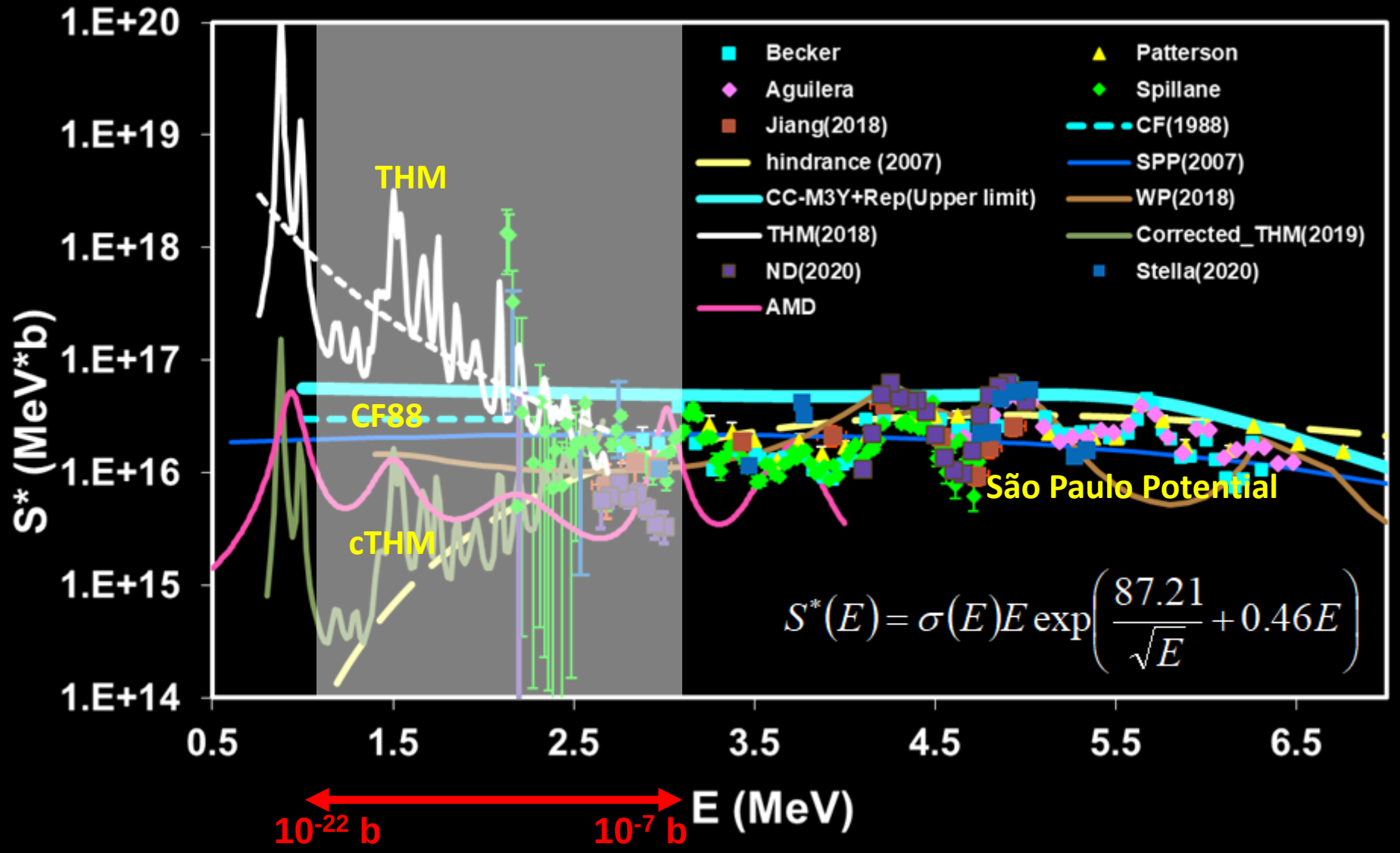


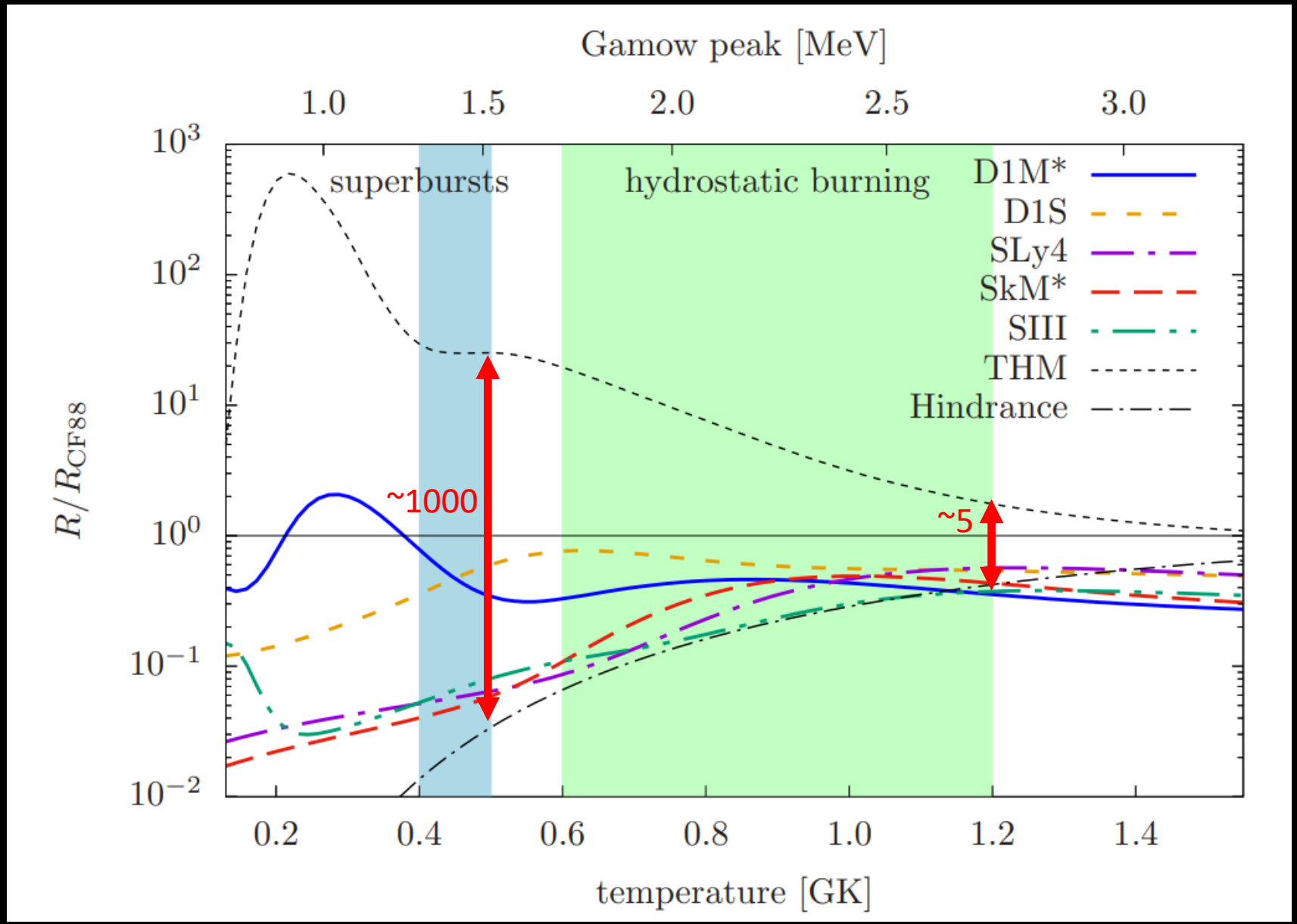




Courtesy of W.P. Liu

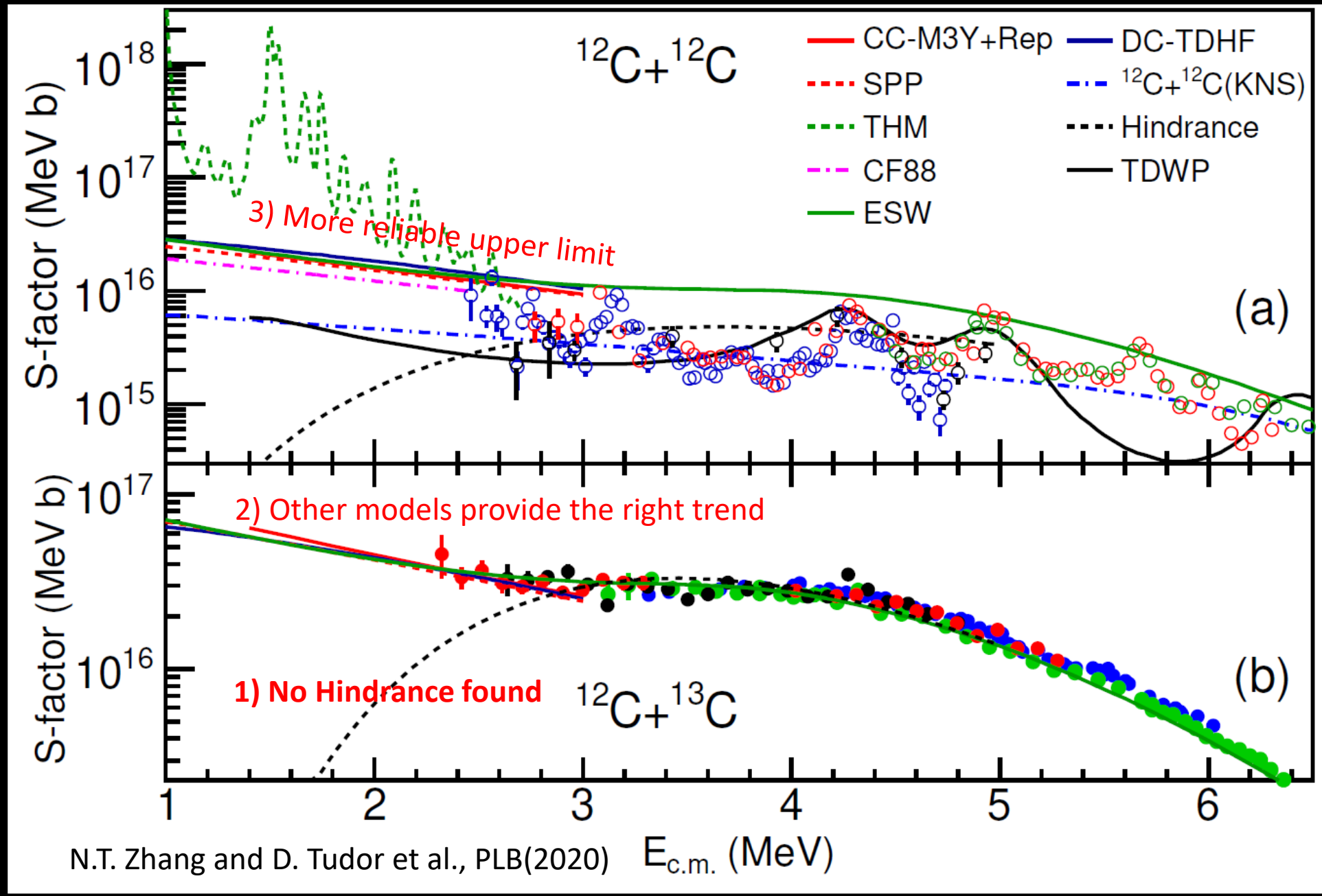
$^{12}C+^{12}C$ Fusion Reaction (1960-)





Taniguchi & Kimura, Phys. Lett. B 849 (2024)

Test of hindrance and upper limit of $^{12}C+^{12}C$ based on systematics



N.T. Zhang and D. Tudor et al., PLB(2020)



N.T.Zhang(IMP)



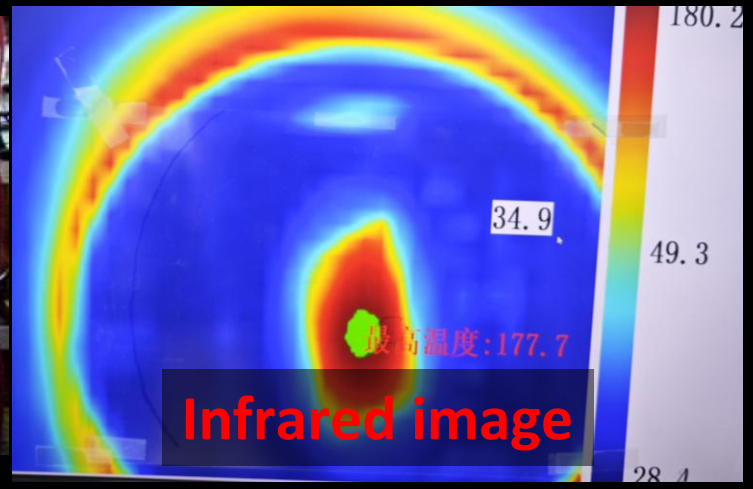
D. Tudor (IFIN-HH)

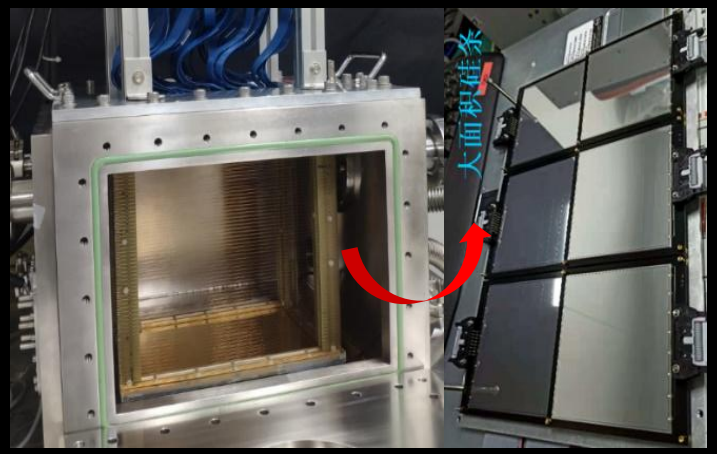


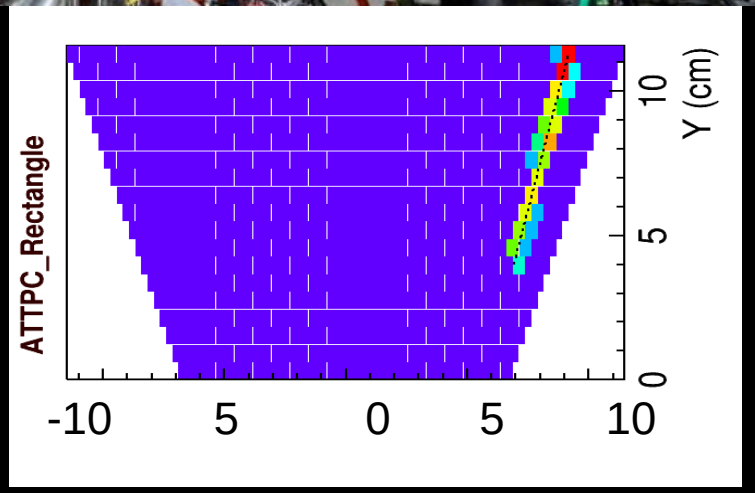
L. Trache (IFIN-HH)

High Intensity+Time Projection Chamber



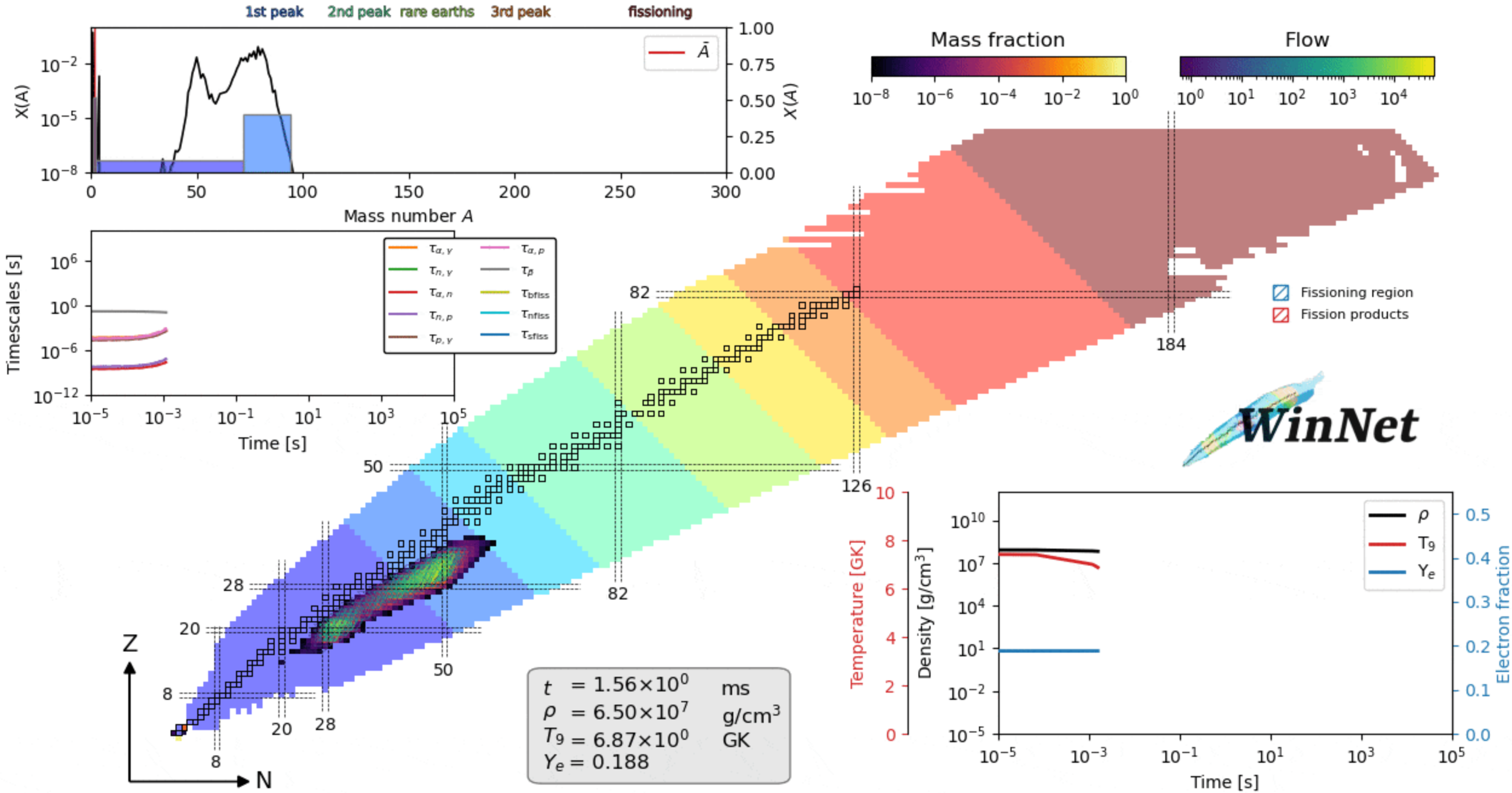




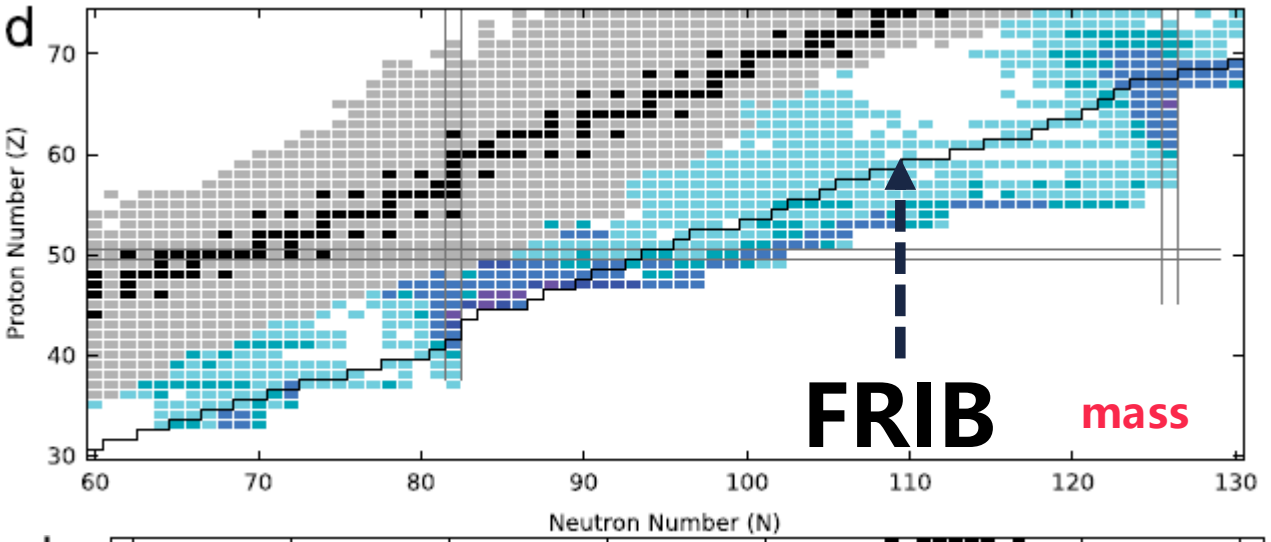


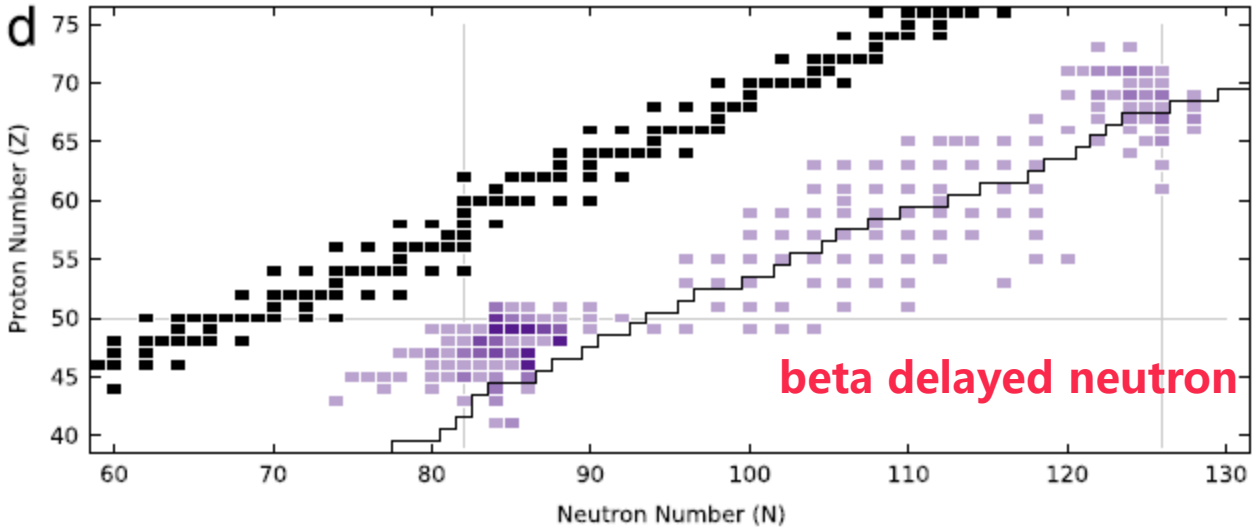


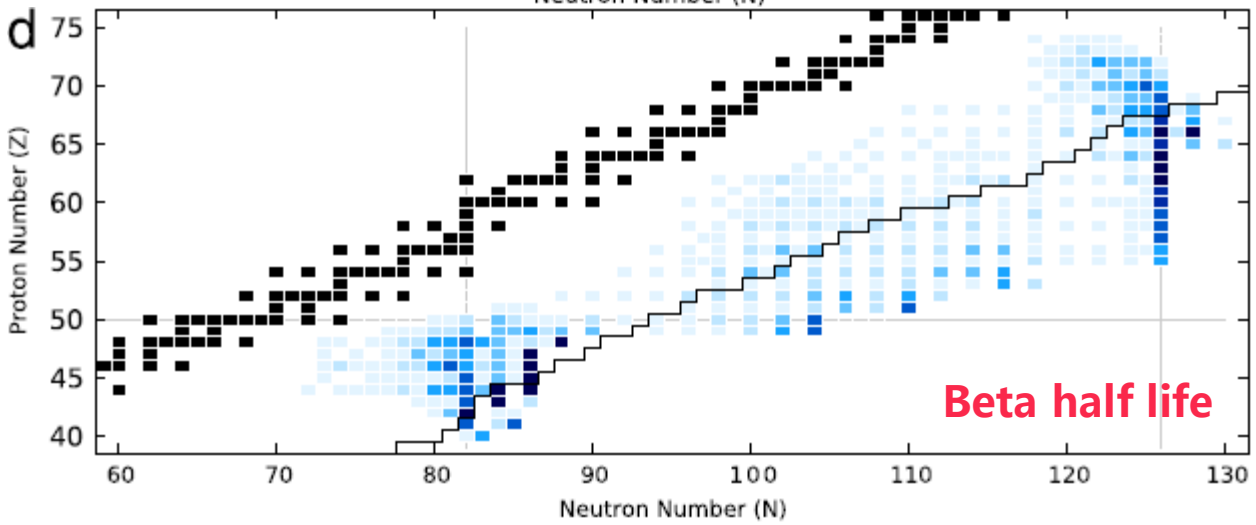
- LINAC: High Intensity beam up to 200 puA
- Time Projection Chamber: Ultra sensitive tracking detector
- Complementary to LUNA-MV underground experiment and other experiments

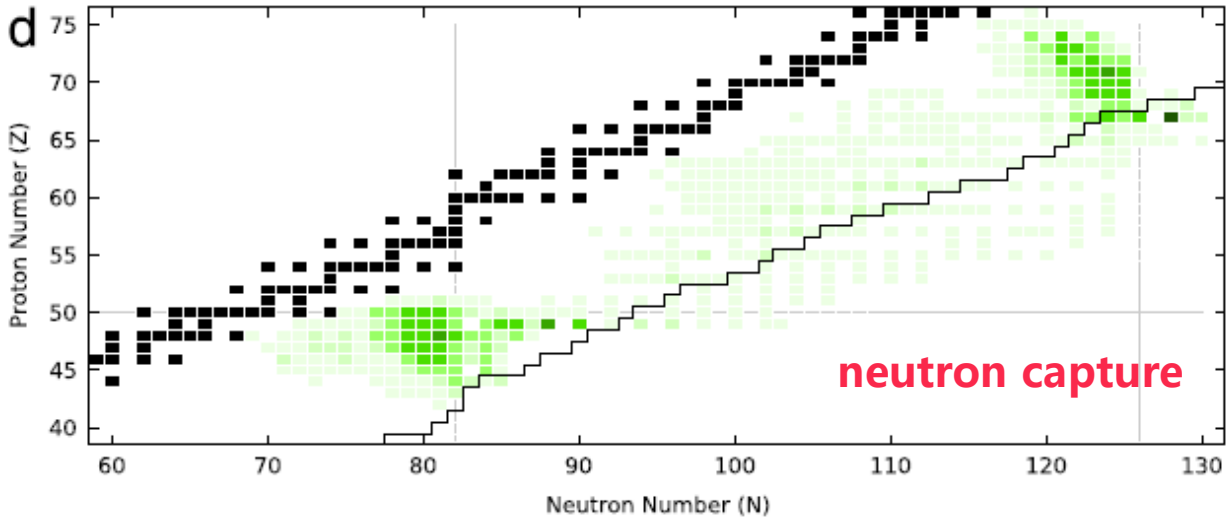

1st peak
2nd peak
rare earths
3rd peak
fissioning
X(A)
$\bar{A}$
Mass number A
Mass fraction
Flow
Timescales [s]
Time [s]
$\tau_{\alpha,\gamma}$
$\tau_{n,\gamma}$
$\tau_{\alpha,n}$
$\tau_{n,p}$
$\tau_{p,\gamma}$
$\tau_{\alpha,p}$
τ_{β}
$\tau_{\beta fiss}$
τ_{nfiss}
τ_{sfiss}
Fissioning region
Fission products
WinNet
Z
N
$t = 1.56\times10^{0}$ ms
$\rho = 6.50\times10^{7}$ g/cm^3
$T_9 = 6.87\times10^{0}$ GK
$Y_e = 0.188$
Temperature [GK]
Density [g/cm^3]
Electron fraction
ρ
T_9
Y_e

Important nuclear physics inputs



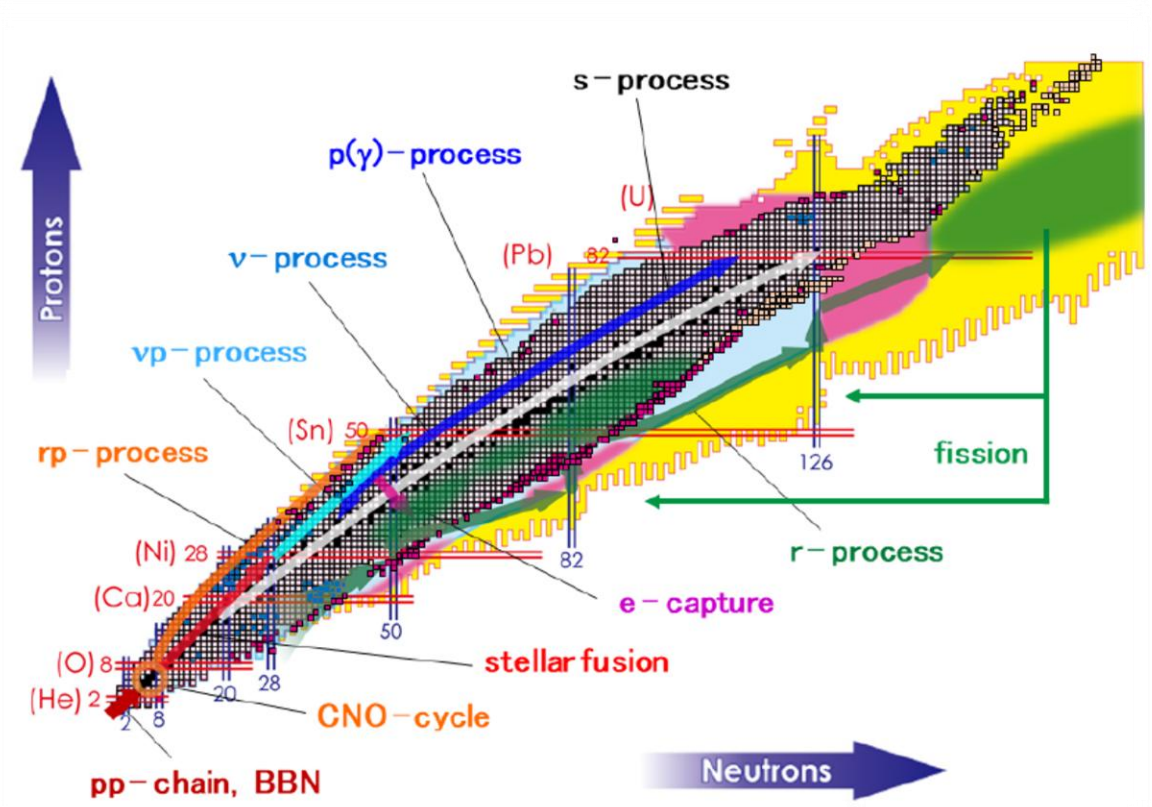


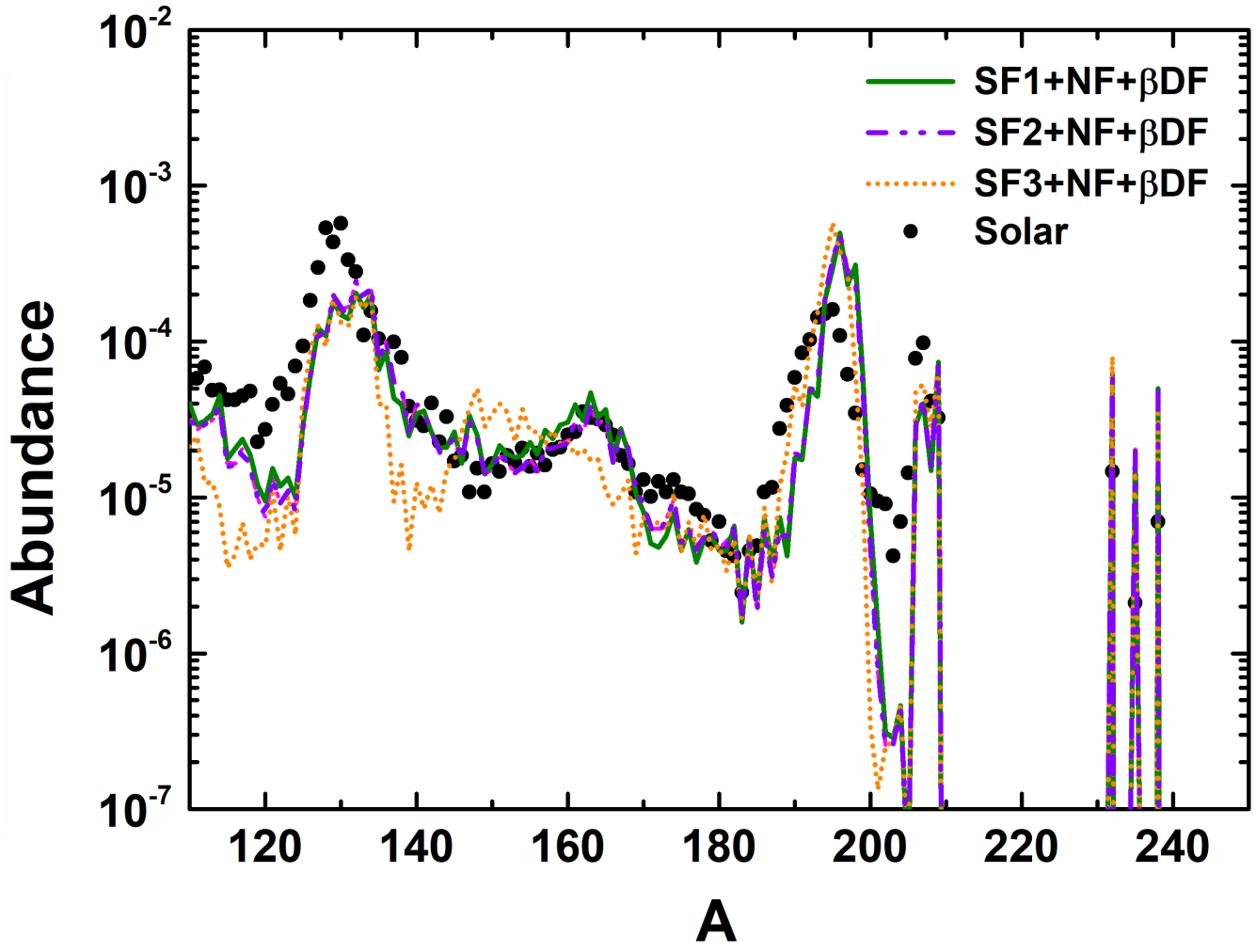




M.R. Mumpower, R. Surmana, G.C. McLaughlin, A. Aprahamian, PPNP 86 (2016) 86–126

Fission: Ending Point of R-process

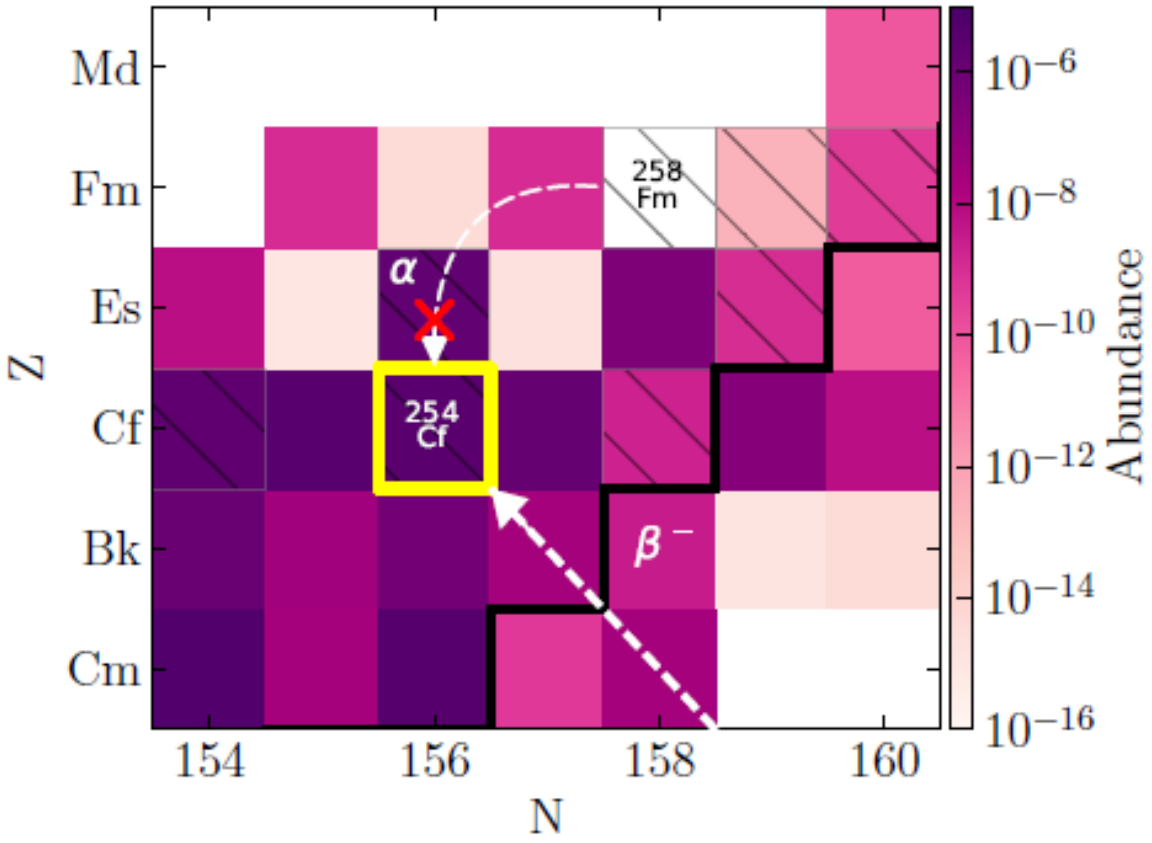




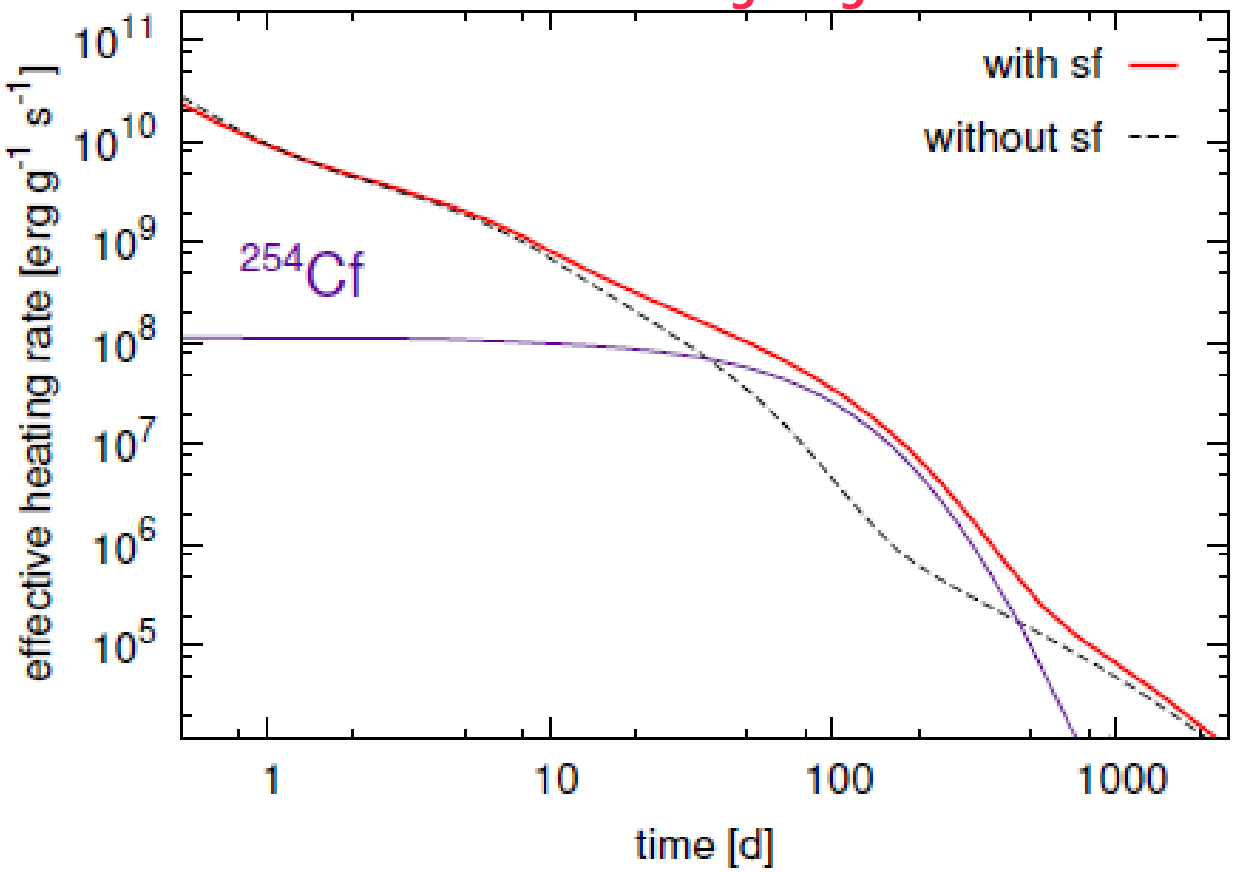
"Progress in Nuclear Astrophysics of East and Southeast Asia", AAPPS bulletin(2021) 31:18

Y. W. Hao, Y.F. Niu et al., APJ, 933, 3 (2022)

Important Nuclear Physics inputs



Neutron star merger light curve



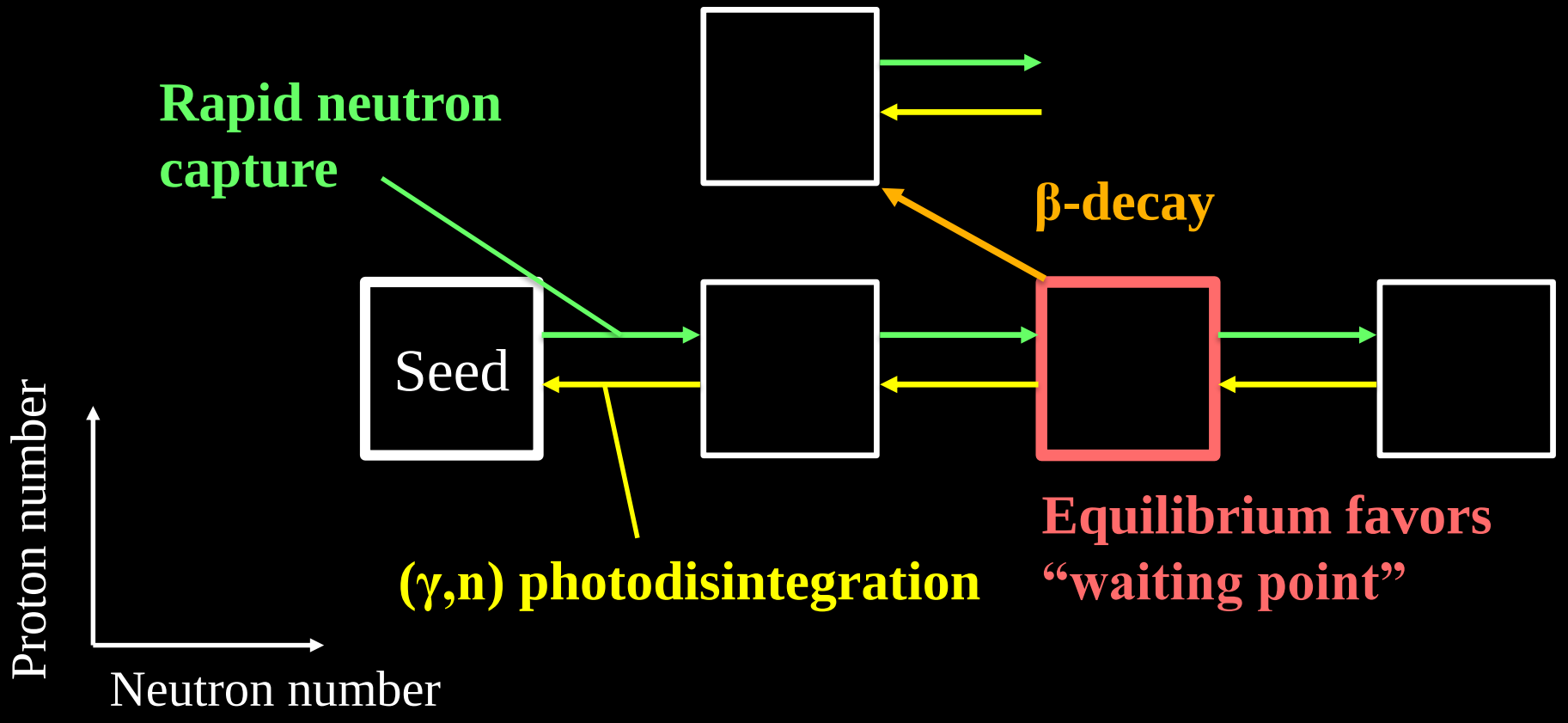
Fission properties of A=254 isotopes are important for the understanding of the light curve of neutron star mergers.

Zhu et al., arXiv:1806.09724v1

The r-process

Temperature: ~1–2 GK
Density: 300 g/cm ^{3} (~60% neutrons!)

neutron capture timescale: ~0.2 μs



Adapted from Schatz's lecture

Waiting point approximation

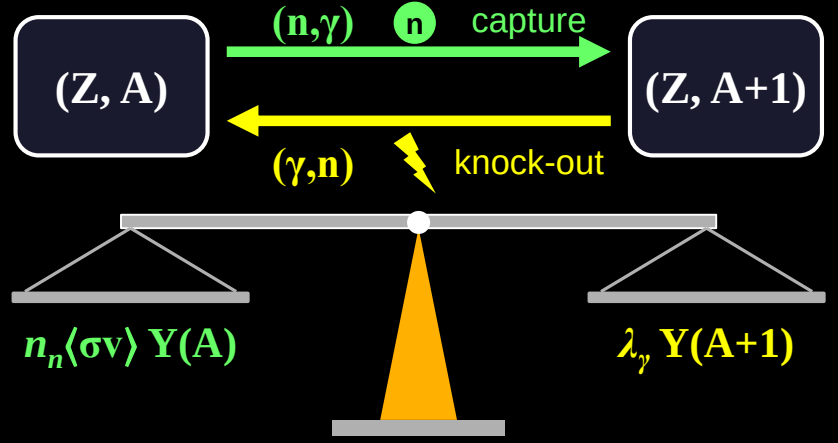
Definition: **ASSUME** (n,γ)–(γ,n) equilibrium within an isotopic chain

How good is the approximation?

This is a valid assumption during most of the r-process

BUT: freeze-out is neglected
Freiburghaus et al., ApJ 516 (1999) 381, showed agreement with dynamical models

(n,γ) flow = (γ,n) flow



Consequences

In (n,γ)–(γ,n) equilibrium the isotopic abundances obey:

$$\frac{Y(Z,A+1)}{Y(Z,A)} = n_n \frac{G(Z,A+1)}{2G(Z,A)} \left[\frac{A+1}{A}\frac{2\pi\hbar^2}{m_u kT}\right]^{3/2} \exp\left(\frac{S_n}{kT}\right)$$

- **Time independent**
  - the whole chain acts as one nucleus in the network
  - only the slow β decays are followed dynamically
- **Independent of the neutron-capture rate**
  so during most of the r-process, n-capture rates do not matter!

Adapted from Schatz's lecture

Why phase space favours the free neutron

① Count the quantum states

One quantum state per phase-space cell **Δx·Δp ≈ h**

$$\lambda = \frac{h}{\sqrt{2\pi m_n kT}} \approx 55\ \text{fm}, \qquad n_Q \equiv \frac{1}{\lambda^3} = \left(\frac{m_n kT}{2\pi\hbar^2}\right)^{3/2}$$

n_Q = quantum concentration: 1 neutron per λ³ cell ≈ 6×10³³ cm⁻³ (T_9 = 1)

Each free neutron has a volume $1/n_n$ to itself, cut into λ³ cells:

$$W_{\text{free}} = \frac{1/n_n}{\lambda^3} = \frac{n_Q}{n_n} \approx 6 \times 10^9 \qquad W_{\text{bound}} \approx 1$$

② Free energy decides: F = E − TS

$$\Delta F_{\text{capture}} = -S_n + kT \ln \frac{n_Q}{n_n}$$

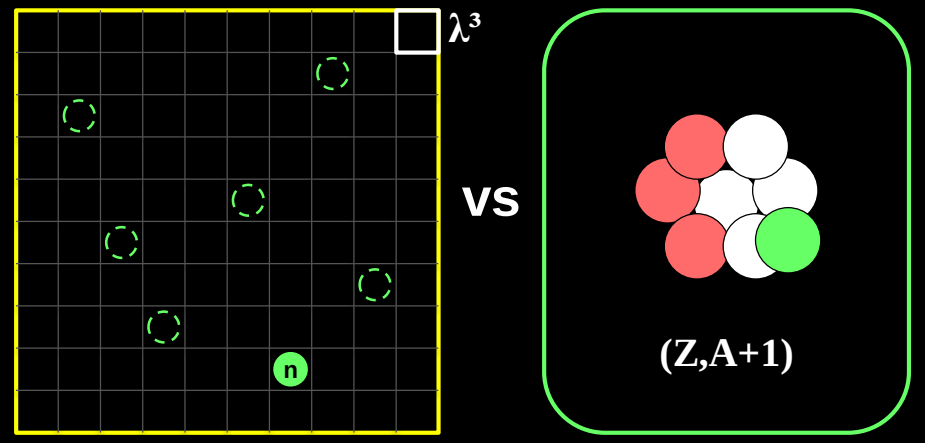
$-S_n$: energy gained by binding **$+kT \ln(n_Q/n_n)$**: entropy lost

ΔF < 0: capture wins (bound) ΔF > 0: (γ,n) wins (free)

ΔF = 0 ⇒ Saha balance: $S_n = kT \ln(n_Q/n_n) \approx 2$ MeV

Knobs: hotter ($n_Q \propto T^{3/2}$) → free more neutrons (n_n ↑) → bound larger S_n → bound

Counting places to be



free: $n_Q/n_n \approx 6\times10^9$ cells
box = $1/n_n \approx (10^5\ \text{fm})^3$

bound: 1 state
but lower by S_n

Same reason, everyday examples

Sun's surface	Puddle	r-process
H ionized, 10^4 K	water evaporates	(γ,n) beats capture
1 eV ≪ 13.6 eV	below 100 °C	86 keV ≪ 2 MeV

Binding ≫ kT, yet the dilute free state wins: e^{22} states

Numbers: T_9 = 1, $n_n = 10^{24}$ cm⁻³

Deriving the (n,γ)–(γ,n) Saha equation

1. Equilibrium, μ(γ) = 0

$$\mu(Z,A) + \mu_n = \mu(Z,A+1)$$

2. Boltzmann gas

$$n_i = G_i \left(\frac{m_i kT}{2\pi\hbar^2}\right)^{3/2} \exp\left(\frac{\mu_i - m_i c^2}{kT}\right)$$

3. Divide: μ's cancel

$$\frac{n(Z,A+1)}{n(Z,A)\,n_n} = \frac{G(Z,A+1)}{G(Z,A)\,g_n}\left[\frac{m_{A+1}}{m_A m_n}\frac{2\pi\hbar^2}{kT}\right]^{3/2} \exp\left(\frac{(m_A + m_n - m_{A+1})c^2}{kT}\right)$$

4. Substitute

$$g_n = 2 \qquad \text{(neutron spin ½)}$$

$$(m_A + m_n - m_{A+1})c^2 = S_n$$

$$\frac{m_{A+1}}{m_A m_n} \approx \frac{A+1}{A\,m_u}$$

$$\frac{n(Z,A+1)}{n(Z,A)} = \frac{Y(Z,A+1)}{Y(Z,A)}$$

$$\frac{Y(Z,A+1)}{Y(Z,A)} = n_n \frac{G(Z,A+1)}{2G(Z,A)}\left[\frac{A+1}{A}\frac{2\pi\hbar^2}{m_u kT}\right]^{3/2} \exp\left(\frac{S_n}{kT}\right)$$

G = Σ (2J+1) exp(−E/kT): nuclear partition function. **No cross section appears!**

Standard statistical-mechanics derivation

Waiting point approximation continued

In the approximation of continuous S_n and abundances Y, the maximum abundance in an isotopic chain occurs for

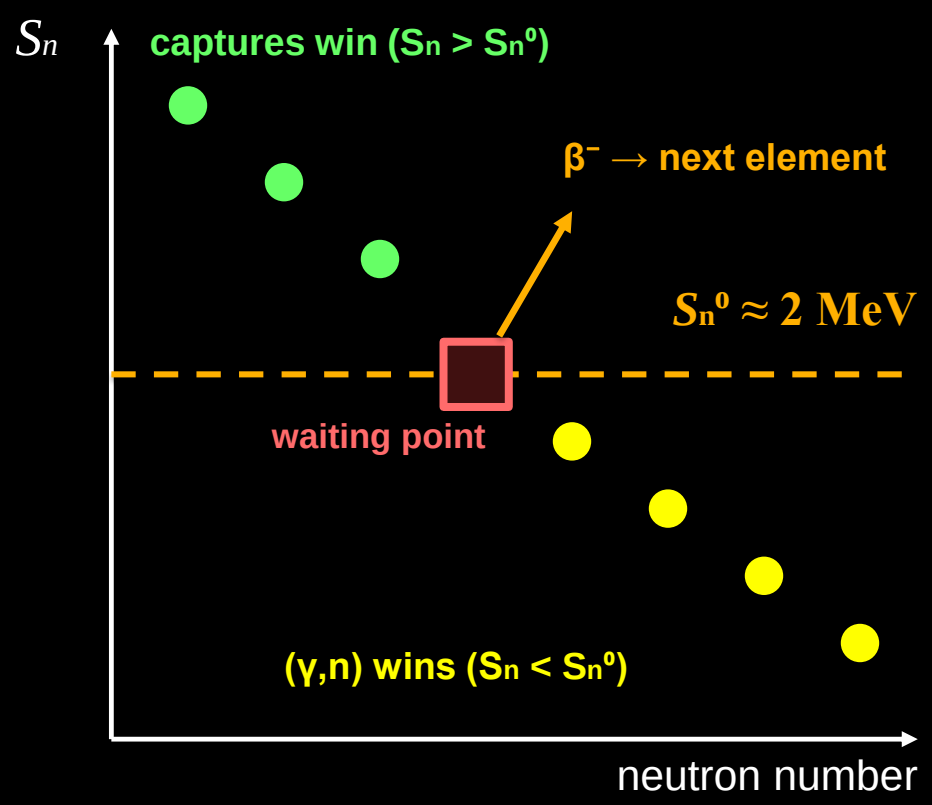
$$\frac{Y(Z,A+1)}{Y(Z,A)} = 1$$

For a given temperature and neutron density one can solve for S_n (assuming A ≈ A+1 and G = 1):

$$S_n = kT \ln\left(\frac{2}{n_n}\left[\frac{m_u kT}{2\pi\hbar^2}\right]^{3/2}\right)$$

$$S_n = \frac{T_9}{11.604}\left[\frac{3}{2}\ln(T_9) - \ln(n_n) + 78.460\right]$$

S_n in MeV; T_9 in 10^9 K; n_n in cm^{-3}



Example: $T_9 = 1$, $n_n = 10^{24}$ cm^{-3}
gives $S_n \approx$ **2.0 MeV**

→ The r-process runs at a fixed neutron separation energy (for given conditions)

Equilibrium r-process path laboratory

Equilibrium-path controls

MRSN cooling r-process (T9~1.5)

t=7.646e-02 s. Default lecture example: equilibrium path is strongly neutron rich.

Temperature T9

1.51

log10 density [g cm^-3]

5.84

Neutron abundance Yn

0.386

Right figure: proton number Z

50

Path range

Z min 20 Z max 100

Match WinNet movie statistical-factor convention

Calculate | Save figure

Standard relation:
Y(Z,N+1)/Y(Z,N) = n_n lambda_T^3
x [(A+1)/A]^(3/2) G_(N+1)/(2 G_N)
x exp[S_n(Z,N+1)/(kT)]

The path selects the maximum relative abundance in each Z chain.

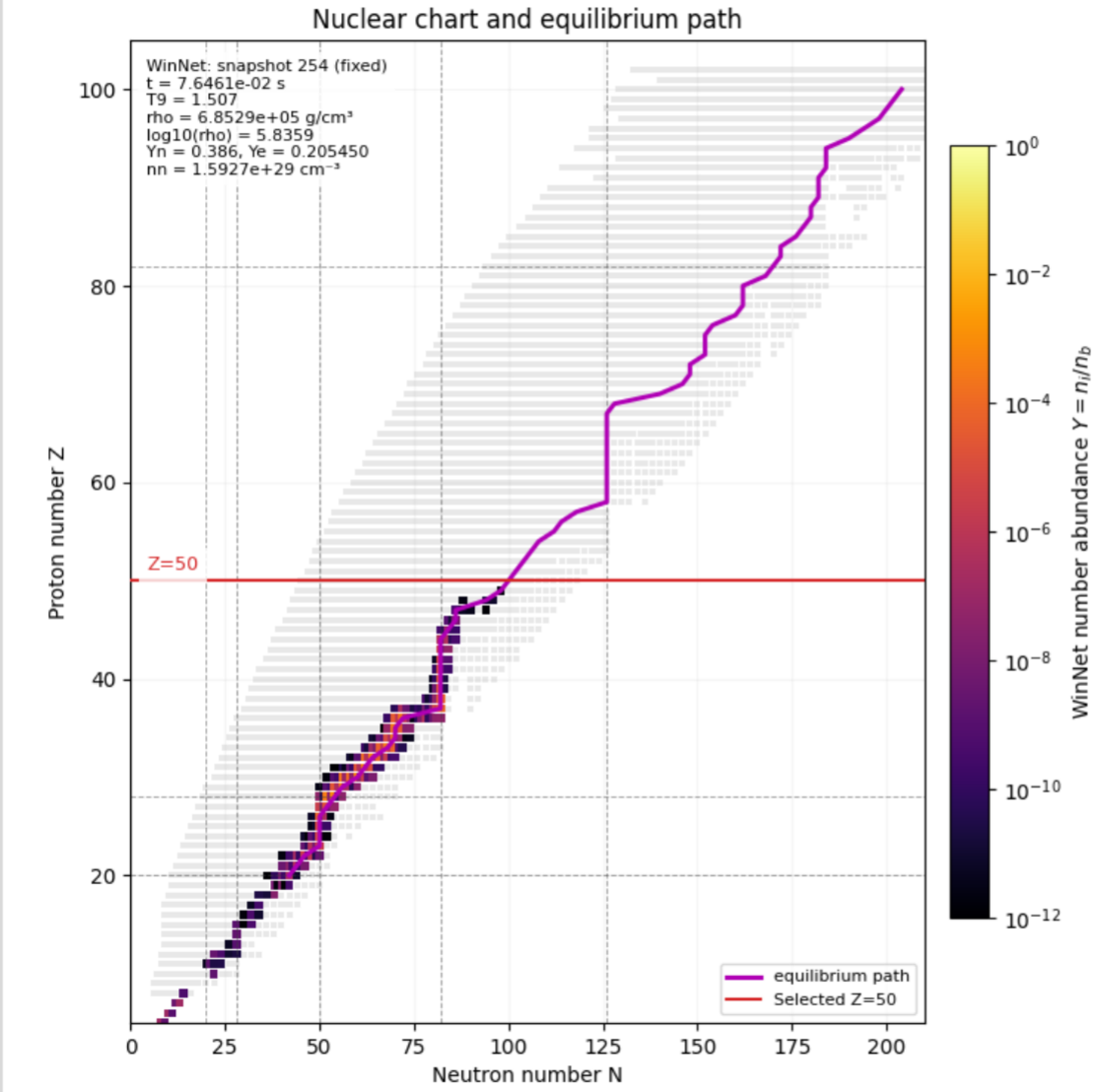
nn = rho × NA × Yn = 1.593e+29 cm⁻³
kT = kB × T9 × 10⁹ K = 0.1298 MeV

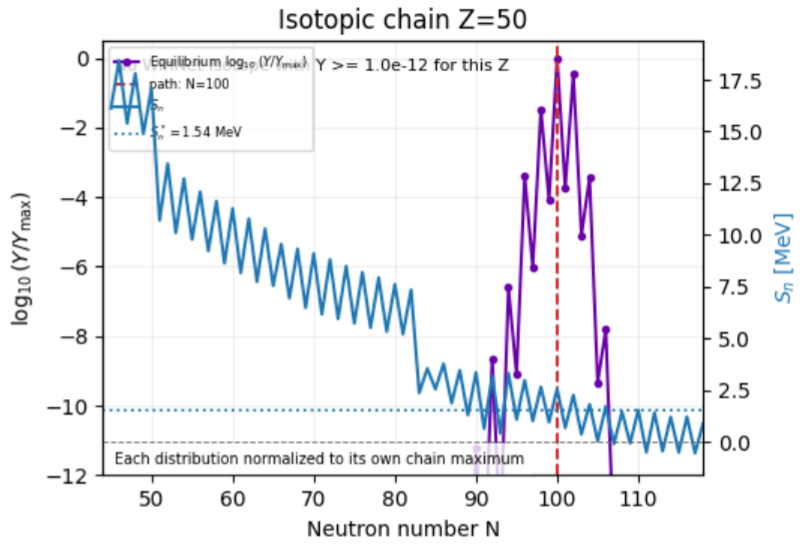
λT³ = [2πℏ² / (mu kT)]³ᐟ²
Sn* ≈ −kT ln(nn λT³ / 2)

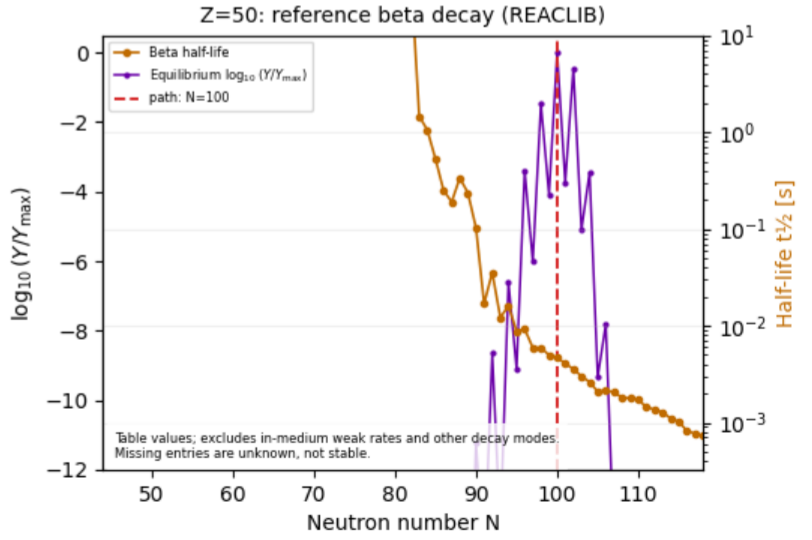
Approximate Sn* = 1.537 MeV
Displayed chain peak: Z=50, N=100

Y min (absolute): 1E-12 Fixed WinNet snapshot: 254 Show snapshot Match snapshot to inputs

WinNet abundance background Load WinNet run Beta-decay table: REACLIB Half-life







Equilibrium r-process path laboratory

Equilibrium-path controls

MRSN near freeze-out (T9~1.0)

t=1.249e-01 s. Equilibrium is becoming less reliable; compare with a full network.

Temperature T9

1.00

log10 density [g cm^-3]

5.30

Neutron abundance Yn

0.237

Right figure: proton number Z

50

Path range

Z min 20 Z max 100

Match WinNet movie statistical-factor convention

Calculate | Save figure

Standard relation:
Y(Z,N+1)/Y(Z,N) = n_n lambda_T^3
x [(A+1)/A]^(3/2) G_(N+1)/(2 G_N)
x exp[S_n(Z,N+1)/(kT)]

The path selects the maximum relative abundance in each Z chain.

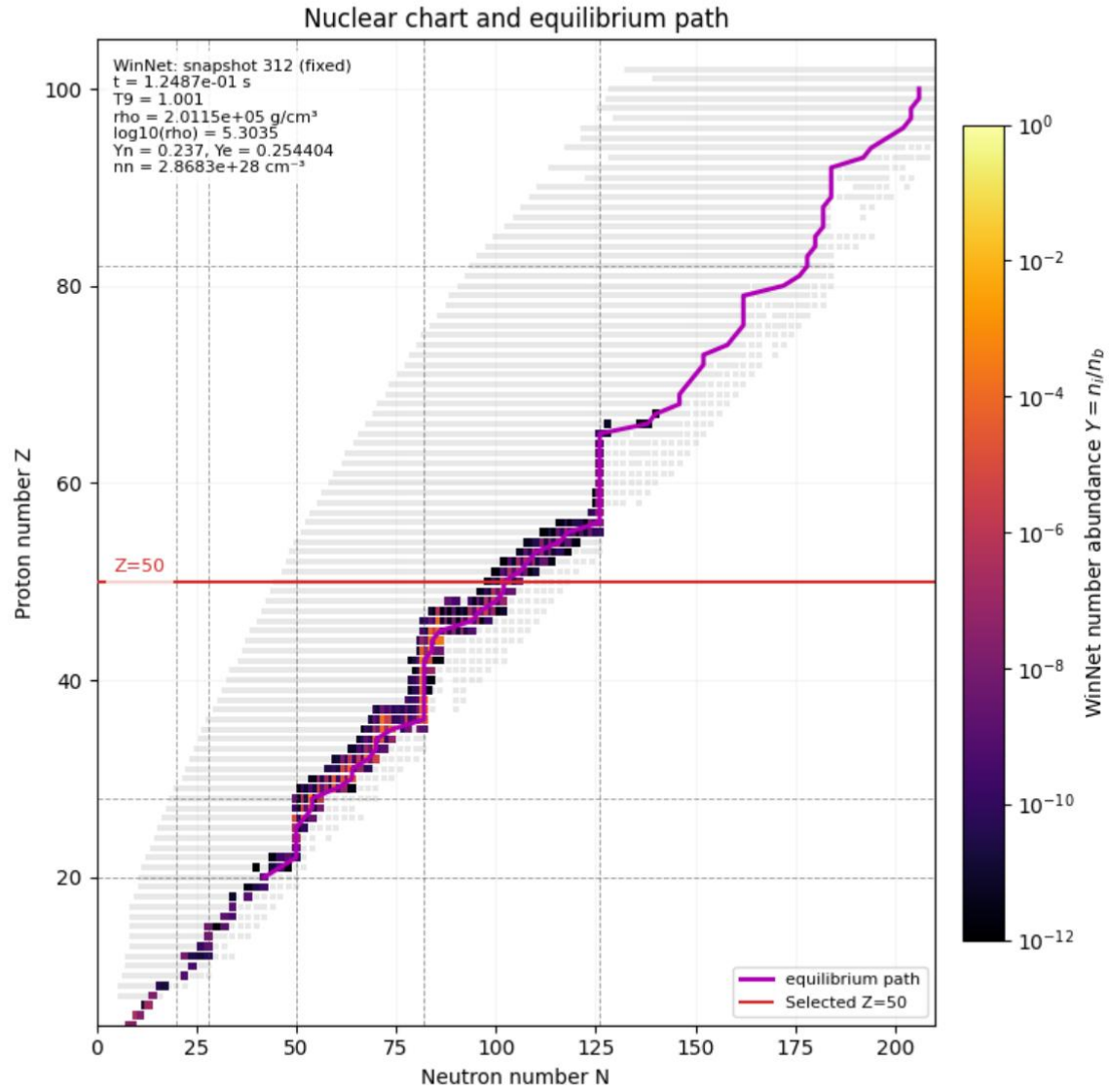
nn = rho × NA × Yn = 2.868e+28 cm⁻³
kT = kB × T9 × 10⁹ K = 0.0863 MeV

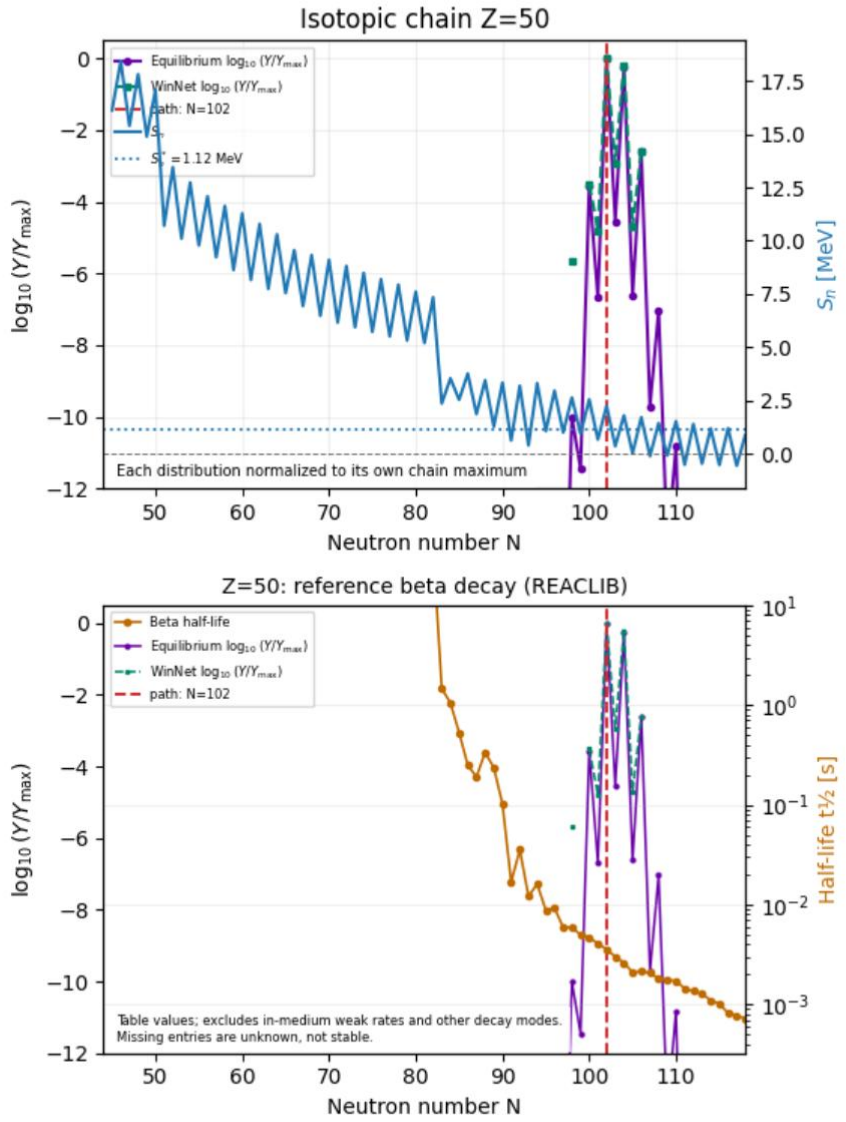
λT³ = [2πℏ² / (mu kT)]^(3/2)
Sn* ≈ −kT ln(nn λT³ / 2)

Approximate Sn* = 1.116 MeV
Displayed chain peak: Z=50, N=102

Y min (absolute): 1E-12 Fixed WinNet snapshot: 312 Show snapshot Match snapshot to inputs

WinNet abundance background Load WinNet run Beta-decay table: REACLIB Half-life





Equilibrium r-process path laboratory

Equilibrium-path controls

MRSN after freeze-out (T9~0.5)

t=2.697e-01 s. Diagnostic only: captures and photodissociations are no longer in equilibrium.

Temperature T9

0.50

log10 density [g cm^-3]

4.40

Neutron abundance Yn

4.42e-08

Right figure: proton number Z

50

Path range

Z min 20 Z max 100

Match WinNet movie statistical-factor convention

Calculate | Save figure

Standard relation:
Y(Z,N+1)/Y(Z,N) = n_n lambda_T^3
x [(A+1)/A]^(3/2) G_(N+1)/(2 G_N)
x exp[S_n(Z,N+1)/(kT)]

The path selects the maximum relative abundance in each Z chain.

nn = rho × NA × Yn = 6.665e+20 cm⁻³
kT = kB × T9 × 10⁹ K = 0.0431 MeV

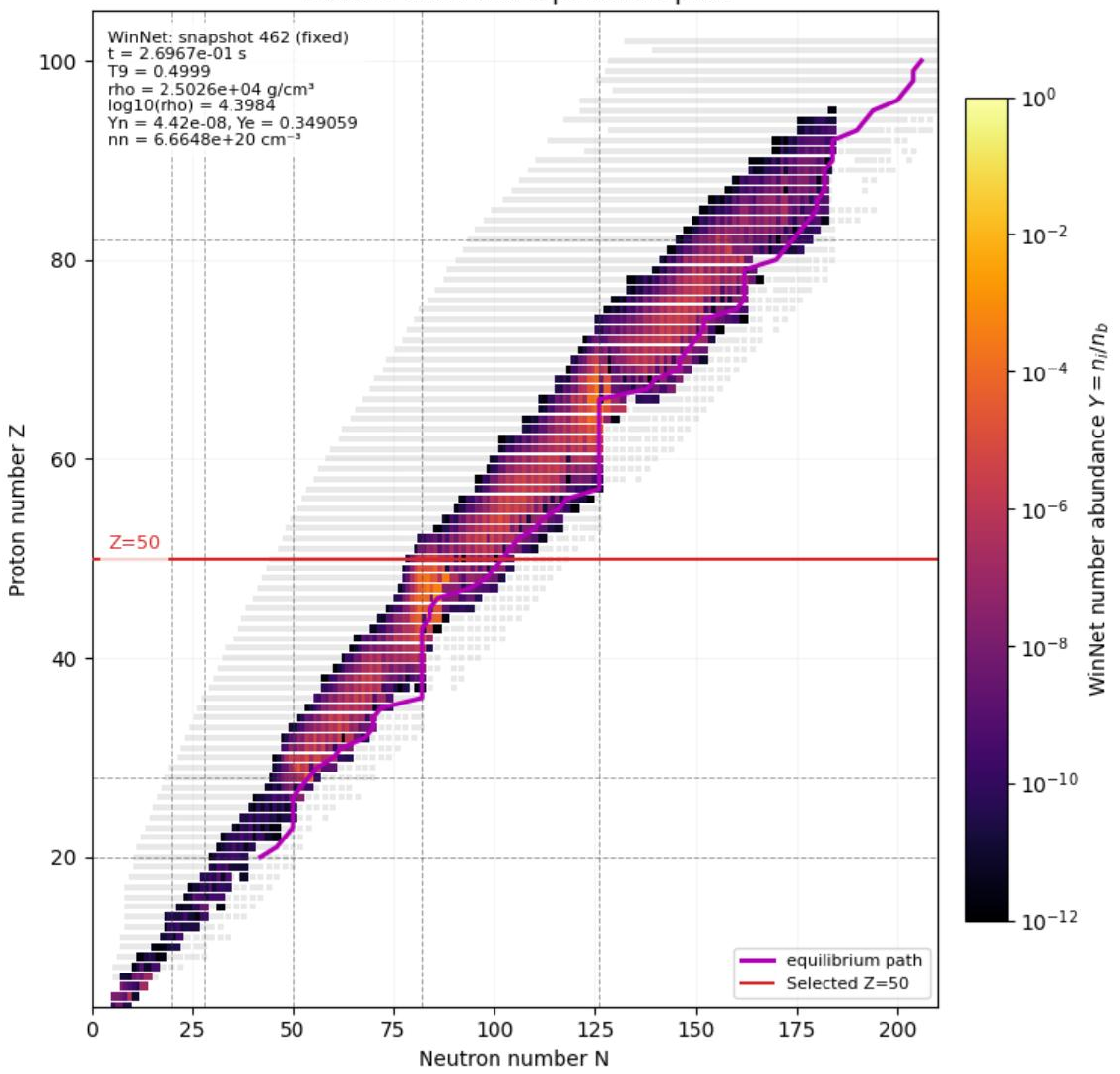
λT³ = [2πħ² / (mu kT)]³ᐟ²
Sn* ≈ −kT ln(nn λT³ / 2)

Approximate Sn* = 1.269 MeV
Displayed chain peak: Z=50, N=102

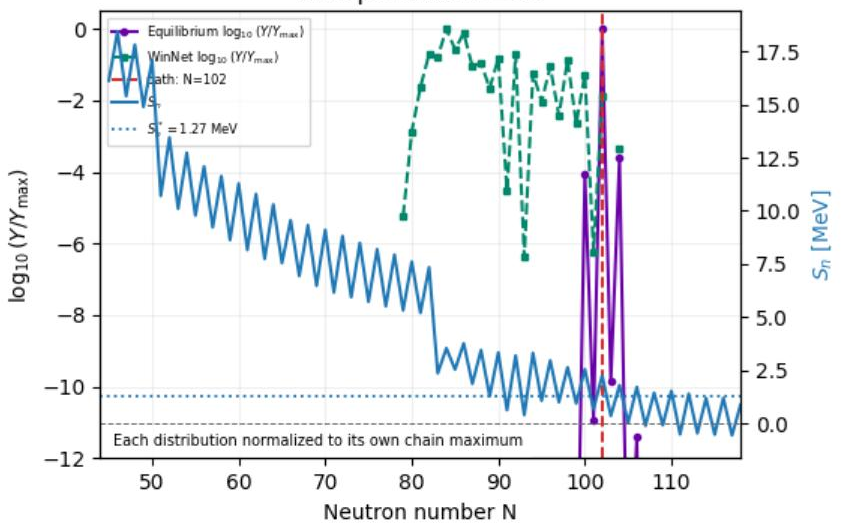
Y min (absolute): 1E-12 Fixed WinNet snapshot: 462 Show snapshot Match snapshot to inputs

WinNet abundance background Load WinNet run Beta-decay table: REACLIB Half-life

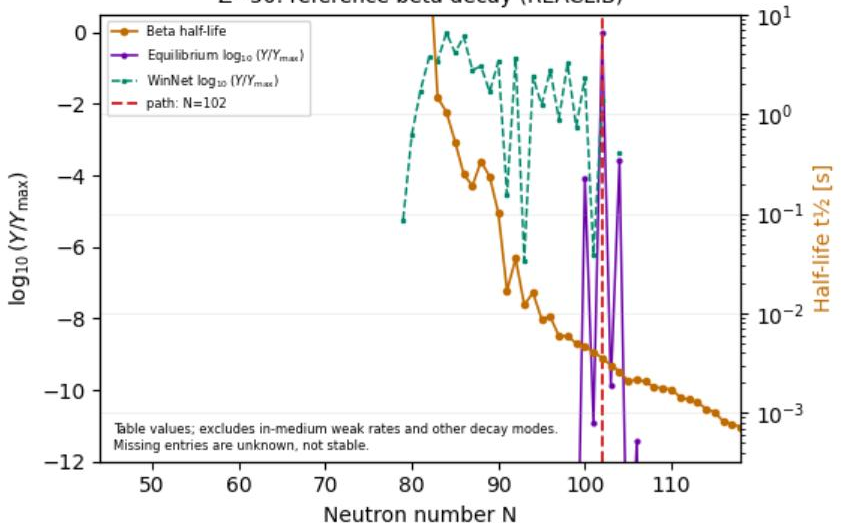
Nuclear chart and equilibrium path



Isotopic chain Z=50



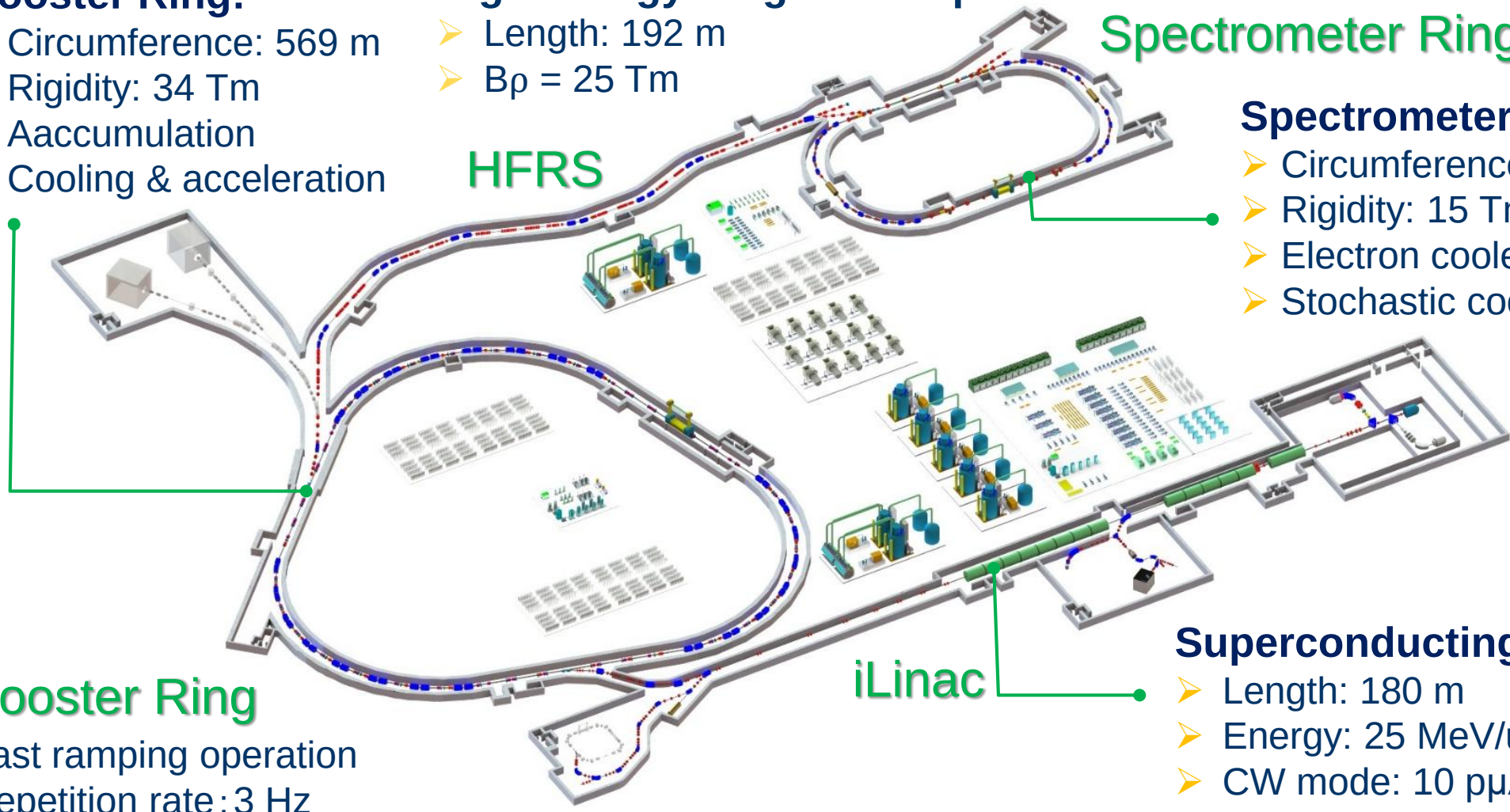
Z=50: reference beta decay (REACLIB)



High Intensity heavy ion Accelerator (HIAF)

Booster Ring:
- Circumference: 569 m
- Rigidity: 34 Tm
- Aaccumulation
- Cooling & acceleration

High Energy Fragment Separator:
- Length: 192 m
- Bρ = 25 Tm



Spectrometer Ring:
- Circumference: 277.2 m
- Rigidity: 15 Tm
- Electron cooler
- Stochastic cooler

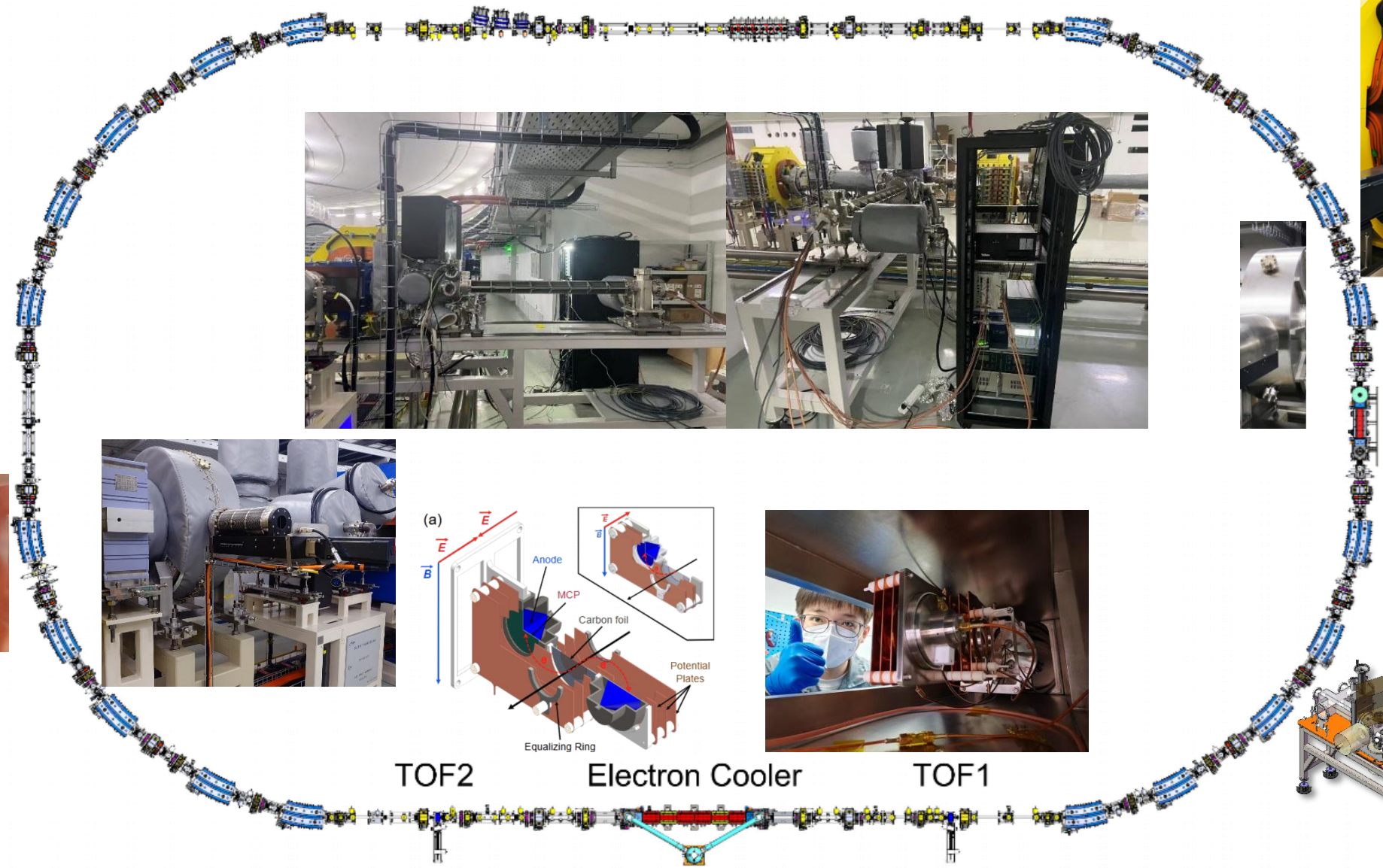
Ion Sources:
- a 45 GHz FECR
- a 28 GHz SECRAL
- a 2.45 GHz ECR

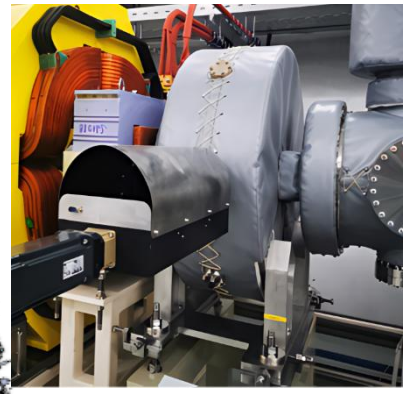
Superconducting Ion Linac:
- Length: 180 m
- Energy: 25 MeV/u ($^{238}U^{34+}$)
- CW mode: 10 pμA with A/Q=2~5
- Pulse mode: 1.0 emA with A/Q=2~7

Fast ramping operation
Repetition rate：3 Hz


High Intensity heavy ion Accelerator facility
(HIAF: 2018. 12–2025. 12)
Ready for User Operation and Global Collaboration
0.8 AGeV, 3×10^10 ppp 238U35+
1.75AGeV, 7.5×10^10 ppp 78Kr19+
2.6~3.0AGeV, 1.0×10^11 ppp 16O6+
iLinac: Superconducting linac
Length:100 m
Energy: 17~22 MeV/u(U35+ ~ 46+)
China Initiated Accelerator Dirven sub-critical System
(CiADS, 2021. 7–2027. 12)
Design Particle proton
Energy 500 MeV
CW Beam current 5 mA
Beam power 2.5 MW
Operation mode CW&Pulse
Beam loss ＜1 W/m
Reactor power 7.5 MWt
Cryogenic 2 /4 K

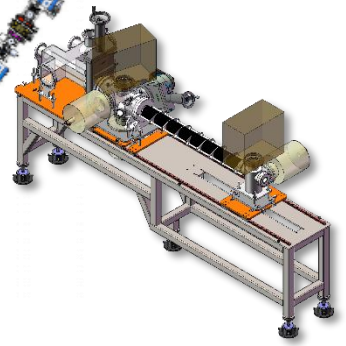
Spectrometer Ring for mass measurement





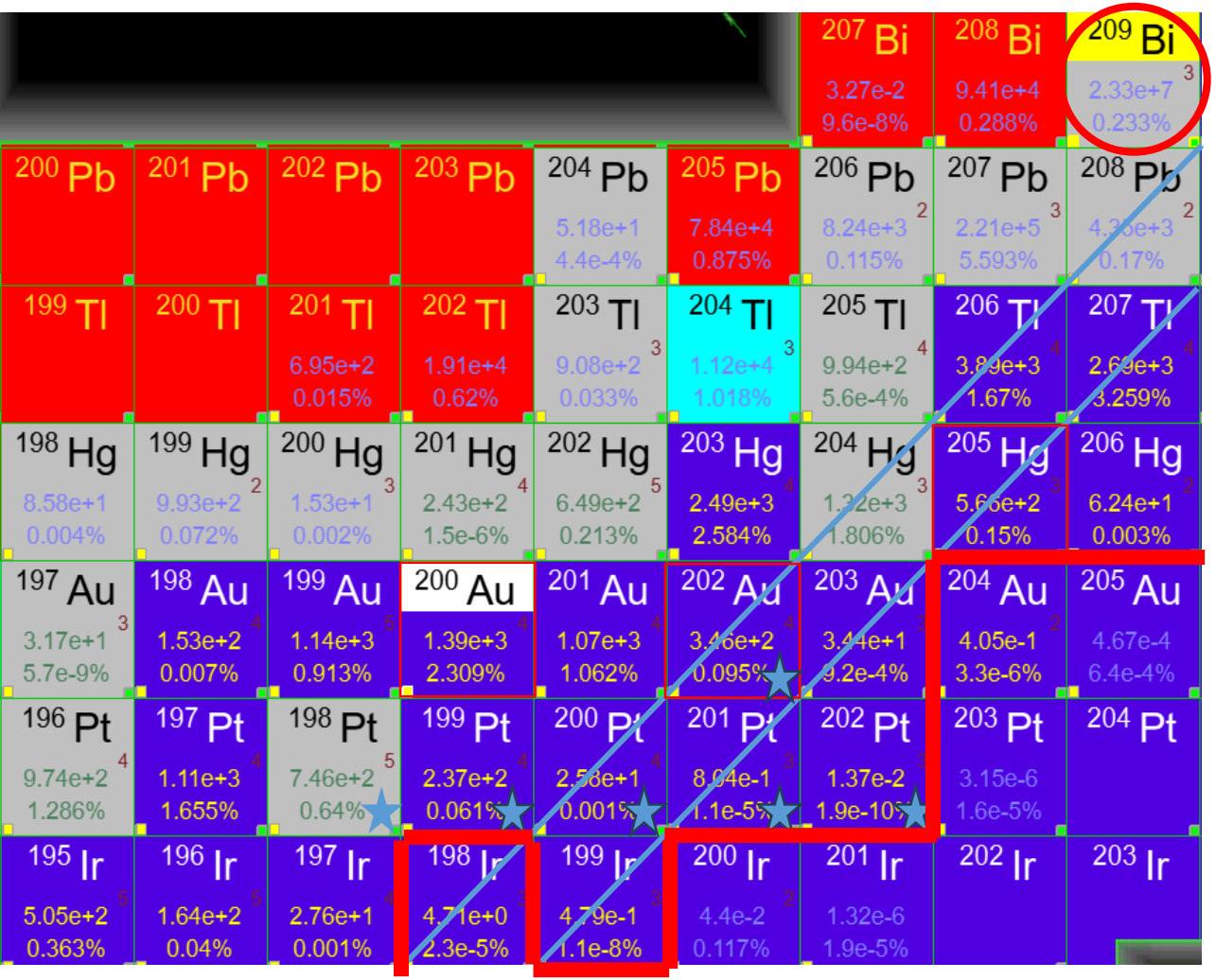


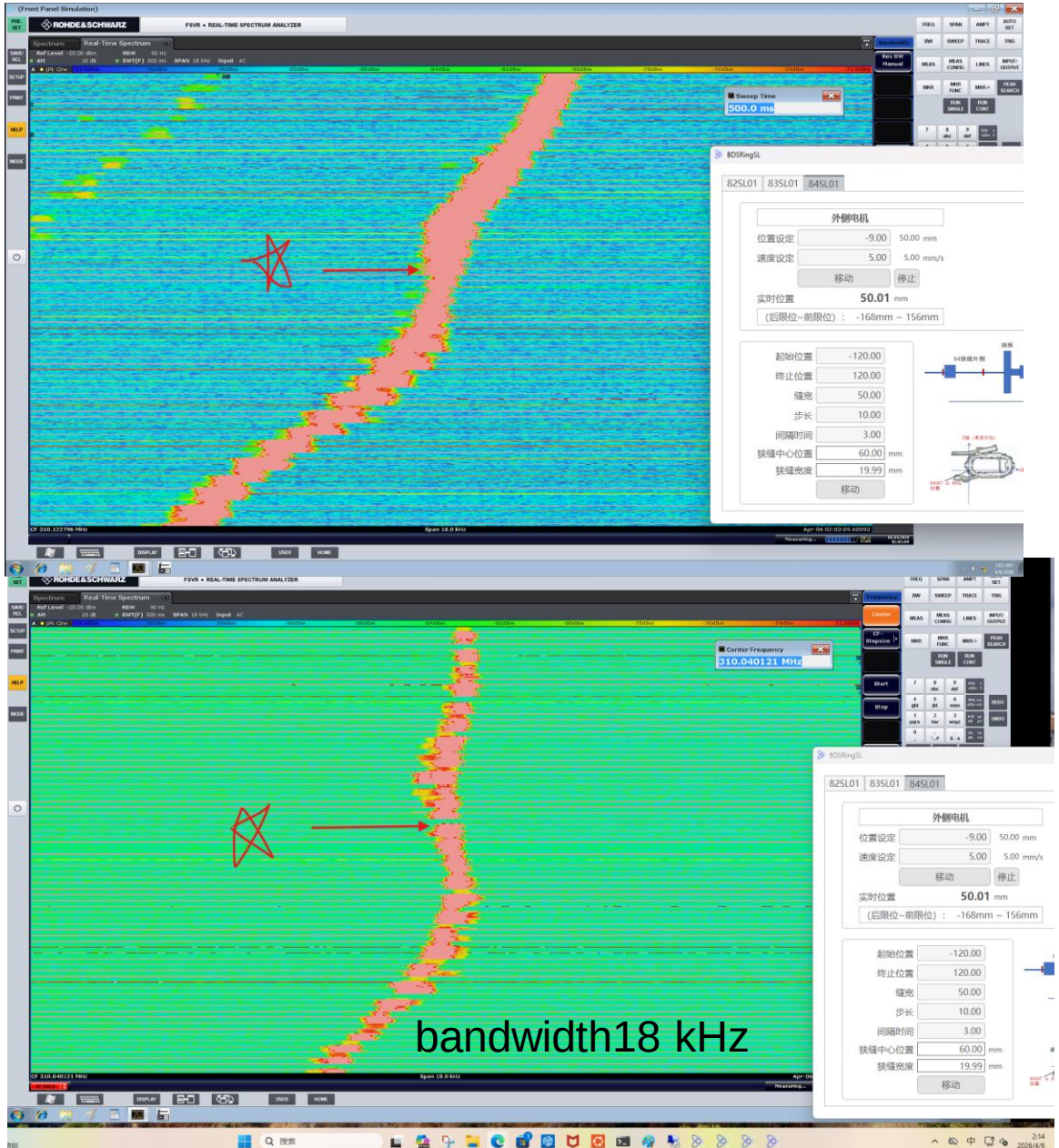
TOF2 Electron Cooler TOF1



Courtesy of M. Wang (IMP)

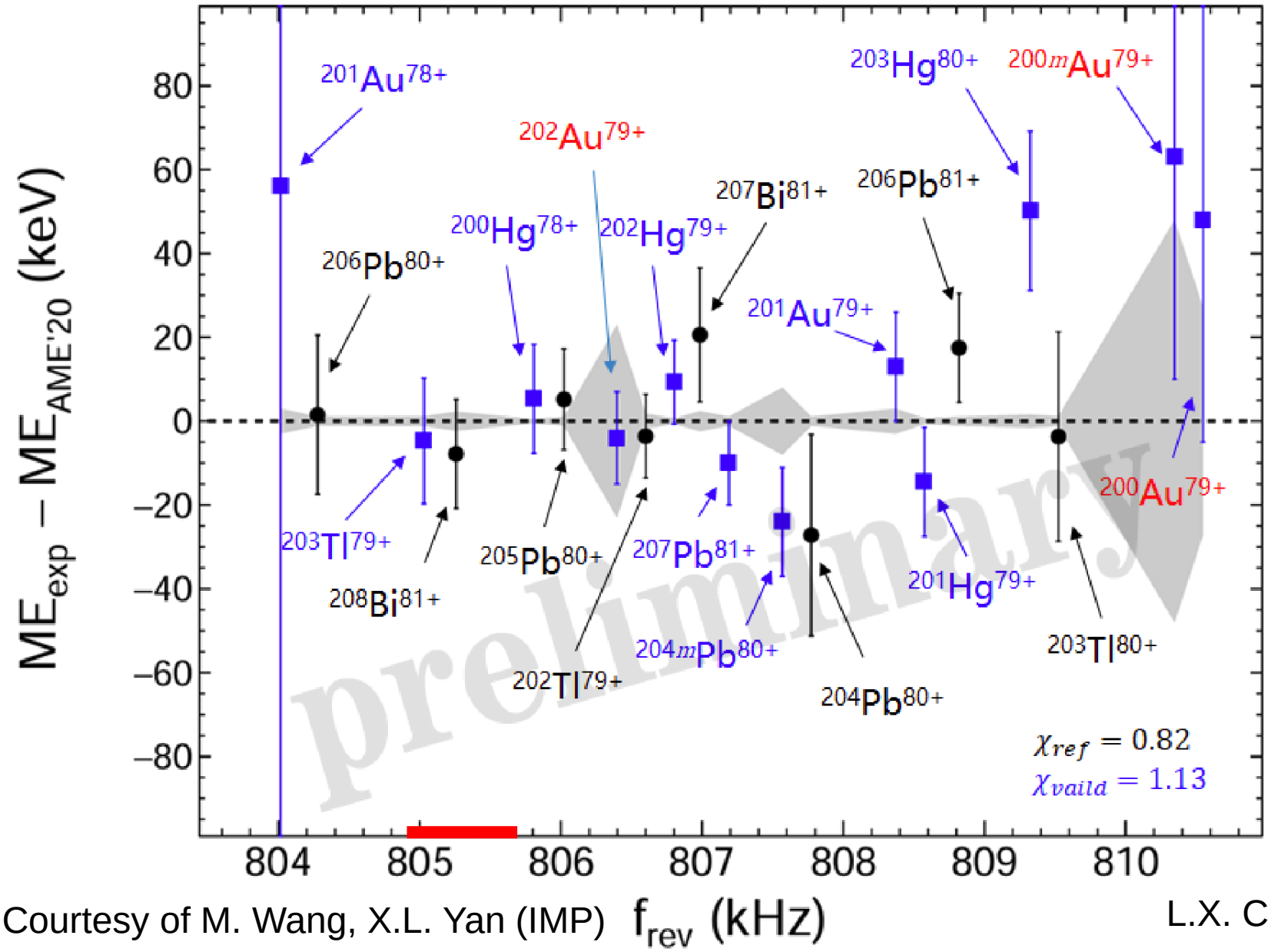
Mass measurement using Schottky Mass Spectrometry





Courtesy of M. Wang (IMP)

Mass measurement using Schottky Mass Spectrometry



ME (^{202}Au)exp = -24357 keV ± 11 keV
ME(^{202}Au)AME = -24353 keV ± 23 keV

$$\frac{\sigma(m)}{m} \sim \frac{11\ keV}{202\ u} \sim 5.8 \times 10^{-8}$$

Highest precision!

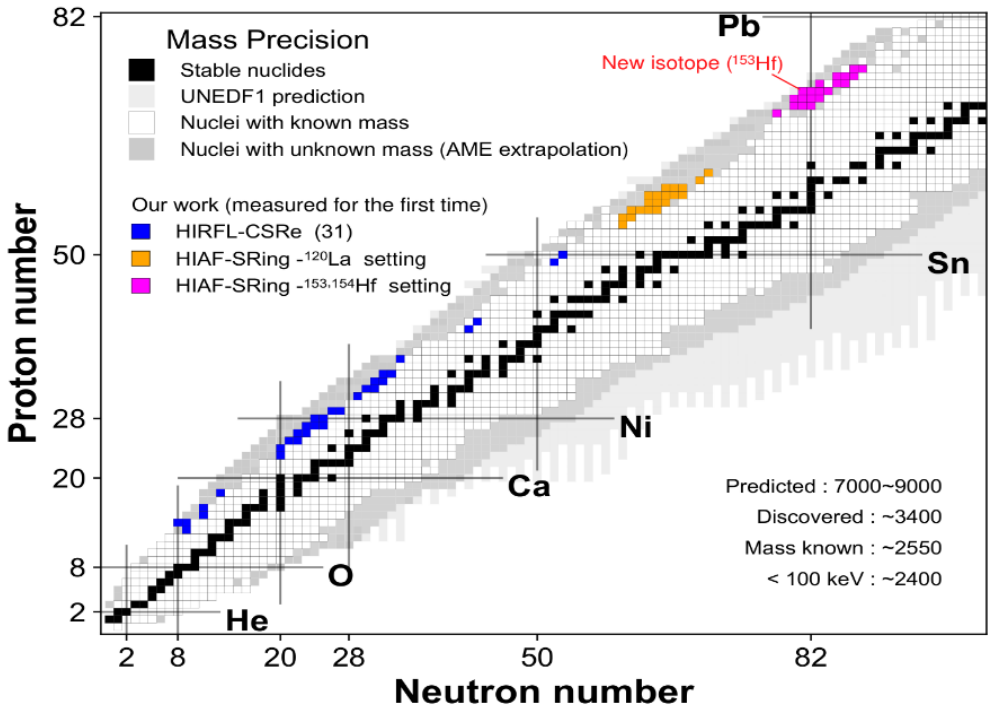
Courtesy of M. Wang, X.L. Yan (IMP)

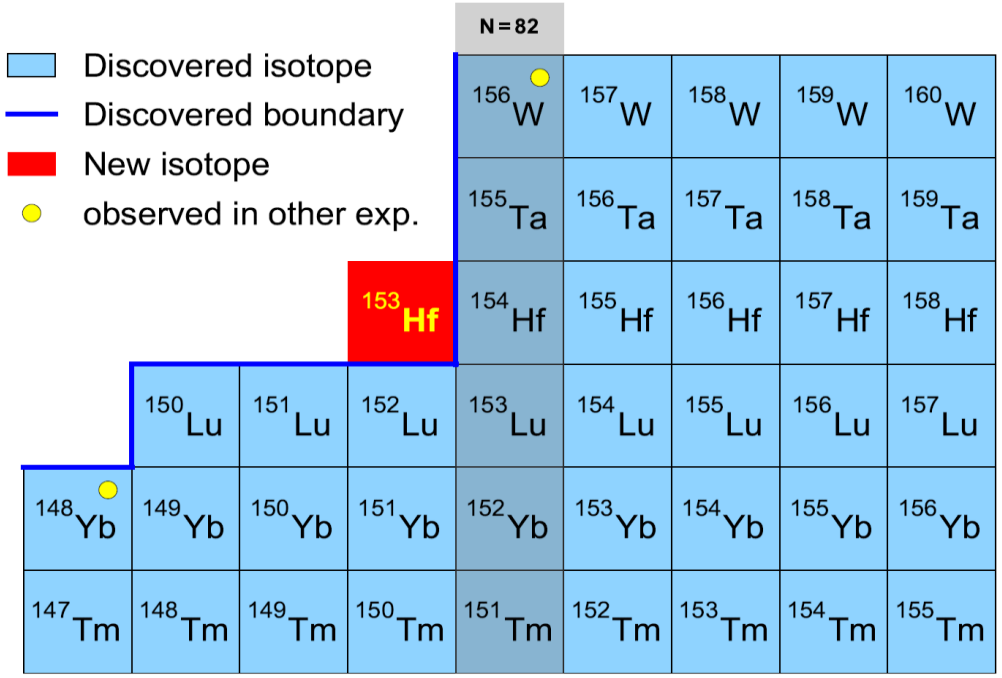
L.X. Chen et al., Nucl. Phys. A 882(2012)71

First Scientific Achievement

☐ High precision spectrometer ring SRing

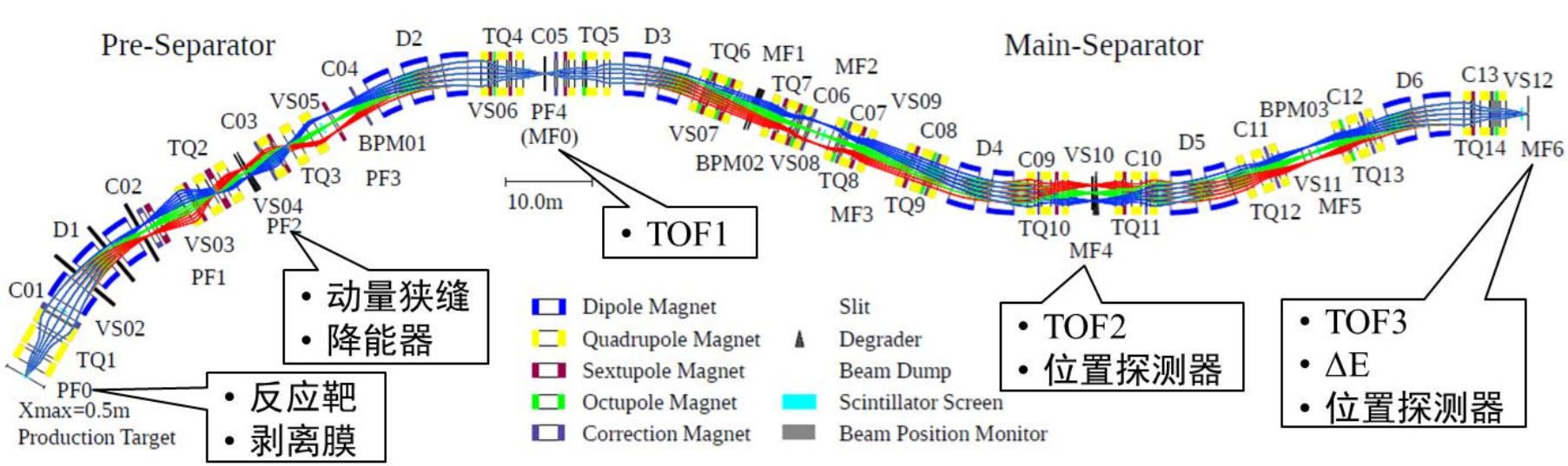
- The new nuclide ^{153}Hf was discovered for the first time.
- Approximately 35 new nuclear masses were simultaneously determined.





HIgh RIgidity Beam Line (HIRIBL)

Production of secondary radioactive ion beams (15 T*m, will upgrade to 25 T*m)





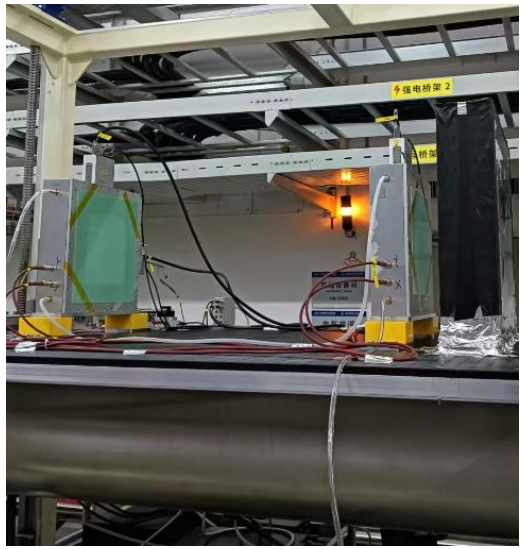


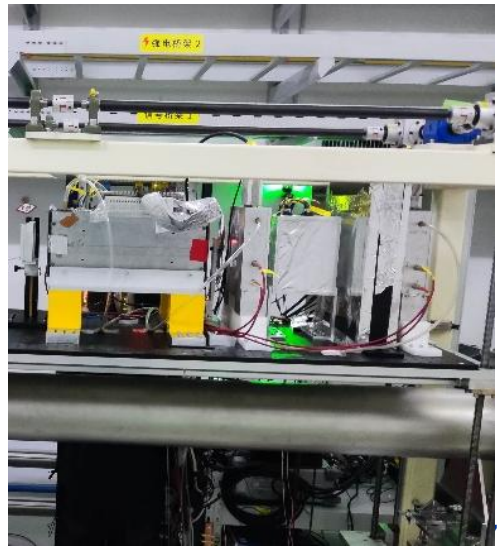


Courtesy of M. Wang (IMP)







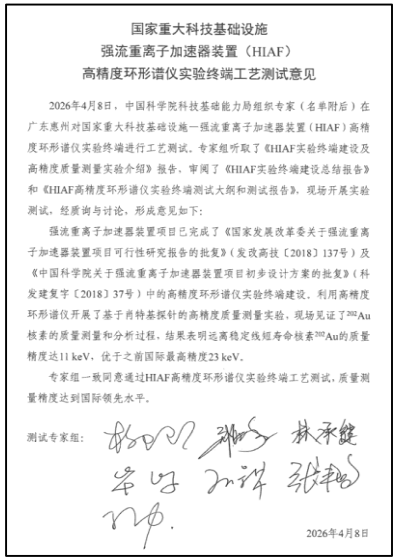


Evaluation of Review Committee

- **HIAF provide excellent beams for several commissioning experiments:**
  - First discovery of the extremely short-lived new nuclide ^{242}Fm (half-life: 4.17 μs).
  - First observation of isomeric states in the neutron-deficient nuclides ^{156}Tm and ^{158}Lu.
  - Highest precision of relative mass measurement accuracy of 10^{-8} for short-lived nuclei
  - Discovery of the new nuclide ^{153}Hf, with ~35 new masses measured for the first time in SRing.

- **These results demonstrate that HIAF are fully capable of consistently producing high-impact scientific outputs.**

Ready for User Operation and Global Collaboration


国家重大科技基础设施
强流重离子加速器装置（HIAF）
高精度环形谱仪实验终端工艺测试意见

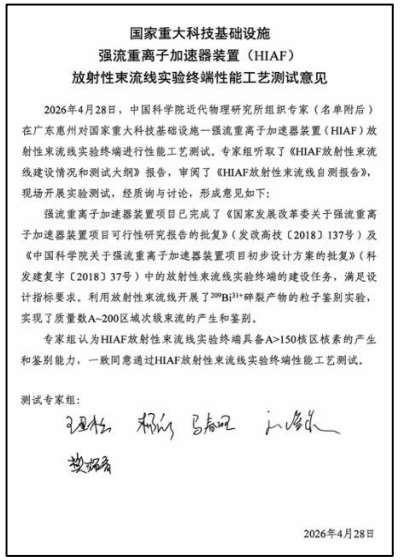
2026年4月8日，中国科学院科技基础能力局组织专家（名单附后）在广东惠州对国家重大科技基础设施一强流重离子加速器装置（HIAF）高精度环形谱仪实验终端进行了工艺测试。专家组听取了《HIAF实验终端建设及高精度质量测量实验介绍》报告，审阅了《HIAF实验终端建设总结报告》和《HIAF高精度环形谱仪实验终端测试大纲和测试报告》，现场开展实验测试，经质询与讨论，形成意见如下：

强流重离子加速器装置项目已完成了《国家发展改革委关于强流重离子加速器装置项目可行性研究报告的批复》（发改高技〔2018〕137号）及《中国科学院关于强流重离子加速器装置项目初步设计方案的批复》（科发建复字〔2018〕37号）中的高精度环形谱仪实验终端建设，利用高精度环形谱仪开展了基于肖特基探针的高精度质量测量实验，现场见证了^{202}Au核素的质量测量和分析过程，结果表明远离稳定线短寿命核素^{202}Au的质量精度达11 keV，优于之前国际最高精度23 keV。

专家组一致同意通过HIAF高精度环形谱仪实验终端工艺测试，质量测量精度达到国际领先水平。

测试专家组：林承键

2026年4月8日


国家重大科技基础设施
强流重离子加速器装置（HIAF）
放射性束流线实验终端性能工艺测试意见

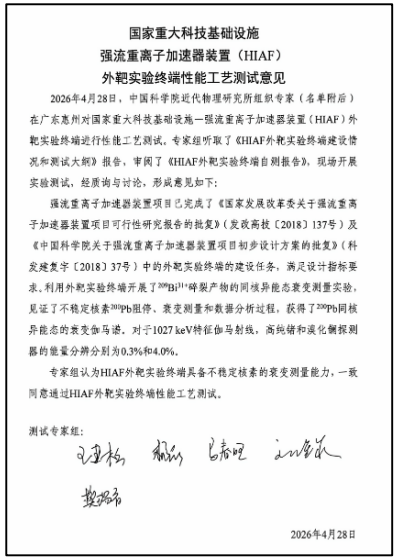
2026年4月28日，中国科学院近代物理研究所组织专家（名单附后）在广东惠州对国家重大科技基础设施一强流重离子加速器装置（HIAF）放射性束流线实验终端进行性能工艺测试。专家组听取了《HIAF放射性束流线建设情况和测试大纲》报告，审阅了《HIAF放射性束流线自测报告》，现场开展实验测试，经质询与讨论，形成意见如下：

强流重离子加速器装置项目已完成了《国家发展改革委关于强流重离子加速器装置项目可行性研究报告的批复》（发改高技〔2018〕137号）及《中国科学院关于强流重离子加速器装置项目初步设计方案的批复》（科发建复字〔2018〕37号）中的放射性束流线实验终端的建设任务，满足设计指标要求。利用放射性束流线开展了^{209}Bi^{31+}碎裂产物的粒子鉴别实验，实现了质量数A~200区域次级束流的产生和鉴别。

专家组认为HIAF放射性束流线实验终端具备A>150核区核素的产生和鉴别能力，一致同意通过HIAF放射性束流线实验终端性能工艺测试。

测试专家组：

2026年4月28日


国家重大科技基础设施
强流重离子加速器装置（HIAF）
外靶实验终端性能工艺测试意见

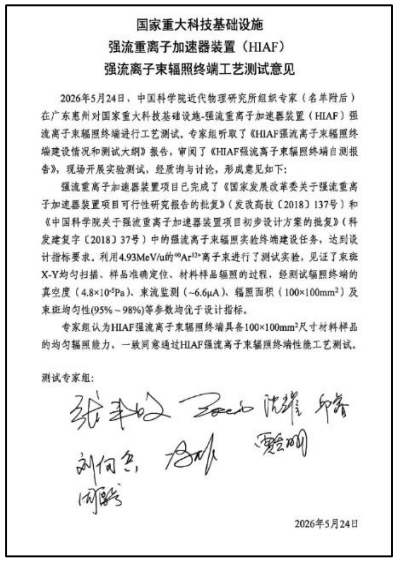
2026年4月28日，中国科学院近代物理研究所组织专家（名单附后）在广东惠州对国家重大科技基础设施一强流重离子加速器装置（HIAF）外靶实验终端进行性能工艺测试，专家组听取了《HIAF外靶实验终端建设情况和测试大纲》报告，审阅了《HIAF外靶实验终端自测报告》，现场开展实验测试，经质询与讨论，形成意见如下：

强流重离子加速器装置项目已完成了《国家发展改革委关于强流重离子加速器装置项目可行性研究报告的批复》（发改高技〔2018〕137号）及《中国科学院关于强流重离子加速器装置项目初步设计方案的批复》（科发建复字〔2018〕37号）中的外靶实验终端的建设任务，满足设计指标要求。利用外靶实验终端开展了^{209}Bi^{31+}碎裂产物的同核异能态衰变测量实验，见证了不稳定核素^{203}Pb组停、衰变测量和数据分析过程，获得了^{200}Pb同核异能态的衰变伽马谱，对于1027 keV特征伽马射线，高纯锗和溴化镧探测器的能量分辨分别为0.3%和4.0%。

专家组认为HIAF外靶实验终端具备不稳定核素的衰变测量能力，一致同意通过HIAF外靶实验终端性能工艺测试。

测试专家组：

2026年4月28日


国家重大科技基础设施
强流重离子加速器装置（HIAF）
强流离子束辐照终端工艺测试意见

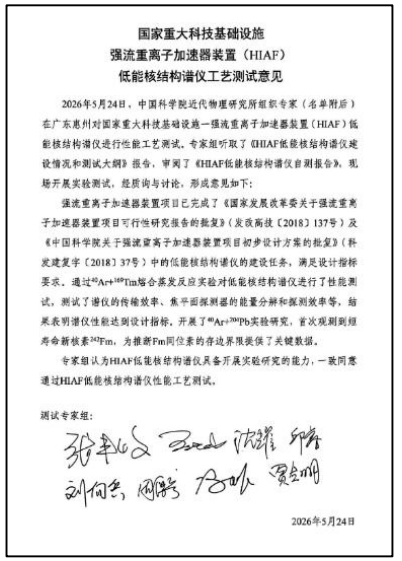
2026年5月24日，中国科学院近代物理研究所组织专家（名单附后）在广东惠州对国家重大科技基础设施-强流重离子加速器装置（HIAF）强流离子束辐照终端进行工艺测试。专家组听取了《HIAF强流离子束辐照终端建设情况和测试大纲》报告，审阅了《HIAF强流离子束辐照终端自测报告》，现场开展实验测试，经质询与讨论，形成意见如下：

强流重离子加速器装置项目已完成了《国家发展改革委关于强流重离子加速器装置项目可行性研究报告的批复》（发改高技〔2018〕137号）和《中国科学院关于强流重离子加速器装置项目初步设计方案的批复》（科发建复字〔2018〕37号）中的强流离子束辐照实验终端建设任务，达到设计指标要求，利用4.93MeV/u的^{40}Ar^{12+}离子束进行了测试实验，见证了束斑X-Y均匀扫描、样品准确定位、材料样品辐照的过程，经测试辐照终端的真空度（4.8×10^{-5}Pa）、束流监测（~6.6μA）、辐照面积（100×100mm^2）及束斑均匀性(95%～98%)等参数均优于设计指标。

专家组认为HIAF强流离子束辐照终端具备100×100mm^{2}尺寸材料样品的均匀辐照能力，一致同意通过HIAF强流离子束辐照终端性能工艺测试。

测试专家组：

2026年5月24日


国家重大科技基础设施
强流重离子加速器装置（HIAF）
低能核结构谱仪工艺测试意见

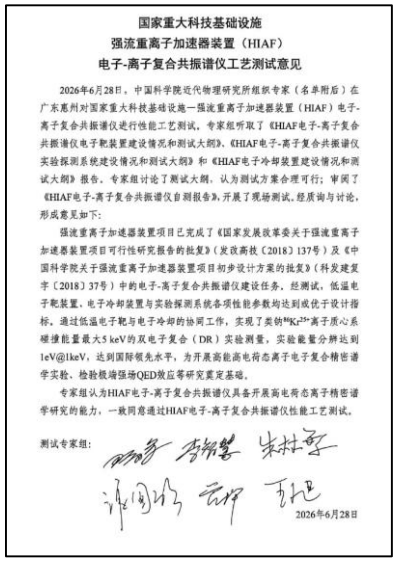
2026年5月24日，中国科学院近代物理研究所组织专家（名单附后）在广东惠州对国家重大科技基础设施一强流重离子加速器装置（HIAF）低能核结构谱仪进行性能工艺测试。专家组听取了《HIAF低能核结构谱仪建设情况和测试大纲》报告，审阅了《HIAF低能核结构谱仪自测报告》，现场开展实验测试，经质询与讨论，形成意见如下：

强流重离子加速器装置项目已完成了《国家发展改革委关于强流重离子加速器装置项目可行性研究报告的批复》（发改高技〔2018〕137号）及《中国科学院关于强流重离子加速器装置项目初步设计方案的批复》（科发建复字〔2018〕37号）中的低能核结构谱仪的建设任务，满足设计指标要求。通过^{40}Ar+^{169}Tm熔合蒸发反应实验对低能核结构谱仪进行了性能测试，测试了谱仪的传输效率、焦平面探测器的能量分辨和探测效率等，结果表明谱仪性能达到设计指标，开展了^{46}Ar+^{209}Pb实验研究，首次观测到短寿命新核素^{242}Fm，为推断Fm同位素的存边界限提供了关键数据。

专家组认为HIAF低能核结构谱仪具备开展实验研究的能力，一致同意通过HIAF低能核结构谱仪性能工艺测试。

测试专家组：

2026年5月24日


国家重大科技基础设施
强流重离子加速器装置（HIAF）
电子-离子复合共振谱仪工艺测试意见

2026年6月28日，中国科学院近代物理研究所组织专家（名单附后）在广东惠州对国家重大科技基础设施一强流重离子加速器装置（HIAF）电子-离子复合共振谱仪进行性能工艺测试，专家组听取了《HIAF电子-离子复合共振谱仪电子靶装置建设情况和测试大纲》、《HIAF电子-离子复合共振谱仪实验探测系统建设情况和测试大纲》和《HIAF电子冷却装置建设情况和测试大纲》报告，专家组讨论了测试大纲，认为测试方案合理可行；审阅了《HIAF电子-离子复合共振谱仪自测报告》，开展了现场测试，经质询与讨论，形成意见如下：

强流重离子加速器装置项目已完成了《国家发展改革委关于强流重离子加速器装置项目可行性研究报告的批复》（发改高技〔2018〕137号）及《中国科学院关于强流重离子加速器装置项目初步设计方案的批复》（科发建复字〔2018〕37号）中的电子-离子复合共振谱仪建设任务，经测试，低温电子靶装置、电子冷却装置与实验探测系统各项性能参数均达到或优于设计指标。通过低温电子靶与电子冷却的协同工作，实现了类钠^{86}Kr^{25+}离子质心系碰撞能量最大5 keV的双电子复合（DR）实验测量，实验能量分辨达到1eV@1keV，达到国际领先水平，为开展高能高电荷态离子电子复合精密谱学实验、检验极端强场QED效应等研究奠定基础。

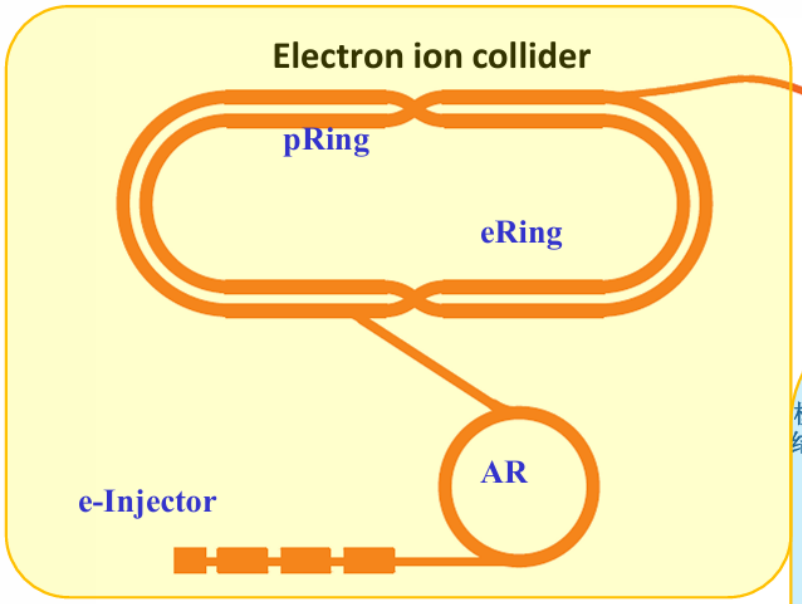
专家组认为HIAF电子-离子复合共振谱仪具备开展高电荷态离子精密谱学研究的能力，一致同意通过HIAF电子-离子复合共振谱仪性能工艺测试。

测试专家组：

2026年6月28日

Future plan

CNUF-China advanced NUclear physics research Facility



☐ Electron ion collider in China (EicC)

Precision measurements of the structure of the nucleon in the sea quark region

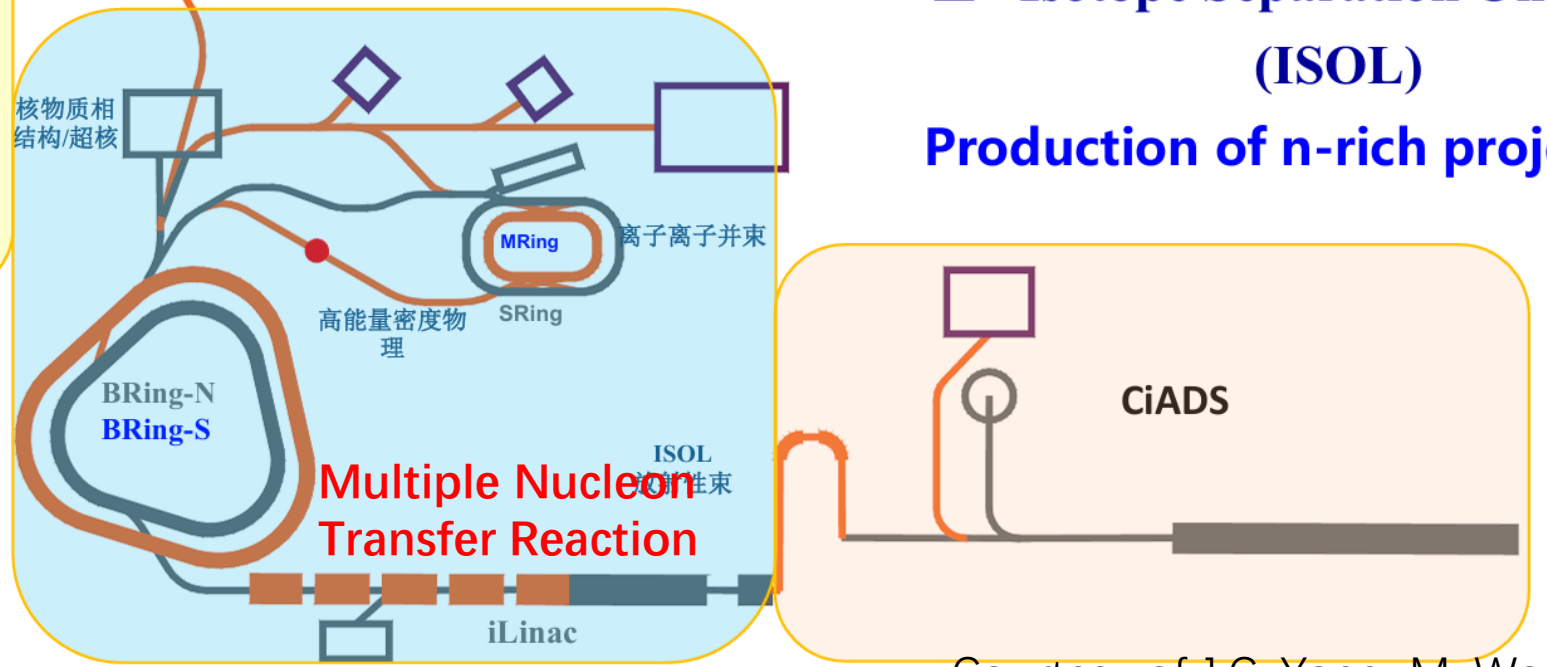
☐ Upgrade of the HIAF (HIAF-U)

Improve the energy up to 25 GeV (p) and 9 GeV/u (U)

New accelerators
Under construction
New terminal

☐ Isotope Separation On-Line (ISOL)

Production of n-rich projectiles



Courtesy of J.C. Yang, M. Wang (IMP)

Conclusions

- Precise nuclear astrophysics experiments play a key role in the multi-messenger era
  Solar neutrino and metallicity problems
  $^{12}C(\alpha,\gamma)^{16}O$: impact on nucleosynthesis and black mass gap
  $^{12}C+^{12}C$: superburst ignition problem

- The studies of $^{12}C(\alpha,\gamma)^{16}O$ and $^{12}C+^{12}C$ are not yet satisfied. More demands are coming from the new multi-messenger observations

- To achieve the best understanding, we need both direct and indirect methods, joint efforts of various facilities, and interdisciplinary collaborations among nuclear physics, astrophysics and astronomy





